KINETIC STUDIES OF THE WATER-GAS SHIFT REACTION - A COMPARISON OF COMMERCIAL CATALYSTS

by

Hebabuddin Ahmed Quazi, B.Sc.(Eng.) Dacca

Thesis submitted for the degree of Doctor of Philosophy
in the Faculty of Applied Science
of the University of Newcastle upon Tyne.

Department of Chemical Engineering,
University of Newcastle upon Tyne,
Newcastle upon Tyne,
England.

September, 1965

ACKNOWLEDGEMENTS

The author would like to express his thanks to Dr. F. Goodridge for his supervision and guidance throughout this work, to Professor J.M. Coulson in whose laboratories the investigations were carried out and to Mr. W.R. Moore who constructed most of the experimental equipment. Thanks are also due to Mr. C. Currie and his staff of technicians who have been most helpful.

The author is indebted to the Association of Commonwealth Universities for awarding him a Commonwealth Scholarship while the present work was carried out. Thanks are also due to the East Pakistan University of Engineering & Technology, Dacca for granting the author leave of absence during the last three years.

A B S T R A C T

There have been many studies on the kinetics of the water-gas shift reaction but the results are in poor agreement. The aim of the present work was to investigate, in the same equipment and under carefully standardised conditions, the behaviour of a number of commercially used catalysts. In this way it was hoped to determine whether the contradiction of results found in the literature could be ascribed to the different kinetic behaviours of these catalysts. As a secondary aim it was intended to obtain some clues to the mechanisms of this reaction although it was realised that the statistical design method used was not particularly suitable for the production of rate equations of great accuracy. A differential reactor was used in this work.

The commercial catalysts studied in this investigation were the products of Girdler Catalysts (G-3A and G-66B), A.B. Svenska Saltpeterverken of Sweden, Power Gas and I.C.I.Limited. All the catalysts except Girdler G-66B worked between 350° to 450°C. Working temperature range of Girdler G-66B was 180° to 320°C. All studies were carried out at atmospheric pressure. Results showed activities of the shift catalysts of the order: Girdler G-66B, SSV (Sweden), Power Gas, I.C.I., Girdler G-3A. Kinetic studies showed that the forward reaction was nearly first order with respect to carbon monoxide for Power Gas, I.C.I. and Girdler G-3A catalysts, but fractional for SSV and Girdler G-66B catalysts. The order of reaction with respect to steam was fractional for all the catalysts. The order with respect to hydrogen was zero for SSV catalyst, but retarding effects were observed for the rest. The forward reaction was unaffected by carbon dioxide for Girdler G-66B, but retarded in the case of the rest of the catalysts.

From these results it is concluded that the divergence in results can be ascribed to the different behaviour of individual catalysts. Comparison with previous work using the SSV catalyst gives good agreement with the present results. An expotential type of rate equation is shown to be of sufficient accuracy to be used for the purpose of reactor design, but a Hougen-Watson type rate equation based on a possible reaction mechanism does not agree with the results obtained.

CONTENTS

Chapter 1. INTRODUCTION

The stoichiometric equation and the thermodynamics of a chemical reaction do not give any indication of the rate at which the reaction will proceed. Thermodynamic studies indicate ultimate change but the magnitude of the thermodynamic functions in no way influence or suggest the time required for the completion of a particular reaction. In the design of industrial scale chemical reactors there is an obvious need for reliable kinetic data. This together with information concerning the relevant physical processes, i.e. heat and mass transfer can then lead to an economic design procedure. Although the importance of such physical processes must not be ignored the following discussion will be confined to the subject of catalysis in general and gas phase solid catalysed reactions in particular.

The research chemist and chemical engineer approach the problems of heterogeneous kinetics from two different viewpoints. The research chemist is concerned with the reaction mechanism, and with the aid of experimental kinetic data attempts to elucidate the simple reaction steps from which the complex overall reaction is built up. The main concern of the chemical engineer however is the determination of a reliable rate equation which will permit accurate reactor design calculations and process control in the practical range of temperatures and pressures. The desire for more reliable reactor design procedures and the need for process optimisation has now necessitated the detailed study of reaction mechanism and its bearing on process potentialities and catalyst characteristics.

The principle difficulty in the determination of mechanism is often the experimental accuracy which is inadequate to determine the relatively small differences resulting from entirely different reaction mechanisms. Many experimental techniques and methods of data evaluation have been used in the past but quite frequently the limitations of the experimental methods are not sufficiently stressed. It will be shown later that apparently different kinetic expressions based on different proposed mechanisms give almost the same results. Hence an agreement between experimental and calculated reaction rates does not necessarily prove the validity of a given reaction mechanism.

The water-gas shift reaction ($CO + H_2O \rightleftharpoons CO_2 + H_2$) in presence of catalyst is of considerable industrial importance for the production of hydrogen from solid fuels, natural gas and heavy petroleum fractions. Utilised first in the ammonia synthesis, today this reaction has become of importance in other synthesis processes, for example, hydrogenations in general, the production of methyl alcohol, and of synthetic petrols by the Fischer Process. The shift reaction is also used to remove carbon monoxide from town gas.

The most widely employed commercial water-gas shift catalyst consists of iron and chromium oxides, either alone or mixed with suitable supports. The usual temperature range extends from 300° to $500^{\circ}C$. Although the principal active constituents are the same, the activities of commercial catalysts vary considerably due to differences either in the method of preparation or in the catalyst composition. The deliberate addition of other constituents as promotors or as binders sometimes not only change the activity of the catalyst but also influence the reaction mechanism. The catalytic activities of the oxides of Nickel, Cobalt, Zinc and Copper have been widely studied but so far Girdler G-66 is the only copper based catalyst commercially available, and exhibits considerable activity at low temperatures (180° - $320^{\circ}C$).

The most common problem facing the chemical engineer when looking for design data lies in the inconsistences in the published literature.

These to mention just a few could be due to differences in experimental technique, insufficient care in observing errors inherent in this technique, and differences in the performance of the actual catalytic materials used. The aim of this work was to investigate, in the same equipment and under carefully standardised conditions, the behaviour of a number of commercially used catalysts. In this way it was hoped to determine whether the contradiction of results on the water-gas shift reaction found in the literature could be ascribed to the different kinetic behaviour of these catalysts. As a secondary aim it was intended to obtain some clues to the mechanisms of this reaction although it was realised that the statistical design method used was not particularly suitable for production of rate equations of great accuracy.

A differential reactor was used in this work but before describing experimental techniques in greater detail it might be useful to consider very briefly some of the theoretical background to heterogeneous catalysis.

Chapter 2 THEORY OF HETEROGENEOUS CATALYSIS

Catalylic gas-phase reactions play an important role in many industrial processes, as in the production of methanol, ammonia, sulphuric acid, nitric acid, and various petrochemicals, and usually involve the high-energy rupture, breakdown or synthesis of low molecular-weight materials. Because of the great industrial importance of catalytic reactions, considerable effort has been put into developing theories that would form a rational basis for the development of kinetic equations of reaction. Various mechanisms have been proposed and are treated in detail in the text books (48, 60, 66, 97 and 105). Here only a very brief review of the salient points can be given.

2.1 CATALYSTS AND THEIR ACTIVITIES

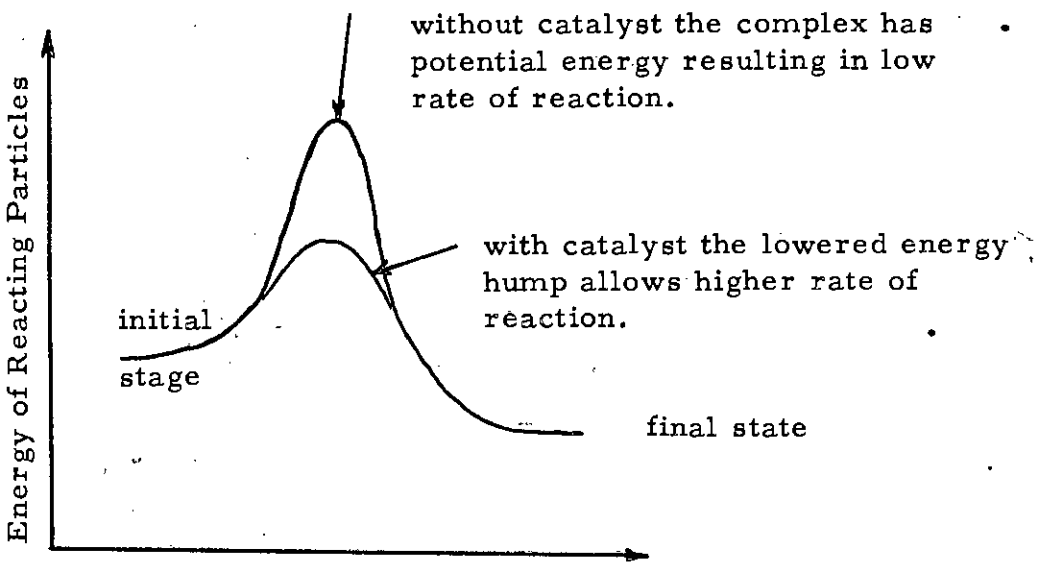

Fig. 2.1 Representation of the action of a catalyst

The selection reasons why a particular catalyst is capable of promoting a specific reaction are not very well understood and in practice extensive trial and error are needed to produce a satisfactory catalyst. It has been observed that the physical or crystalline structure is as important in imparting catalylic activity to a material as its chemical constitution. It is thought that reactant molecules are somewhat changed, energized, or affected to form intermediates in the regions close to the catalyst surface, and various theories have been proposed to explain this catalylic activity (41). In terms of the transition state theory the catalyst reduces the potentional energy barrier over which the reactants must pass to form products. Catalyst influences the form and development of the kinetic rate equations needed in design, but it never determines the equilibrium or end point of a reaction. Since the solid surface is responsible for catalytic activity, highly porous catalytic materials are desirable.

2.2 RATE EQUATION

In developing rate expressions for the continuous-reaction model, the various processes that may cause resistance to reaction must be taken into account. For a single porous catalyst particle we may visualise these processes as follows:-

(a) Gas film resistance: Reactants must diffuse from the main body of the fluid to the exterior surface of the catalyst.

(b) Pore diffusion resistance: Because the interior of the pellet contains so much more area than the exterior of the particle most of the reaction takes place within the particle itself. Therefore the reactants must in general move into the pellets through the pores.

(c) Surface phenomenon resistance: At some points in their wanderings the reactant molecules are associated with the surface of the catalyst where they react to give products that are released to the fluid phase within the pore.

(d) Pore diffusion resistance for products: Products then diffuse out of the pellet.

(e) Gas film resistance for products: Products then move from the mouth of the catalyst pores into the main gas stream.

Of the foregoing processes it is usually found that one or two offer appreciable resistance and therefore become rate controlling. Let us now consider the various forms taken by the rate equation when one of steps (a) - (e) is rate controlling.

2.2.1 FILM RESISTANCE CONTROLS

When the gas film resistance is much greater than that of pore diffusion or surface phenomenon, the rate of reaction is limited by the rate of flow of reactant to the surface as given by the mass transfer coefficient k_g between gas and solid. The rate based on unit exterior surface of particle S_{ex} is then

$$-\frac{1}{S_{ex}}\frac{dN_A}{dt} = k_g (C_{Ag} - C_{Ae}) \qquad (2.1)$$

where C_{Ag} is the concentration of reactant A in the gas stream and C_{Ae} is its equilibrium concentration on the surface. The observed overall reaction rate will be the same for both catalytic and non-catalytic fluid-solid reactions if the gas film resistance is the controlling.

2.2.2 SURFACE PHENOMENON CONTROLLING

A good number of very detailed mechanisms have been proposed in this connection. The most useful for our purposes supposes that reaction takes place on an active site of the surface of the catalyst and three steps are considered to occur successively at the surface.

Step 1. A molecule is adsorbed on to the surface and is attached to an active site.

Step 2. It then reacts either with another molecule on an adjacent site (duel-site mechanism), or with one coming from the main gas stream (single-site mechanism), or it simply decomposes while on the site (single-site mechanism).

Step 3. Products are desorbed from the surface, which gives the site further opportunity to absorb fresh reactants.

In addition, an equilibrium is assumed to exist between species involved in the three steps.

For design purposes the real value of the active site theory is that it gives a qualitative idea of what may happen on extrapolation to new operating conditions. Imagine a molecule adsorbing, reacting and desorbing from the surface. From findings in adsorption we know that a rise in pressure results in an increase in amount of material adsorbed. Hence if adsorption is rate controlling, an increase in reactant concentration will result in an increase in rate of reaction.

Suppose desorption controls. Desorption, being an equilibrium process between site attached and free product molecules, is unaffected by an increase in concentration of reactants. Hence we get no increase in rate.

with a rise in reactant concentration. When chemical reaction controls, we visualise that all the active sites are constantly and continually in use.

Whatever form the rate equations take they will be based on some relation between the concentration of species in the immediate vicinity of the surface and the amount of this species actually adsorbed on the surface. This relationship may be represented by an adsorption isotherm. Before discussion of the actual rate expression it will be therefore useful to review briefly the most important of these isotherms. Of these, those by Langmuir, Freundlich and Temkin are probably the most important. Each is characterised by certain assumptions, in particular as to the manner in which the differential heat of adsorption varies with adsorbed amount and each is applicable to certain experimental systems (41). In deriving theoretical isotherms, three approaches are possible. First, in kinetic terms, the condition for equilibrium is that the velocities of adsorption and desorption are equal, and isotherms may be obtained by equating these velocities. Second, in statistical terms, the equilibrium constant is given by a ratio of partition functions of vacant sites, adsorbed molecules and gas phase molecules, and isotherms may be obtained by equating this ratio to the corresponding ratio of concentrations. The statistical approach is more powerful than the kinetic approach because it gives numerical values for constants which cannot be evaluated by the kinetic method. Third, equilibrium may be approached thermodynamically, either using the condition that the change in free energy on transferring an infinitesimal amount of gas from the gas phase to the surface at constant temperature is zero, or alternatively using the Gibbs adsorption equation.

The Langmuir Isotherm

The kinetic and statistical derivations of the Langmuir isotherm are based on the following assumptions:-

(a) Adsorption is localised and takes place only through collision of gas molecules with vacant sites.

(b) Each site can accommodate one and only one adsorbed particle.

(c) The energy of an adsorbed particle is the same at any site on the surface, and is independent of the presence or absence of nearby adsorbed molecules.

The assumptions underlying the thermodynamic derivation differ from those given above in that the adsorption is considered to be non-localised. It can be shown (41) that the Langmuir isotherm is represented by $\Theta = \frac{ap}{1 + ap}$ where Θ is the coverage of surface, p is the pressure and 'a' is dependent on temperature alone.

The Freundlich Isotherm

Early during the study of adsorption it became clear that many experimental data did not obey the Langmuir isotherm. An alternative isotherm, which was empirical at the time of its proposal, was suggested by Freundlich. The Langmuir isotherm assumes the product $f_a \cdot e^{q/RT}$ to be constant at all values of Θ where f_a is the complete partition function of adsorbed molecules, q is the heat of adsorption, T the temperature and R the gas constant. Since the separate quantities f_a and $e^{q/RT}$ are not likely to vary to an equal but opposite extent with Θ, this implies that both f_a and q must be constant. The Freundlich isotherm, however, assumes that q decreases logarithmically as Θ increases.

This gradual decrease in the heat of adsorption is ascribed to the variation in the activity of the surface sites, the most active being occupied first. The Freundlich isotherm may be in the form $v = c\, p^{1/n}$, where v is the volume of gas adsorbed, c and n are constants at a given temperature, the former depending on some properties of the adsorbent, like the surface area, while the latter is characteristic of the particular gases being adsorbed, its value always being greater than unity.

The Temkin Isotherm

Of the two isotherms considered so far, that of Freundlich is likely to be more widely obeyed than the Langmuir isotherm, because heats of chemisorption normally fall with increasing in surface coverage. However, relatively few experimental q - Θ curves are logarithmic in form, and for this reason the Freundlich isotherm is in many cases only an approximation to the truth. Very often, the heat decreases approximately linearly with Θ, and it is with this type of behaviour that the Temkin isotherm is concerned. The isotherm is in fact derived by inserting in to the Langmuir isotherm the condition that the heat of adsorption decreases linearly with Θ. Such a decrease can arise either on a uniform surface due to repulsive forces, or from surface heterogeneity.

The Temkin isotherm is characterised by a linear variation of lnp with Θ and can be represented as $\Theta = \frac{RT}{q_o \alpha} \ln A_o p$, where α is a constant, q_o is the heat of adsorption at $\Theta = o$ and $A_o = a_o e^{q_o/RT}$, which is independent of Θ.

Based on the above mentioned three isotherms a number of methods are in use for the derivation of rate equations. Amongst these the Langmuir-Hinshelwood, Hougen-Watson and Temkin methods are probably the best known

The Langmuir-Hinshelwood Method

The Langmuir-Hinshelwood method has in many cases given a good qualitative, and sometimes also a quantitative interpretation of experimental data by employing an assumed reaction mechanism. Consider a reaction of the type

$$A + B = R + S \tag{2.2}$$

This is studied by measuring the conversion at different partial pressures p_A while the other partial pressures are kept constant. If a low conversion is chosen the consumed and produced amounts of A, B, R and S are so small that only slight corrections have to be made to the initial pressures p_A, p_B, p_R and p_S. When reversible reactions are studied it is usually convenient to choose pressure conditions such that the backward reaction can be neglected. The same measurements are performed with the other gas components and finally the rate can be expressed as a function of all reactants and products involved, i.e.

$$r_f = f\left[(p_A), (p_B), (p_R), (p_S)\right] \tag{2.3}$$

This function can then after closer inspection of the constant pressure terms involved be written in the form of a rate equation. The backward rate r_b is also evaluated in the same manner as r_f and the net rate then becomes $r = r_f - r_b$.

Assume for instance (100) that, experimental data could have resulted in the expression

$$r_f = f\left[(p_A), (p_B/(b + K_B\, p_B)), (1/(c + K_R\, p_R)), (p_S)\right] \tag{2.4}$$

and that closer examination of the constants b and c revealed the relationships $b = 1 + K_R\, p_R$ and $c = 1 + K_B\, p_B$. The rate equation can then be formulated as

$$r_f = \frac{k\, p_A\, p_B}{1 + K_B\, p_B + K_R\, p_R} \tag{2.5}$$

Equation (2.5) should describe the reaction rate not only for the experimental conditions used in the derivation of (2.5) but also give the rate of the forward reaction under actual condition when the reactants are converted simultaneously. Equation (2.5) can be accounted for by assuming the collision between gaseous A and absorbed B as the rate determining step, the product R diminishing the rate by partly covering the active surface.

The Hougen-Watson Method

An extension of the Langmuir-Hinshelwood approach has been developed by HOUGEN and WATSON (49) and HOUGEN and YANG (111) and this method is often been used for the kinetic investigation of technical processes.

The Hougen-Watson method uses an elegant formal way of expressing the chemisorption of a gas on the active catalyst surface and together with other simplifications it is possible to derive the rate equation for every possible reaction mechanism with a minimum of calculations.

The Hougen-Watson technique can, for instance, be used to derive the rate equation for the mechanism of the before mentioned example (equations 2.4 and 2.5). The first reaction step is assumed to be the collision of A from the gas-phase with B adsorbed on the surface. The products formed are adsorbed R and S in the gas phase. If the adsorptions of B and R are fast in comparison with the first step, they can be treated as adsorption equilibria and the first step becomes rate determining. The rate of the reversed reaction is then the collision of S with adsorbed R.

The concentrations of the adsorbed particles are represented by c_B and c_R, the concentration of free active centres by c_1 and the total concentration of active centres by L. The chemisorption can then be written as a chemical reaction between a gas particle and an active centre 1. In this case

$$B + 1 = B1 \tag{2.6}$$

$$R + 1 = R1 \tag{2.7}$$

$$A + B1 = R1 + S \tag{2.8}$$

where the last expression (2.8) constitutes the rate determining step. The rate, the adsorption equilibria and the surface-concentrations can now be written as

$$r = k_1 p_A c_B - k_2 p_S c_R \tag{2.9}$$

$$K_R = \frac{c_R}{p_R c_1} \tag{2.10}$$

$$K_B = \frac{c_B}{p_B c_1} \tag{2.11}$$

$$L = c_1 + c_B + c_R \tag{2.12}$$

The elimination of the unknown surface concentrations gives the rate equation expressed in measurable partial pressures

$$r = \frac{k_1 K_B \left(p_A p_B - \frac{1}{K} p_R p_S\right)}{1 + K_B p_B + K_R p_R} \tag{2.13}$$

where K is the equilibrium constant for the reaction. For the forward reaction this expression is identical with the one (2.5) in the foregoing example. However, this rate equation could have been written directly with the help of formula tables which have been constructed by HOUGEN and YANG (111).

The formal ease with which the different rate equations can be derived has often influenced the experimental approach when the Hougen-Watson method is used. The calculations involved have been discussed in detail by CORRIGAN (24).

The Temkin Method

In their derivation in 1940 of the rate equation for the ammonia synthesis, TEMKIN and PYZHEV (35) started with a non-ideal adsorption isotherm assuming a linear decrease in the heat of adsorption with coverage of the surface. The mechanism was considered to be

$$N_2 \rightleftharpoons N_2\text{-ads} \tag{2.14}$$

$$3H_2 + N_2\text{-ads} \rightleftharpoons 2NH_3 \tag{2.15}$$

The adsorption of nitrogen (2.14) is taken as rate determining and reaction (2.15) is assumed to be in equilibrium. The rate of the slow reaction is now the difference between the rates of adsorption and desorption, i.e.

$$r = k_a p_{N_2} e^{-g\Theta} - k_d e^{h\Theta} \tag{2.16}$$

where g, h, k_a and k_d are constants. The adsorption isotherm in this case has the form

$$\Theta = \frac{1}{g+h} \ln a_o p_{N_2} \tag{2.17}$$

The equilibrium (2.15) gives

$$P^*_{N_2} \equiv (N_2\text{-ads}) = K_N \frac{(p_{NH_3})^2}{(p_{H_2})^3} \tag{2.18}$$

where $P^*_{N_2}$ is the fictitious pressure that gives the equivalent N_2 adsorption. If this "pressure" or fugacity is taken as in equilibrium with Θ and is substituted into the adsorption isotherm and then Θ is eliminated from the rate equation the final equation becomes (35)

$$r = k_1 p_{N_2} \left[\frac{(p_{H2})^3}{(p_{NH3})^2}\right]^{\alpha} - k_2 \left[\frac{(p_{NH3})^2}{(p_{H_2})^3}\right]^{1-\alpha} \tag{2.19}$$

where $\alpha = \frac{g}{f}$

Discussion of the Rate Derivation Methods

The Langmuir-Hinshelwood and Hougen-Watson methods have been critically discussed by WELLER (109) and BOUDART (17) and the use of Hougen-Watson method in technical investigations has been questioned. Weller points out that the Langmuir adsorption isotherm, which is the basis of both methods, has been derived on the assumption of a constant heat of adsorption which is independent of surface coverage. Experiments however always give a heat of adsorption decreasing with increasing coverage. This interaction of adsorbed molecules or atoms has also been observed when several gases are adsorbed simultaneously.

Furthermore the adsorption of one gas can sometimes increase the degree of adsorption of another gas. If the adsorption of A increases when B also is adsorbed the amount of adsorbed A, c_A, can according to Weller be expressed in the following form:

$$c_A = \frac{k\, p_A}{(1 + K_A\, p_A - K_B\, p_B)} \qquad (2.20)$$

This expression has a negative adsorption constant which in the Hougen-Watson method was a characteristic mark of physical unsound rate equations which therefore were ruled out.

According to Weller the Langmuir-Hinshelwood method should be used with care and then for qualitative considerations only. He states further that the Hougen-Watson method should really be considered primarily as an empirical technique of data fitting and a mechanism deduced by this method should be regarded with caution.

Instead he recommended the use of exponential expressions of the form $r = k\,(p_A)^m\,(p_B)^n\,(p_R)^u$ ..... where the exponents have integral or

half-integral valves or zero. Weller demonstrates on several investigations described in the literature how a simple exponential expression with only one constant gives the same data fittings as complicated Hougen-Watson expressions with up to four constants. Rate equations of the simple exponential form can therefore with advantage be used for technical calculations.

The real difference between Weller's exponential expressions and the Langmuir-Hinshelwood and Hougen-Watson expressions is, however, not so large (100). It is a matter of choice of the adsorption isotherm. Weller uses indirectly the Freundlich isotherm and the other expressions are based on Langmuir.

BOUDART (17) shows that the good agreement shown by Langmuir's isotherm when applied to non ideal surfaces can be explained by the broad energy distribution of the active centres and also by the possible mathematical approximation

$$\Theta_F = k\, p^n \approx \Theta_L = \frac{bp}{(1 + bp)} \qquad (2.21)$$

This means that the purely empirical Freundlich isothern, Θ_F with an exponantial distribution of the heat of adsorption can always be approximated by an expression Θ_L of the same mathematical form as the Langmuir isotherm. This is of course the reason why Weller can fit his simple one-constant expressions with about the same deviations as those found with the Hougen-Watson method.

Some rate equations which are believed to be uniquely expressed in the exponential form must by the same argument be derivable from the Langmuir isotherm and Boudart shows how this can be done for Temkin-Pyzhev rate equation for the ammonia synthesis.

TEMKIN (102) has shown that the expression (2.19) could also be derived using the Freundlich isotherm and Boudart (17) demonstrated that the Temkin equation could be obtained by means of Langmuir-Hinshelwood type of argument.

Using the formal Hougen-Watson method of derivation and assuming the slow step to be $N_2 + 2l = 2\,Nl$ the rate equation can be shown to be (100)

$$r = \frac{k\,L^2\left[p_{N_2}\,(p_{H_2})^3 - (p_{NH_3})^2/K\right]}{\left[(p_{H_2})^{1.5} + K_{N_2}^{0.5}\,p_{NH_3}\right]^2} \qquad (2.22)$$

with the approximation $kx/(1 + kx) \approx a\,x^{1-\alpha}$ and with $x = K_N^{0.5}(p_{NH_3})/(p_{H_2})^{1.5}$ the equation above is transformed into the Temkin equation.

These different ways of deriving the Temkin rate equation have demonstrated that rate equations seem to be quite insensitive to the choice of adsorption isotherm. The exponential form of rate equations may be easier to fit to the experimental data, but the Langmuir form has the advantage of covering the whole pressure range.

To sum up it can be said the Langmuir isotherm although strictly valid only for ideal surfaces, nevertheless can be used with advantage for the derivation of rate equations. It must be stressed, however, that the constants involved are not real adsorption constants but rather a kind of average parameters for the different areas contained in a heterogeneous surface. These parameters do not describe the real nature of the variation in the heat of adsorption, which may be due to surface heterogeneity, interaction between adsorbed particles or to some form of electron effects of the bulk of the catalyst.

From this discussion it is also apparent that there is no real disadvantage in using the simplest available correlating rate expression which satisfactorily represents the data.

2.2.3 PORE DIFFUSION RESISTANCE CONTROLS

From the previous discussion it can be seen that diffusion through the gas film and surface reaction steps are in a series relationship to each other; however the pore diffusion step cannot be related in any simple way to the other steps. In consequence film and surface reaction resistances can be treated separately in turn, whereas the pore diffusion resistance can never be treated independently. LEVENSPIEL (66) has dealt very fully with this problem. The effect of pore diffusion on the rate of reaction can be accounted for by a separate correction factor $\mathcal{E}$, called the effectiveness factor and is defined as

$$\mathcal{E} = \frac{\text{(average reaction rate within pore)}}{\text{(maximum reaction rate if pore diffusion is absent)}}$$

This factor $\mathcal{E}$ involves not only a diffusion term but a surface reaction term as well in the form of the rate constant. Thus pore diffusion can never become controlling in the sense that it alone will determine the rate of reaction.

The experimental design of kinetic investigations is considered in Chapter 4.

Chapter 3 SURVEY OF PREVIOUS WORK

The water-gas shift reaction ($CO + H_2O = CO_2 + H_2$) was first observed by Thaddeus Lowe, an american in 1870, and the first commercial use of this reaction over an iron oxide catalyst was made by the Badische Anilin und Soda Fabric of Germany to produce hydrogen for the Haber ammonia synthesis. Due to the growing industrial importance of the shift reaction a good deal of work have been carried out to investigate the equilibrium relationships, catalytic activities and the kinetic behaviour of a number of materials under different operating conditions.

3.1 EQUILIBRIUM STUDIES

As early as 1909, HABER (39) experimentally obtained values of the equilibrium constant K for the water-gas shift reaction between 200° to 600°C, by the application of the law of mass action. Tabulated values of K for different temperatures are available from many sources (78, 90, 91, 92, 99, 104) but, for the purpose of developing rate equations, it is convenient to have a functional relationship for the equilibrium constant.

A sufficiently accurate equation given by MOE (72), is applicable to the range of temperatures encountered in using iron base shift catalysts (600° - 900°F) is

$$K = \exp. \left(\frac{8240}{T} - 4.33\right) \qquad (3.1)$$

where T is in °Rankine.

For the temperature range of 700° to 900°K KASSEL (55) has given the relationship of the form:

$$\log K = \frac{1914}{T} - 1.782 \qquad (3.2)$$

where T is in °K.

ANOKHIN, TRAKER and MUKHLENOV (1) have suggested an equation of the form:

$$\ln K_p = \frac{2203}{T} + 5.16 \times 10^{-5} T + 2.54 \times 10^{-7} T^2 - 7.46 \times 10^{-11} T^3 - 2.3 \quad (3.3)$$

where T is in ^{o}K. The differences between the "K" values obtained by the three equations given above are not large however this will be discussed in Chapter 7.

At high pressures the partial pressure of the reactant gas is not a true measure of its active mass and hence, even in gaseous systems in which reactions take place with no change in total volume, the value of the equilibrium constant K_p shows a drift with progressive changes in total pressure. The effects of pressure upon the equilibrium constants for the water-gas shift reaction were studied by SARTORI and NEWITT (95) up to 100 atm., by PARATELLA (82) up to 200 atm., by FAUSER (37) up to 250 atm., by SORGATO and ANGELIN (98) up to 300 atm., and by DODGE (32) up to 2000 atm. Dodge has shown that at P = 2000 atm. and t = 400°C, the constant K_p decreases from a value of 11.62 to 4.3.

3.2 WORK ON IRON OXIDE BASED CATALYSTS

Iron oxide by itself or in combination with other inorganic materials has been used extensively in commercial operations, because of its physical properties and because of the fact that most iron oxide base catalysts are not susceptable to sulphur poisoning (18). Natural iron ores, roasted sulphide ores and waste oxides, hydroxides and carbonates of iron were used for many years although all these catalysts had low activities.

In view of this most of the emphasis in the survey will be placed on this type of catalyst although in section 3.3 a brief review will deal with other materials. The first commercial chromia promoted iron oxide catalyst was patented by JOHNSON (53) in 1913.

3.2.1 KINETIC STUDIES

A great deal of work has been done in this field and as will be seen results are often contradictory. ~~A table summarising results so far will be found in Chapter 7.~~

BELONOGOV and POPOV (9) studied the kinetics of the shift reaction on an iron oxide catalyst between 300° to 400°C and observed that a kinetic equation of the 1st order satisfactorily represented the data when any of the reaction products are absent in the inlet mixture.

The kinetics of the shift reaction was investigated by BOHLBRO (11) at atmospheric pressure over a commercial iron oxide - chromium oxide catalyst in the temperature range 330° to 500°C. 3.0 and 12.0 gms of catalyst with particle size between 0.8 to 1.2 mm. were used in the experiment and the feed rate was 2.4 gm. mols/hr. with wide variation of composition (CO, H_2O, CO_2, H_2). The experimental data were fitted with an exponential type of rate equation. The forward rate is represented by $r_f = k\,(CO)^l(H_2O)^m(CO_2)^n$, where (CO), ($H_2O$), ($CO_2$) are partial pressures of CO, H_2O and CO_2 respectively. The rate was observed independent of H_2 partial pressure. The exponents l, m and n varied only slightly with temperature and were situated within the following ranges, l = 0.80 to 1.00, m = 0.20 to 0.35, and n = -0.65 to -0.50. By application of an average rate expression for the whole temperature range the apparent energy of activation was found to be 27.4K.cal/mole.

Further work of BOHLBRO (14) dealt with a comparison of the kinetic expressions obtained with laboratory-prepared catalysts with and without alkali present in minor quantities. Quite substantial influences of the alkali on the kinetic expression were found. It was further observed that CO_2 concentrations above a certain limit produced a relatively slow decrease of activity of the alkali-impregnated catalysts, the effect being dependent on the

temperature of drying of the catalyst prior to the impregnation. The results are given in the following table:

Table 3.1 Values of exponents of (CO), (H_2O), (CO_2) and (H_2) with different catalysts at 380°C.

Catalysts	exponent of (CO)	exponent of (H_2O)	exponent of (CO_2)	exponent of (H_2)
Catalyst A (alkali free)	0.75	0.30	-0.35	-0.05
Catalyst E (1.9% NaOH) (low CO_2 range)	1.35	-0.15	-0.40	0.00
Commercial Catalyst (Ref. 11)	1.00	0.25	-0.60	0.00

In his discussion Bohlbro pointed out that the rate of catalyst E was more than proportional to the partial pressure of the reducing agent CO as well as negatively influenced by an increase of the partial pressure of the oxidizing agent H_2O might indicate that the activity of the catalyst E was dependent on the state of oxidation of the surface layer and that the lower state of oxidation was a more active catalyst than the higher state of oxidation. Another hypothesis to explain the fact that exponent of CO became greater than one in the presence of alkali was the assumption that some rate-determining steps involved a compound containing more than one CO group (8).

HEINZE and REINACKER (42) studied the kinetics of the water-gas shift reaction on iron oxide and iron oxide-chromium oxide catalysts. The catalysts were prepared by thermally decomposing the respective nitrates. With Fe_3O_4 as catalyst the conversion was found to be 1st order reaction with respect to the CO concentration and zero order with respect to the H_2O content (up to 300°C).

Addition of varying amount of Cr_2O_3 to Fe_3O_4 did not show any definite change to catalytic effect.)

The principles of statistical design (27, 103) were used by HULBURT and SRINI VASAN (50) to elucidate the reaction mechanism of the shift reaction. Instantaneous reaction rates "r" (for 25% conversion it was defined as $r = \frac{(p_{CO})_{20} - (p_{CO})_{30}}{t_{20} - t_{30}}$, where $(p_{CO})_{20}$ and $(p_{CO})_{30}$ are the partial pressures of CO in the exit gases at which 20% and 30% of the feed CO were converted respectively. The contact times at 20% and 30% conversion are given as t_{20} and t_{30} respectively.) were determined for sixteen different combinations of the following five variables: partial pressures of carbon monoxide, water, carbon dioxide, hydrogen and temperature. Nitrogen gas was used as an innert diluent to make up the total pressure to 1 atm. The statistical factorial design method was used after assuming an exponential type of rate equation for the forward reaction. The analysis of variance of the data showed strong effect from T with weaker effects from p_{H_2} and amongst interactions T x p_{H2} was quite strong with weaker effects from $p_{H_2} \times p_{H_2O}$ and T x p_{H_2O}. The interactions with temperature suggested a different kinetic model with more than one temperature dependent rate constants. Experimental data were finally correlated with the help of Hougen-Watson approach by assuming the surface oxidation by H_2O step as rate controlling. The final correlated form is given by

$$r = \frac{0.2107 p_{H_2O}}{1 + 1.063 \frac{p_{H_2O}}{p_{H_2}}} \qquad (3.4)$$

The above observations and the rate equation are of course applicable in the range of variables covered (in this case the change in composition was

very small) with 20 to 30% conversion, atmospheric pressure, 310° to 340°C. In the work of KIRILLOV (57) an inactivated Fe_2O_3 and a Fe_2O_3 activated at low temperature were used as catalysts. An equation was developed for the velocity of the reaction which was in good agreement with the experimental data (300° to 380°C).

$$\frac{d\,p_{CO}}{dt} = k_f\, p_{H_2O} \left[\frac{p_{CO}}{p_{CO_2}}\right]^{0.5} - k_b\, p_{H_2} \left[\frac{p_{CO_2}}{p_{CO}}\right]^{0.5} \qquad (3.5)$$

The activation energies obtained were 17.5 K cal/mole at 300° - 380°C and 37.6 K cal/mole at 280° to 300°C.

KODAMA, FUKUI, TAME and KINOSHITA (58) used Fe_2O_3 with 10% Cr_2O_3 as catalyst. The work was carried out with mixtures of CO and steam (1:1, 1:2 and 1:3) only at 1 atm. between 350° to 450°C. A rate equation was derived on the assumption that the process consisted simply of bimolecular reaction between CO and H_2O in which the surface sites of Fe_3O_4 acted as an oxygen supplier. The equation was of the form:

$$-\frac{d\,[CO]}{dt} = \frac{k\,(\,[CO]\,[H_2O] - K\,[H_2]\,[CO_2]\,)}{(\,[CO_2] + E\,[H_2O]\,)} \qquad (3.5a)$$

where [ ] represents concentration and E is an empirical constant. The work on an industrial catalyst by KODAMA, MAZUME, FUKUBA and FUKUI (59) showed that the values of k were fairly constant over the contact time range 0.1 to 0.8×10^{-3} hr. and various inlet gas compositions at 350°C. At 400°C, k varied somewhat with the concentration of CO in the feed, which was attributed to the catalytic decomposition of CO. With relatively small [CO] in the feed, however, the dependence was negligible.

KULKOVA and TEMKIN (62) studied in detail the kinetic behaviour of the shift reaction over a pure iron oxide and an iron oxide based composite catalysts. X-ray investigation of the sample of iron oxide catalyst showed that γ - Fe_2O_3, in the course of the reaction, transformed itself into magnetic Fe_3O_4 with a low Fe_2O_3 content. Suggested mechanism of the reaction leads to alternate reduction of the catalyst surface by CO and oxidation by water, whereupon the oxygen atoms randomly situated on the surface of the catalysts are regarded as adsorbed. On the basis of the experimental data the limiting phase reaction was considered to be the reciprocation of CO with surface oxygen. The form of the reaction rate expression given below agreed satisfactorily with experimental data.

$$r = k_f p_{CO} \left[\frac{p_{H_2O}}{p_{H_2}} \right]^{0.5} - k_b p_{CO_2} \left[\frac{p_{H_2}}{p_{H_2O}} \right]^{0.5} \qquad (3.6)$$

The activation energies for iron oxide and composite catalysts were obtained as 16.5 K cal/mole and 12.5 K cal/mole respectively. Later KULKOVA, KUZNETS and TEMKIN (61) studied the mechanism of the shift reaction on an iron oxide catalyst by using isotopic oxygen. The result showed that there was an isotopic exchange between the oxygen of the catalyst and that in the reaction mixture.

POPOV (85) used a compressed iron oxide catalyst in the shape of a hollow cylindrical tube through the inner bore of which the reaction mixture was passed (cappillary method). In the 300° - 400°C range, the experimental data were in satisfactory agreement with a rate equation for a reversible monomolecular reaction. The reaction was first order with respect to CO and zero order with respect to H_2O. For the temperature range of 400° to 500°C, the reaction order for H_2O and H_2 found to change. The reaction would be retarded by hydrogen. Later work by LEBEDER and POPOV (65) on an

unactivated iron oxide catalyst at 300°, 400°, 500°C showed that the reaction was zero order with respect to H_2O when it was present in excess of the stoichiometric ratio, and first order with respect to CO. The velocity of the reaction was decreased by CO_2 and was independent of H_2. An equation for the velocity of the reaction was presented which satisfactorily represented the experimental data. The equation stands as

$$\frac{d\,x}{dt} = k_f \frac{1 - x}{1 + a\,(p^o_{CO_2} + x\,p^o_{CO})} \qquad (3.7)$$

where $x = \frac{p^o_{CO} - p_{CO}}{p^o_{CO}}$, p^o_{CO} and $p^o_{CO_2}$ are partial pressures of CO and CO_2 in the initial gaseous mixture, and 'a' is the adsorption coefficient of CO_2. In the early work of POPOV (84), and BELONOGOV and POPOV (9) a simple rate equation of the form:

$$\frac{d\,x}{dt} = k\,(x_m - x) \qquad (3.8)$$

was used, where x is the degree of conversion and x_m is the equilibrium conversion.

In his work MOE (72) used a commercial iron oxide-chromium oxide catalyst ($\frac{1}{4}$ inch diameter x $\frac{1}{4}$ inch long tablets) and developed a rate equation by assuming that the reaction rate was proportional to the displacement of the gas composition from its thermodynamic equilibrium value. The equation for the reaction rate was given as

$$r = k\,(ab - \frac{cd}{K}) \qquad (3.9)$$

where a, b = concentration of reactants

c, d = concentration of products.

The calculated rates as reported showed good agreement with the experimental data (600° to 750°F) and the activation energy obtained was 17,500 Btu/lb. mole.

ATWOOD, ARNOLD and APPEL (6) claimed that their data as well as the data of the other investigators using iron oxide catalyst (64, 81 and 113) could be represented adequately by the simple first order rate equation neglecting possible effects due to the retardation by CO_2 (69). Integration of the equation gave:

$$k_e = 2.303\ V\ (R + 1) \log \frac{1}{1 - CO_t} \qquad (3.10)$$

where

CO_t = (moles of CO converted)/(moles of CO converted at equilibrium).

k_e = isothermal rate constant of the forward reaction.

R = moles of steam per mole of feed gas.

V = volume at normal temperature and pressure of dry gas treated per unit volume of catalyst per hour.

This equation has also been used by MARS (68), MARSH and ROBSON (70), OLIVER and BELA (80) and HOOGSCHAGEN and ZWIETERING (45).

In the studies of R1(86), and PADOVANI and LOTTERI (81), a rate expression was used based on a bimolecular reaction mechanism and is given by

$$\frac{d\,x}{dt} = k_f (1 - x) \left[1 - C_o (1 + x)\right] - k_b C_o\ x^2 \qquad (3.11)$$

where x is the degree of conversion and C_o is the CO concentration in the feed mixture (85). SAKSIN (94) obtained a rate equation of the form:

$$\frac{d\,[CO]}{dt} = k_f\,[H_2O]\,\frac{[CO]^{0.5}}{[CO_2]^{0.5}} \qquad (3.12)$$

where [ ] represent the concentration. Reaction order with respect to H_2 was zero.

ROITER et al (89) studied the shift reaction on a Fe catalyst and obtained the following reaction sequences; $2CO = CO_2 + C$; $C + 2H_2O = CO_2 + 2H_2$. They found that H_2 did not affect the rate of the reaction but that CO_2 retarded it (85).

DEBAUN and ADLER (28) uses the rate equation

$$\frac{d\,(p_{CO})}{dt} = k_f\,p_{CO}p_{H_2O} - k_b\,p_{CO_2}\,p_{H_2} \qquad (3.13)$$

for reactor design purposes with the help of an electronic computer.

STELLING and KRUSENSTIERNA (100) studied the shift reaction on an iron oxide catalyst. By closer inspection of the data the authors suggested the form of rate equation for the forward reaction

$$r_f = k_f\,\frac{p_{CO}\,p_{H_2O}}{p_{CO_2} + K_{H_2O}\,p_{H_2O}} \approx k_f\,p_{CO}\left[\frac{p_{H_2O}}{p_{CO_2}}\right]^n \qquad (3.14)$$

The experimental data indicated that H_2O and CO_2 were strongly adsorbed and that H_2 did not take part in the reaction. The work of MARS (68) has confirmed the above findings (100).

LAUPICHLER (64), in his work, used a large excess of steam and finally derived a rate equation

$$\frac{d\,x}{dt} = k\,\left[H_2O\right]_{\text{average}}\,(x_m - x) \qquad (3.15)$$

where [ ] is the concentration, x is the degree of conversion and x_m is the equilibrium conversion.

3.2.2 STUDIES AT HIGH PRESSURE

The stoichiometric form of the water gas shift reaction indicates that the equilibrium is not significantly influenced by pressure. An increase in operating pressure results in a longer contact time, which should increase the capacity of a given reactor, thus reducing the initial cost of the reactor per unit mass of gas reacted. In 1914 BOSCH and WILD (16) were granted a patent covering the production of hydrogen by the water-gas shift reaction at elevated pressure and it was suggested that pressures of between 4 and 40 atmospheres be employed.

ATWOOD, ARNOLD and APPEL (6) investigated the influence of pressure on the rate of the shift reaction over a commercial iron oxide-chromium oxide catalyst in the pressure of 1 to 30 atmospheres at 655° and 760°F. They observed that activity of the catalyst approximately doubled as the pressure was raised to 10 atmospheres, and increased only slightly as the pressure was further increased. The work of PADOVANI and LOTTERI (81) showed that the activity of a commercial iron oxide catalyst increased to a maximum at 10 to 20 atmospheres, and decreased with further increase in pressure.

A threefold increase in the activity of "brown oxide" catalyst with an increase of operating pressure from 1 to 11 atmospheres has been reported for a pilot plant unit (113). HOLROYD (43) claims that in German commercial practice an eightfold increase in the activity of iron oxide-chromium oxide catalyst was obtained by increasing the operating pressure from 1-25 to 30 atmospheres.

BOHLBRO (12) studied the kinetics of the shift reaction over a commercial iron oxide-chromium oxide catalyst at elevated pressures ($380^{\circ}C$). In conclusion the author said that the results largely confirm the results obtained at atmospheric pressure (11) and further that the same rate equation was valid at total pressure up to about 20 atmospheres.

MOE (72) gives the relation between the increase in activity with increase in pressure which is given in the figure below:

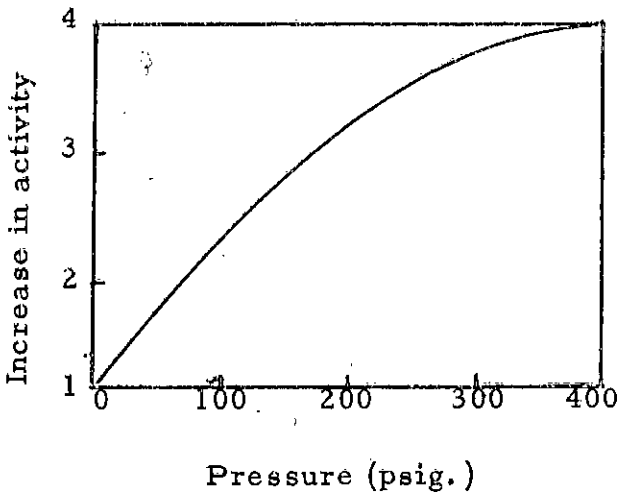

Fig. 3.1 Effect of Pressure on Girdler Shift Catalyst

Almost similar relation is given by the Svenska Salpeterverken of Sweden for their shift catalyst.

The influence of pressure on the activity of catalysts is probably affected by gross particle size, and it is probable that a greater increase in catalyst activity with increasing pressure would be obtained in commercial units than in the small experimental reactors where small particle size catalysts are used.

3.2.3 WORK ON CATALYST POISONING

In practice water-gas contains H_2S as impurity, the amount depending on the source of the feed gas. This H_2S acts as poison to the iron-oxide catalysts. When the H_2S concentration is a few thousand ppm. then there is every possibility that the iron oxide will more or less be transformed into iron sulfide. H_2S concentration less than a thousand ppm. may influence the kinetics by being adsorbed on the active sites.

RI's work (86) showed that when a small amount of H_2S was added to the reaction mixture, the activity of the catalyst (Fe_2O_3 and $Fe_2O_3 + Cr_2O_3$) decreased and stayed at a definite value (400° - 500°C), but when a pure gas mixture was led through the catalytic chamber, the reactivity gradually returned to the original value. This observation has been confirmed by EVANS and NEWTON (36). BRIDGER, GARNES and THOMPSON (18) reported that though some additives like boron and phosphorous reduces the activity of an iron oxide catalyst, surphur compounds do not have much effect on it.

BOHLBRO (13) studied the effect of H_2S on the kinetic behaviour of the shift reaction over a commercial iron oxide-chromium oxide catalyst at 380°C. The results showed that with the presence of H_2S, the strong retarding influence of CO_2 previously found (11) was considerably decreased and a small retarding effect of H_2 was found. The H_2O exponent was increased but that of CO was decreased in the presence of H_2S.

MARSH and ROBSON (70) studied a different type of iron oxide catalyst poisoning (a better term is catalyst fouling). They used Power-Gas, I.C.I. and Girdler iron oxide based commercial catalysts to remove CO from carburatted water-gas. The presence of butadine or cyclo-pentadiene along with acetylene, nitric oxide and oxygen was found to cause fouling.

Use of nickel subsulphide guard prevented any loss of shift catalyst activity.

3.2.4 MASS TRANSFER STUDIES

The fact that mass transfer processes could retard the reaction rate has been noted in a number of papers. BELONOGOV and POPOV (9) investigated the role of diffusion processes in the shift reaction on an iron oxide catalyst and observed that at 300° to 400°C, the CO conversion could be satisfactorily described by a kinetic equation of the 1st order if other reaction products were absent, but at higher temperatures a deviation from the equation was noted. The inhibition of the reaction at 400°C for the particular catalyst studied did not go beyond 10% and the authors considered it to be caused by an insufficient supply of the reactants to the catalyst surface (external diffusion). They also observed that the diffusion to the internal surface of the catalyst was greatly inhibited above 350°C. POPOV (84, 85) studied mass transfer by using a capillary method (10), the essence of which was that the catalysts were arranged in the shape of a hollow cylindrical tube through the inner bore of which the reaction mixture was passed. Samples were withdrawn for analysis at varying positions along the length of the capillary tube, and a process rate constant taking into account the effect of mass transfer was calculated. It was observed that the degree of utilisation of the internal catalyst surface was close to 100% for granules less than 3 mm. in diameter over the 300° to 400°C range, i.e. diffusional retardation was absent. Above 400°C for granules with diameter larger than 2 mm. the degree of utilisation of internal surface was significantly less than 100%.

LAUPICHLER (64), in his work, did derive equations for both mass transfer rate and reaction rate for the shift reaction (450°-570°C). Under the conditions of the tests (3000 to 5000 cubic meters per hour) the diffusion

resistance was found to be negligible in comparison with the chemical resistance, and considered that in industrial practice mass transfer would usually play a minor role.

MOE (72) and ATWOOD, ARNOLD and APPEL (6) have reported that the size of the catalyst particles has quite an influence on the rate of reaction.

BOKHOVEN and HOOGSCHAGEN (15) studied the diffusion in Fe_2O_3 - Cr_2O_3 shift catalyst (tablets crushed down to 2.8 to 3.4 mm. size). The activity line at atmospheric pressure showed a bend near 350°C. Correction with observed value of $D_{eff}/D_{gas} = 0.054$ did yield a straight line for the true activity between 275° and 450°C, where D is diffusion co-efficient.

3.2.5 REVERSE SHIFT REACTION

In the present work conditions were arranged to make the reverse reaction ($CO_2 + H_2 \longrightarrow CO + H_2O$) of small importance. Nevertheless it is felt that a brief discussion of some work done on this reaction might be of value.

DOEHLEMAN (32a) examined the reverse shift reaction over iron foil at 910°C and atmospheric pressure, and postulated a reaction mechanism in which the iron functioned as a "carrier" of oxygen. The final form of the rate equation derived by him, considering the step $CO_{2_{gas}} = CO_{gas} + O_{ads}$ rate controlling, can be represented by

$$\frac{d\,p_{CO_2}}{dt} = k_f\, p_{CO_2} - k_b\, \frac{p_{CO}\, p_{H_2O}}{p_{H_2}} \qquad (3.16)$$

Experimental data also showed that the forward reaction rate also increased with increasing pressure of hydrogen.

BARKLEY and co-workers (7) used a commercial copper oxide promoted iron oxide catalyst (cylindrical pellets - 3 mm. diameter and 1.75 mm. in length) to study the reverse shift reaction (1000°F). The rate equation obtained was:

$$r = \frac{k\left(p_{CO_2} p_{H_2} - \frac{p_{CO} p_{H_2O}}{K}\right)}{\left(1 + K_{CO_2} p_{CO_2} + K_{CO} p_{CO}\right)} \qquad (3.17)$$

NAKANISHI and TAMARU (76) studied the reverse shift reaction on an iron oxide 79% and chromium oxide 5.3% (with SiO_2, CaO, K_2O and Al_2O_3) catalyst. The catalyst size was 20-50 mesh. The reaction was carried out in a chromatographic column where the catalyst is used as a adsorbing material. It was shown that the properties of the catalyst surface in the working state underwent appreciable changes, depending upon the composition of the reacting gas (alternate oxidation and reduction). It was suggested that the reaction rate was proportional to the reduction of oxide surface with hydrogen.

3.2.6 MISCELLANEOUS WORK

Some of the work done on the water-gas shift reaction does not fall readily into a convenient classification and will therefore be mentioned in the present section.

ATWOOD and ARNOLD (5) studied the effect of added constituents on the activity of an iron oxide-chromium oxide shift catalyst. No promoters out of 33 elements were found. The majority of the additives had no

significant effect on the initial catalyst activity whilst boron and phosphorous reduced activity to a considerable extent. CHRISTAIN and BOYD (22) compared five commercial iron oxide based catalysts on the basis of activity and durability.

A catalyst with 74% Fe_2O_3 and 10% Cr_2O_3 gave the highest activity and did not dust or spall. The conclusion was drawn that the method of manufacture had a considerable influence on the activity of a catalyst, and is the major factor in determining the physical properties.

MARS (68) investigated the factors governing the behaviour of the adiabatic water-gas shift reactor using an iron oxide catalyst. The temperature profile was calculated on the basis of laboratory measurements with the aid of a computer. The laboratory data used comprise: the intrinsic activity of the catalyst, the effect of sintering, the influence of diffusion in the catalyst pores and the poisoning effect of hydrogen sulphide. The influence of mass transfer to the surface of the pellets was neglected. The results agreed on the whole with that found in practice but further work was advocated. The influence of the activity of the catalyst and of the particle size on the temperature profile and on the conversion was also calculated. MOE (72) has given the relation for temperature rise ($^{\circ}F$) in an adiabatic reactor and is given with sufficient accuracy by the simple relation:

$$\text{moles CO converted} = \frac{\left(9 \frac{\text{steam}}{\text{gas ratio}} + 7\right) \Delta t}{164} \qquad (3.18)$$

The relationship is based on 100 moles of dry gas entering the reactor.

If a porous catalysts possessing a large internal surface area is kept at a sufficiently high temperature, the surface area will gradually diminish due to sintering. HOOGSCHAGEN and ZWIETERING (45) studied the sintering phenomena of the shift catalyst (Fe_2O_3 - Cr_2O_3) quantitatively and found that the decrease in surface area could be correlated by the following equation

$$\frac{1}{A^n} - \frac{1}{A_o^n} = K\, t \exp(-E/RT) \qquad (3.19)$$

where:

A = surface area.

A_o = original surface area.

t = time.

n = experimentally determined constant.

The constant n, as reported, varied with the method of preparation and decreased with an increase in the chromium content of the catalyst. This observation suggested that the chromia serves to stabilise the surface area, since chromia alone has very slight activity for the shift reaction.

RI (86) studied several iron oxide based shift catalysts at 400° to 500°C. The activation energy calculated from integrated form of the Arrhenius equation ($\frac{d \ln k}{dt} = \frac{E}{RT^2}$) was 5100 cal. and was the smallest when the catalyst of Fe_2O_3 containing 7% of Cr_2O_3 was used, hence the catalyst was most powerful.

A study on the optimisation of the water-gas shift reaction on a commercial (I.C.I.) Fe_2O_3 - Cr_2O_3 catalyst has recently been carried out by RIPPIN and KISIEL (88).

Information on the removal of undesirable CO from gaseous mixtures with the help of shift reaction in presence of iron oxide catalyst may be obtained in the following literature (19, 20, 21, 25, 54, 70, 71, 74, 75, 79, 96).

3.3 WORK ON OTHER OXIDE CATALYSTS

Some of the metallic oxides other than Fe_2O_3 show considerable activity for the water-gas shift reaction at a low temperature range but most of them generally lack the other qualities needed for a commercial catalyst. So far Girdler G66, a copper based catalyst, is the only "low temperature" commercial catalyst available in the market, and has in fact been studied in the present work.

EVANS and NEWTON (36) measured the activity of precipitated oxides. Cobalt oxide had the highest activity in the absence of surphur compounds, iron oxide was next in activity, followed by chromium oxide. Oxides of manganese, nickel, copper, uranium, titanium, tungsten and vanadium gave little shift conversion at 450°C and a throughput of 1000 $hr.^{-1}$.

WHITE and SCHULTZ (110) studied fused cobalt oxide catalysts containing promoters added to prevent methane synthesis from occurring simultaneously with the shift conversion. The catalysts were made by fusing the nitrates together in an oxy-hydrogen flame, and were activated by reducing in hydrogen at 310°C. On these catalysts, shift conversion was brought to near equilibrium even at 283°C. Chromia promoter improved the activity and reduced the amount of methane synthesis. Iron oxide promoter also reduced the amount of methane formation. The best catalyst, which gave no methane, contained 42.1% cobalt and 37.7% of copper. Copper oxide alone was even more active, but treated gas contained about 0.5% of methane. Rate constants for the shift conversion on these catalysts at 310°C were about 15 times greater than those on iron oxide-chromia. Sulphur free gas was used in this work.

STORCH and PINKEL (101), in their study, improved the method of making cobalt-copper catalyst mentioned above (110). They discovered that if a mixture of cobalt carbonate and small amount of copper oxide (5 to 15%) is heated rapidly (in about 3 minutes) from room temperature to between 900° and 1100°C, a sintered mass of granules is obtained. The product had excellent mechanical properties that permit prolonged use without appreciable spalling. It was also a very active catalyst when properly reduced and subsequently protected from surphur poisoning. Lost activity due to poisoning could be readily regenerated by heating to 900°C and passing a stream of air over it. Subsequent reduction and use with water-gas-steam mixture yielded an activity identical with the original catalyst.

B.P.M. in the Netherlands devised a copper catalyst made initially by co-precipitation from a solution containing equimoler concentrations of copper, magnesium and aluminium nitrates, using caustic soda solution. This catalyst covered by British patents 609, 166 and 638, 340 was said to be active at 260°C and to have some resistance to poisoning by sulphur compounds.

FUKUDOME and KUSANO (38) tested ferrites made by a dry method at above 1000°C as a shift catalyst. Activity was poor in most cases, but at 300°C the cobalt ferrite gave 90% conversion; nickel ferrite, the next most active, gave 10% conversion.

RIGAMONTI and AGLIARDI (87) studied the kinetics of the shift conversion on zine oxide made by decomposing the basic carbonates. Shift equilibrium was approached in the range 270° to 440°C. The rate was independent of H_2O vapour, but depended on the concentration of CO. The apparent order of the reaction with respect to the latter was between 0.5 to 1. The apparent energy of activation varied markedly with the temperature within the experimental range, diminishing with the rising temperature.

The catalytic action of MgO and ZnO on the shift reaction was studied by NATTA and RIGAMONTI (77). ZnO was much more effective than MgO as a catalyst. Addition of K_2CO_3 increased the percentage conversion at 363°C from a value of 58.5% with ZnO to 93% with K_2CO_3, while 5% Na_2CO_3 raised the percentage conversion only to 78%.

IVANOVSKII et al (52) investigated mixtures of co-precipitated oxides of zine, chromium and copper as shift catalysts. The most active mixture was $ZnO:Cr_2O_3:0.5CuO$. The catalyst must be activated at 250° to 300°C; it was then said to be highly active even at 175°C.

ATROSHENKO and IVANOVA (4) used $ZnO.Cr_2O_3$ in the form of 2 to 3 mm. grains as catalyst. The temperature varied from 300° to 450°C, and the pressure from 1 to 16 atmospheres. The reaction was found to be of 1st order in respect to CO and the calculated energy of activation to be 15 K cal/gm.mol. The rate was thought to be controlled by the rate of reaction of CO with oxygen layer on the catalyst surface. Some experiments with a more finely ground catalyst (1-2 mm.) had shown that the size of the grains had no effect on the rate of conversion and implied that the reaction was not inhibited by the diffusion processes.

ATROSHCHENKO and BIBR (3) studied the kinetics of the shift reaction at high pressures (6-21 atm.) on a catalyst containing MgO-61%, Cr_2O_3-2.5%, Fe_2O_3 - 30%, Al_2O_3-1.5% and K_2O-1% (578°-820°C). The rate equation obtained was

$$\frac{d\,p_{CO}}{d\tau} = k\,\frac{(p_{CO} - p^{*}_{CO})}{p_{H_2}}\,(p_{H_2O})^{0.5} \qquad (3.20)$$

where τ is the contact time and p^{*}_{CO} is the partial pressure of CO at equilibrium.

ROITER et al (89) reported a study of the shift reaction between 400° and 500°C over K - carbon catalyst. Results were explained by the reaction scheme: $2\,KOH + CO = K_2CO_3 + H_2$; $K_2CO_3 + H_2O = 2\,KOH + CO_2$. ROYEN and EHRHARD (93) studied the effect of alkali soaked activated carbon. The mechanism as presented follow the pattern:

$$K_2CO_3 + 2\,CO + H_2O = 2KOOCH + CO_2$$

$$2KOOCH + H_2O = K_2CO_3 + CO_2 + 2H_2$$

ARMSTRONG and HILDITCH (2) studied the shift reaction on pure copper. The assumed mechanism can be given in the following two steps. $CO + H_2O \rightleftharpoons H.COO\,H$ and $H.COO\,H \longrightarrow CO_2 + H_2$. Between 200° to 300°C copper was found more active than iron oxide. The activity somewhat declined after 350°C, and the maximum change affected appeared to be greater the higher the proportion of CO in the feed gas.

Early in 1963 Girdler announced the availability of their G-66 low temperature shift catalyst (112). This is a Zn-Cu-Cr. catalyst and mainly for use in gases containing up to 1 or 2 ppm. of sulphur compounds. Girdler claimed that, by using this catalyst, the initial cost of a typical hydrogen plant (50 million cu. ft. per day) could be reduced to $1 million from $ 4 million for the one using iron oxide-chromia catalyst.

Later MOE (73) published some information about this G-66 catalyst. According to him the rate equation is the same as that for the G-3A $Fe_2O_3 - Cr_2O_3$ commercial catalyst (eqn. 3.9). Based on commercial and extensive laboratory tests, the rate constant is given as:

$$k = \exp\left(15.92 - \frac{7050}{T}\right) \qquad (3.21)$$

where T is in °Rankine.

. The effect of pressure on the activity of G-66 is given in the fig. 3.2.

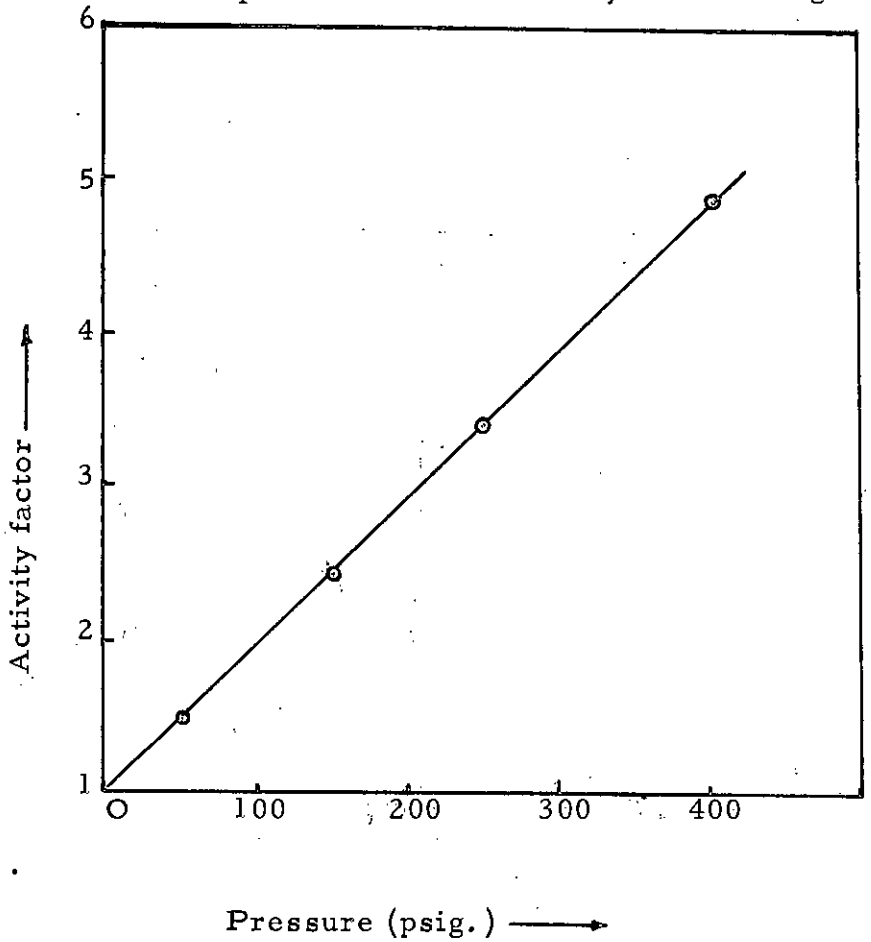

Fig. 3.2 Effect of Pressure on G-66 Catalyst

MOE has also stated that copper chromites exhibited reasonable activity at temperatures as low as 350°F. These compounds had a spinel-type of crystal structure (26, 30) and were not reduced to a simple mixture of the two metals by a water gas mixture.

Chapter 4. DESIGN OF EXPERIMENT

In this chapter methods of investigating the kinetics of heterogeneous reactions are discussed. By necessity the treatment must be brief, but further details are found in the text books (48, 60, 66, 97, 105).

To explore the kinetics of the catalytic reactions any type of reactor usually batch or continuous, may be used. In most cases a steady-state flow reactor is the most convenient to use. The differential equation expressing the rate of disappearance of A at steady state

$$(F_{AO})(dx_A) = (-r_A)\,dV \qquad (4.1)$$

(where F_{AO} is moles of A fed per hr. and dx_A is moles of A reacted per moles of A fed.) has on the left-hand side the dimensions of quantity of A reacted per unit time; hence the right-hand side must have the same dimensions, no matter whether rates are based on unit mass, unit area, or unit volume of solid and voids, or bulk volume of catalyst bed.

A catalytic flow reactor is considered to be a differential reactor if the rate of reaction is the same at all points in the reactor; it is defined as an integral reactor if the rate varies with position in the reactor.

4.1 DIFFERENTIAL REACTOR

As mentioned previously in a differential reactor the rate is assumed constant at some average value throughout the reactor. Since reaction rates are dependent on concentration, the assumption of constant rate is reasonable when composition changes in the experimental reactor are small. A differential reactor is usually visualised to be small, as the name implies; however, this is not necessary because if the rate is slow the change in reactant composition is small, even in a large reactor.

Assuming plug flow rates of reaction in differential reactors are found in a straight forward manner since integration of the design equation becomes quite simple. Thus we have

$$\frac{V}{F_{AO}} = \int_{x_{A,\,in}}^{x_{A,\,out}} \frac{dx_A}{-r_A} = \frac{1}{(-r_A)_{av.}} \int_{x_{A,\,in}}^{x_{A,\,out}} dx_A = \frac{x_{A,\,out} - x_{A,\,in}}{(-r_A)_{av}}$$

$$\text{or} \quad (-r_A)_{av} = \frac{F_{AO}\,(x_{A,\,out} - x_{A,\,in})}{V} \qquad (4.2)$$

In order to investigate the kinetics of a given reaction a number of runs are made giving different average concentrations $C_{A\,ave}$. From these data one obtains $-r_A$ as a function of $C_{A\,ave}$ and hence if the kinetic process is simple the order of the reaction can be obtained.

4.2 INTEGRAL REACTOR

In the integral reactor the reaction rate and the change in composition are so large that these variations are to be considered in the method of analysis. We may follow one of two procedures in searching for a satisfactory rate expression.

In integral analysis a specific mechanism with its corresponding rate equation is put to the test by integrating the rate equation for the reactor flow conditions. A series of runs varying V and/or F_{AO} are obtained in such a manner that a wide range of conversions is obtained. Again assuming plug flow the integrated form of design equation is given by

$$\frac{V}{F_{AO}} = \int_{o}^{x_A} \frac{dx_A}{-r_A} \qquad (4.3)$$

The rate equation is tested by substituting for $-r_A$ into Eq.(4.3). A linearity test can then be performed to test the rate equation (66). Integral analysis provides a straight forward rapid procedure for testing some of the simpler rate expressions. But the integrated forms of these expressions become unwieldy when more complicated rate expressions are used. In these situations, the differential method of analysis becomes more convenient when searching for a rate equation. Re-arranging Eq.(4.1), we obtain the expression that allows us to find rates of reaction in integral reactors. Thus we have

$$-r_A = \frac{dx_A}{dV/F_{AO}} = \frac{dx_A}{d(V/F_{AO})} \qquad (4.4)$$

In differential analysis a series of runs are made using feed of the same composition C_{AO} but varying the feed rate F_{AO} or reactor volume V to obtain a series of different V/F_{AO} values. The best fit curve to the $x_{A\ out}$ vs V/F_{AO} data is to be obtained and it should pass through the origin. Equation (4.4) shows that the rate of reaction at any value of x_A is simply the slope of this curve; hence at a number of x_A values, the slopes of this curve (i.e. rates of reaction) as well as the corresponding concentrations of reaction C_A can be obtained. We now have a series of rates versus concentrations which can be correlated in the manner mentioned in the differential reactor data analysis.

4.3 A TYPICAL PROGRAMME FOR KINETIC EXPERIMENTS

(a) Diffusion effects: The effect of the external diffusion is determined at the highest temperature used in the investigation (highest rate) by the relation between the conversion x and the feed F at constant W/F (W is the weight of catalyst used). If above a certain limiting gas velocity F_D the conversion x is constant, this would indicate that diffusion is no longer rate

controlling step.

The internal diffusion (pore diffusion) is determined by measuring x at constant W/F and varying the diameter of the catalyst particles d. Under a certain diameter d_p the conversion x is constant when the pore diffusion becomes negligible.

(b) Preliminary data: Integral reactor data with $F \geqslant F_D$ and $d \leqslant d_p$ are taken for different contact times W/F and the function $x = f(W/F)$ is obtained. This function can be considered as a graphical form of the rate equation and can be used for preliminary calculations.

(c) Initial-rate data with variation of one partial pressure: Initial-rate data are produced in the following way: The total pressure and all the partial pressures except one (and the inert gas) are kept constant. One partial pressure is varied over a wide range while the composition of the gas mixture is kept away from equilibrium to avoid the influence of the reverse reaction. As the conversion x is kept low the reaction rate is $r = x(F/W)$. All reactants and products are studied in this way and the experimental data are graphically represented. Inspection of the curves with the help of the Langmuir-Hinshelwood reasoning gives hints to possible mechanisms and these can be further investigated by experimentation.

(d) Tests with the established rate equation: The final rate equation with its mechanism (for derivations the Hougen-Watson method can also be used with advantage) is established and the expressions for the forward and backward reaction are examined from a thermodynamic point of view. A fit to the integral-reactor curves is made and constants are evaluated by graphical methods.

(e) Influence of temperature: After the establishment of the rate equation measurements at two relatively different temperatures are started.

Only a limited number of runs are necessary as the rate equation is known. Activation energies are calculated from the temperature variation of the constants.

(f) Investigation of other catalysts: If the purpose of the investigation was not only the establishment of the rate equation but also information about the catalyst, the change in mechanism when promoters are added etc., the investigation can with advantage be carried out with the initial-rate method. Determination of the activation energy can give information concerning the influence of additives and of different methods of treatment.

4.4 PROGRAMME FOR THE PRESENT WORK

(a) Catalytic activity of the reactor material: Since reactor and other parts of the equipment are made of stainless steel and the fact that iron has catalytic activity for the water-gas shift reaction, a study had to be made at the highest temperature of the experiment at a number of mass velocities. A mass velocity above which no catalytic activity of the reactor material is in evidence has to be determined.

(b) Diffusion effect: The procedure is the same as in section 4.3(a). From the knowledge of the mass transfer studies on the shift catalysts (section 3.2.4) a very small particle size (500-600 microns) catalyst is used.

(c) Preliminary data: The procedure is the same as in section 4.3(b).

(d) Initial-rate data and to establish rate equation based on possible mechanisms: The method described in the sections 4.3(c) and 4.3(d) are not used. Instead differential rates are obtained experimentally and an exponential rate expression is fitted by means of a least square method. When the number of variables involved are large, the evaluation of initial rate data and establishment of rate equation by the method described in sections 4.3(c) and 4.3(d) becomes a very lengthy procedure. Under these circumstances

the use of a statistical design method helps in reducing considerably the main bulk of the work and produces data of reasonable accuracy.

For the water-gas shift reaction the more generalised form of exponential type rate expression can be written as:

$$r = k\,(p_{CO})^{a}\,(p_{H_2O})^{b}\,(p_{CO_2})^{c}\,(p_{H_2})^{d} \qquad (4.5)$$

where

r = differential reaction rate.

k = rate constant.

p = partial pressure of the particular component.

a, b, c, d are constants. Employing a simple Arrhenius relation we can write:

$$r = (A \exp - E/RT)\,(p_{CO})^{a}\,(p_{H_2O})^{b}\,(p_{CO_2})^{c}\,(p_{H_2})^{d} \qquad (4.6)$$

where

R = gas constant.

E = activation energy.

T = absolute temperature.

Taking logarithms on both sides we have

$$\log r = \log A - \frac{E}{R} \cdot \frac{1}{T} + a \log p_{CO} + b \log p_{H_2O} + c \log p_{CO_2} + d \log p_{H_2} \qquad (4.7)$$

Experimental conditions are chosen to test the validity of the above equation (4.7) and also to evaluate the parameters A, E/R, a, b, c and d. Since there are five independent variables in the equation i.e. partial pressures of CO, H_2O, CO_2, H_2 and temperature, a half replicate of 2^5 factorial design suggested itself (the principles of statistical design method

are discussed briefly in the later part of this chapter). Here each factor or variable will have two levels of value and experimentally 16 values of "r" are to be obtained for 16 combinations of 5 factors at their high and low level values. Now the analysis of variance of the 16 values of log r will help in sorting out the factors actually involved in controlling the rate and thus a possible mechanism could be established.

(e) Influence of temperature: The method is the same as described in section 4.3(e).

(f) Investigation of other catalysts: For the reasons mentioned in section 4.3(f) five commercial shift catalysts are studied in the way described in sections 4.4(d) and 4.4(e).

4.5 STATISTICAL DESIGN METHOD - FACTORIAL EXPERIMENTS

For the study of the variation brought about by deliberate changes in the experimental conditions a generally useful technique is provided by the Factorial Experiment. A considerable advantage is gained if the experiment is so designed that the effect of changing any one variable can be assessed independently of the others. One way of achieving this object is to decide on a set of values, or levels, for each of the factors to be studied, and to carry out one or more trials of the process with each of the possible combinations of the levels of the factors. Such an experiment is termed a Factorial Experiment; the term is extended to modified designs in which the number of trials is restricted in certain well-defined ways.

The advantages of factorial design can be summed up: (a) when there are no interactions the factorial design gives the maximum efficiency in the estimation of the effects. (b) when interactions exist, their nature being unknown, a factorial design is necessary to avoid misleading

conclusions. (c) in the factorial design the effect of a factor is estimated at several levels of the other factors, and the conclusions hold over a wide range of conditions. These conclusions not only true when two factors are used but hold with even greater emphasis when more than two factors are involved.

The simplest class of factorial design is that involving factors at two levels, that is, the 2^n class, n being the number of factors. For convenience a factor is denoted by a capital letter, and the two levels of the factor by "1" and the corresponding small letter. The levels of a factor A are thus denoted by "1" and "a". By convention "1" refers to the lower level, while "a" refers to the higher level. Also "+" means that the factor is at its higher level and "-" means that at lower level.

When more factors are investigated simultaneously the appropriate factorial design may be larger than can be carried out at uniform conditions or too large to handle at one time. The most efficient way of dealing with this situation is to divide the experiment into smaller blocks in a particular manner, such that the main effects of the factors and their more important interactions are investigated under uniform conditions. This method is called confounding and in confounding the number of observations capable of being carried out under strictly comparable conditions is less than the number required for the whole design.

For a 2^5 factorial experiment, as in the case of the present work one can have two blocks. The treatment combinations with a plus sign fall into one block and those with a minus sign fall into the other. The appropriate blocks are then:

(1): a, b, c, d, e, abc, abd, abe, acd, ace, ade, bcd, bce, bde, cde, abcde.

(2): 1, ab, ac, ad, ae, bc, bd, be, cd, ce, de, bcde, acde, abde, abce, abcd.

In the present work block (1) has been chosen and 16 treatment combinations of half replicate of 2^5 factorial design are given in table 4.1.

Table 4.1 Experimental Design for the Present Work

Treatment Combination Number	Levels of Factors				
	$\log p_{CO}$	$\log p_{H_2O}$	$\log p_{CO_2}$	$\log p_{H_2}$	$\frac{1}{T}$
TCN-1	+	-	-	-	-
TCN-2	-	+	-	-	-
TCN-3	-	-	+	-	-
TCN-4	+	+	+	-	-
TCN-5	-	-	-	+	-
TCN-6	+	+	-	+	-
TCN-7	+	-	+	+	-
TCN-8	-	+	+	+	-
TCN-9	-	-	-	-	+
TCN-10	+	+	-	-	+
TCN-11	+	-	+	-	+
TCN-12	-	+	+	-	+
TCN-13	+	-	-	+	+
TCN-14	-	+	-	+	+
TCN-15	-	-	+	+	+
TCN-16	+	+	+	+	+

From now on a particular treatment combination will be represented by the corresponding treatment combination number.

The actual values of the levels used in the experiment (except Girdler G-66 catalyst) are given below.

Table 4.2 Values of variables at two levels

Variables	Levels -	Levels +
$\log p_{CO}$	log (0.10 atm.)	log (0.15 atm.)
$\log p_{H_2O}$	log (0.10 ")	log (0.15 ")
$\log p_{CO_2}$	log (0.10 ")	log (0.15 ")
$\log p_{H_2}$	log (0.10 ")	log (0.15 ")
$\frac{1}{T}$	$\frac{1}{(350+273)^{\circ}K}$	$\frac{1}{(380+273)^{\circ}K}$

To cover the high temperature range, another Factorial Experiment was performed for each catalyst changing the values of temperature levels only.

$$\frac{1}{T} = \frac{1}{(400+273)^{\circ}K} \quad \text{and} \quad \frac{1}{(430+273)^{\circ}K}$$

For Girdler G-66 catalyst all the values given above in the table 4.2 except the values of temperature were used. The values taken were

$$\frac{1}{T} = \frac{1}{(250+273)^{\circ}K} \quad \text{and} \quad \frac{1}{(285+273)^{\circ}K}$$

The analysis of variance and the significance of the effect as well as factorial design in general are dealt with very fully in the text books (27, 103). In Chapter 11 however calculations involved in the analysis of variance and significance tests will be considered.

Chapter 5. EXPERIMENTAL EQUIPMENT

The equipment was designed primarily for the purpose of testing the comparative behaviour of a number of catalysts in order to investigate the seemingly contradictory results obtained by other workers.

A general view and layout of the equipment are shown in Fig. 5.1 and Fig. 5.2 respectively. The system required to mix the gases to a required volume and to produce steam in known quantities. This steam-gas mixture should pass through the catalyst in the reactor at the reaction temperature. After reaction unreacted steam is to be measured after condensing. The exit gas mixture is measured and analysed. A mass balance then gives the reaction rate. The equipment consists of the following main items: (a) Jet Mixer, (b) Gas-Steam Mixer, (c) Water Tank, (d) Boiler, (e) Steam Superheater, (f) Differential Reactor, (g) Condenser, (h) Condensate Knock-out Drum, (i) Condensate Tank. Besides these temperature, pressure and flow measuring, heating and gas analysing instruments are also included.

5.1 DESIGN AND CONSTRUCTION

(a) Jet Mixer: This is a 2 ft. 6 inch long, 3 inch N.B. Copper pipe (Fig. 5.3a) one end of which is closed with a 1/16 inch brass disc. At the centre of this disc a $\frac{1}{4}$ inch N.B. copper tube was connected for the injection of nitrogen gas. 3 more $\frac{1}{4}$ inch N.B. copper tubes were inserted inside the main body at 4 inch, 8 inch and 12 inch along the length from the closed end. These three tubes had short right angles bent at the axis of the main pipe and were facing along the direction of flow. About the last foot of the pipe was packed with dry ceramic packing rings. This end was closed with

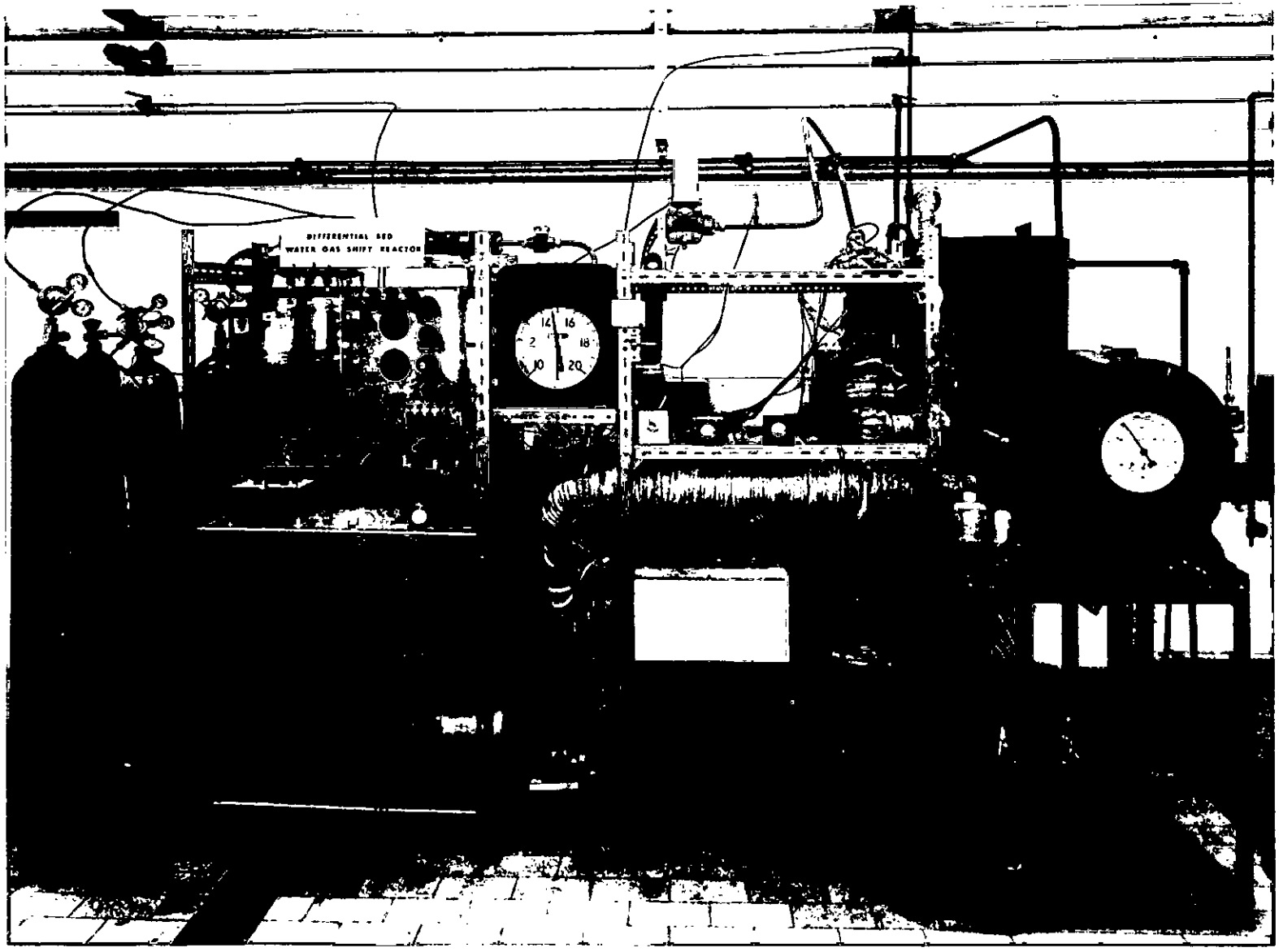

Fig. 5.1 General View of Equipment.

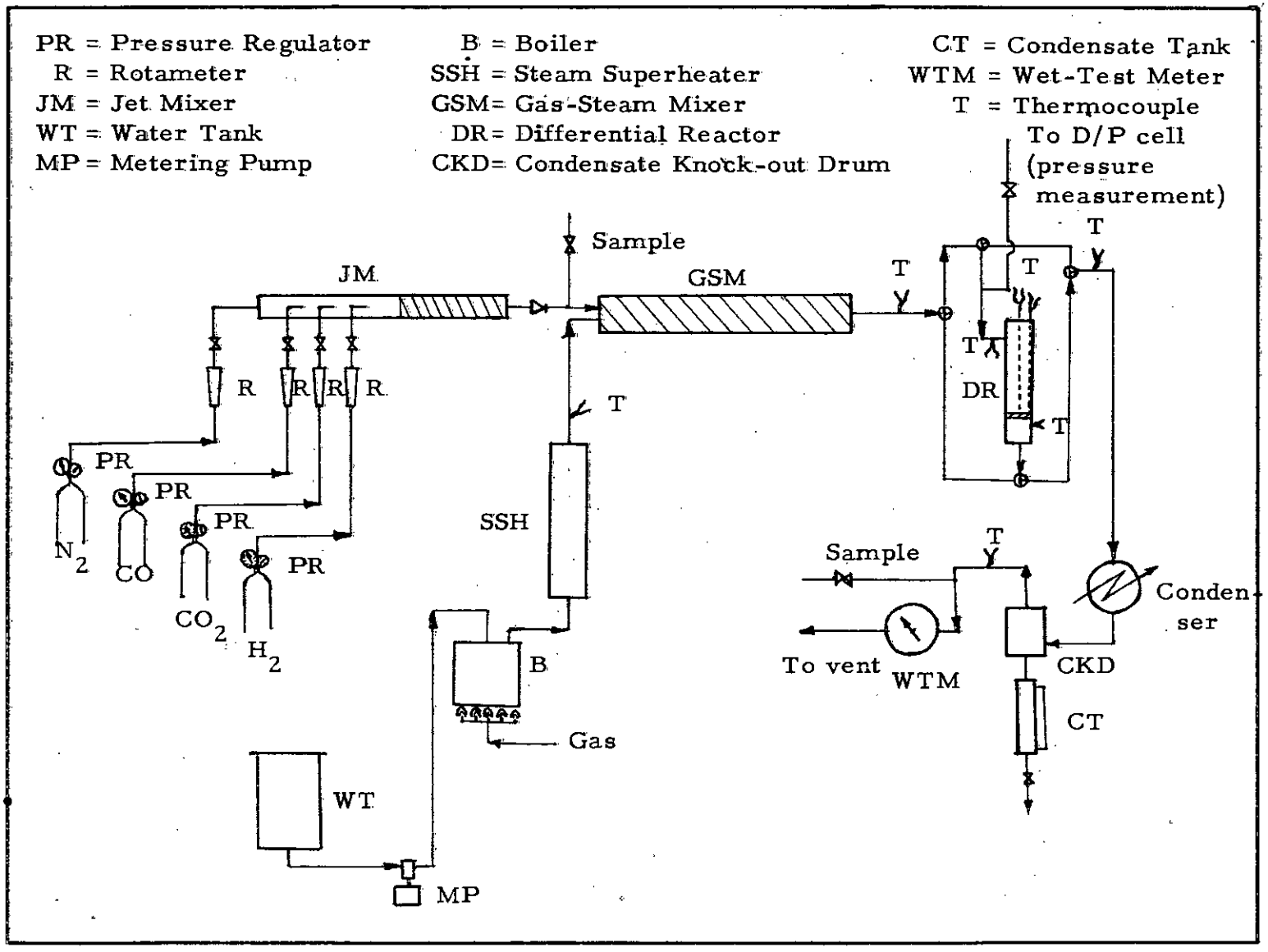

Fig. 5.2 Layout of Equipment

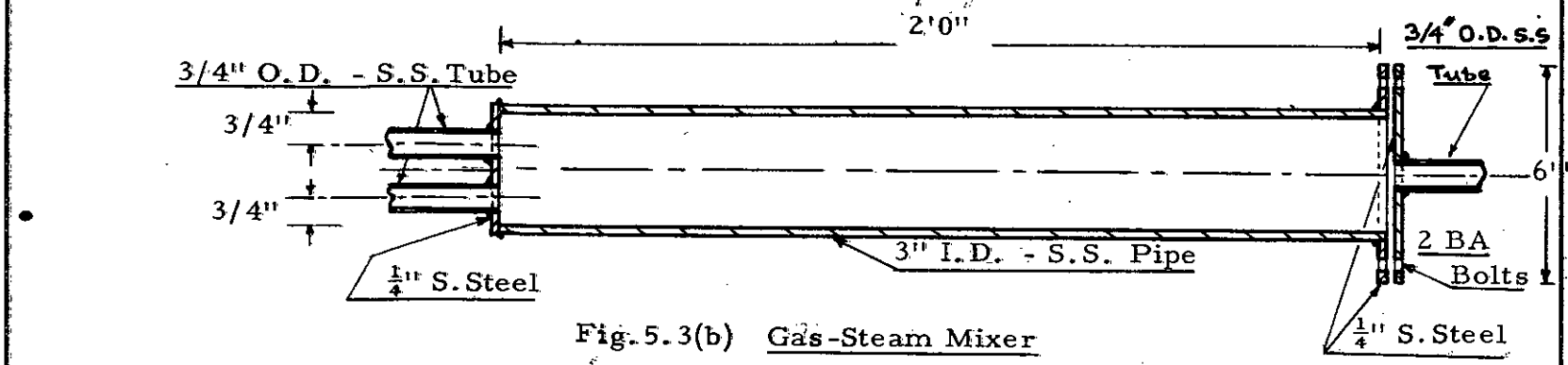

Fig. 5.3(b) Gas-Steam Mixer

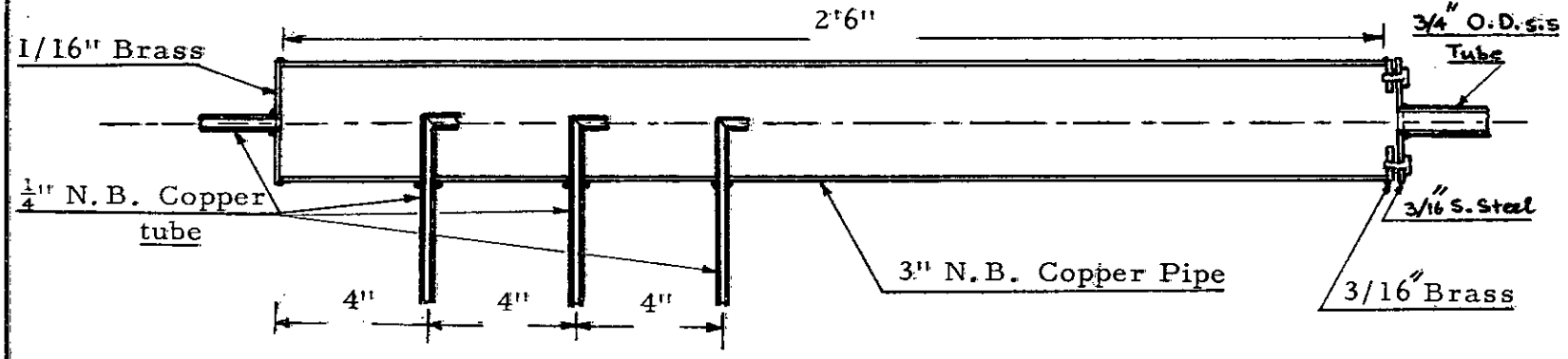

Fig. 5.3(a) Jet-Gas Mixer

Scale: 1/5 Full Size

a stainless steel 3 inch dia. x 3/16 inch thick flange leading to a 3/4 inch O.D. S.S. tube as shown in the figure (5.3a). 8 2BA S.S. screws were used in the flange. The seams were brazed.

(b) Gas-Steam Mixer: This is a 2 feet long 3 inch I.D. Stainless Steel pipe (Fig. 5.3b) one end of which is connected with two 3/4 inch O.D. S.S. tubes through a $\frac{1}{4}$ inch thick S.S. disc. The other end was connected with a 3/4 inch O. D. S.S. tube through a pair of 6 inch dia. x $\frac{1}{4}$ inch thick S.S. flanges. 8 2BA S.S. nuts and bolts were used. A high temperature resistant gasket material was placed between the two flanges and the seams were silver-soldered. The whole 'Mixer' was packed with 2 mm. glass balls.

(c) Water Tank: This is a 2 ft. high cylindrical tank with 1 ft. in diameter. The cylindrical shell was built with 1/16 inch thick S.S. sheet and the base was of 1/8 inch thick S.S. plate. At the centre of the base a $\frac{1}{2}$ inch O.D. S.S. tube was connected to lead the water to the pump. The lid was made of wood. The seams were silver-soldered.

(d) Boiler: Boiler is a closed cylindrical Stainless Steel tank with two pipes connected at the top (Fig. 5.4). The cylindrical body (10 inch in diameter and 1 ft. high) and the top was made of 1/16 inch thick S.S. sheet. The base was 1 ft. dia. x 1/8 inch thick S.S. disc. The water inlet pipe was at the centre of the top and was a 10 inch long and 3/4 inch O.D. S.S. tube at the top of which a brass tube (3/4 inch O.D.) with a hypodermic needle facing downward was connected up by a coupling. The seams were silver-soldered. The steam outlet was provided through a pipe of 3/4 inch O.D. S.S. tube and was connected at a side of the top. About 2 inch S.S. gauge packing was placed at the bottom.

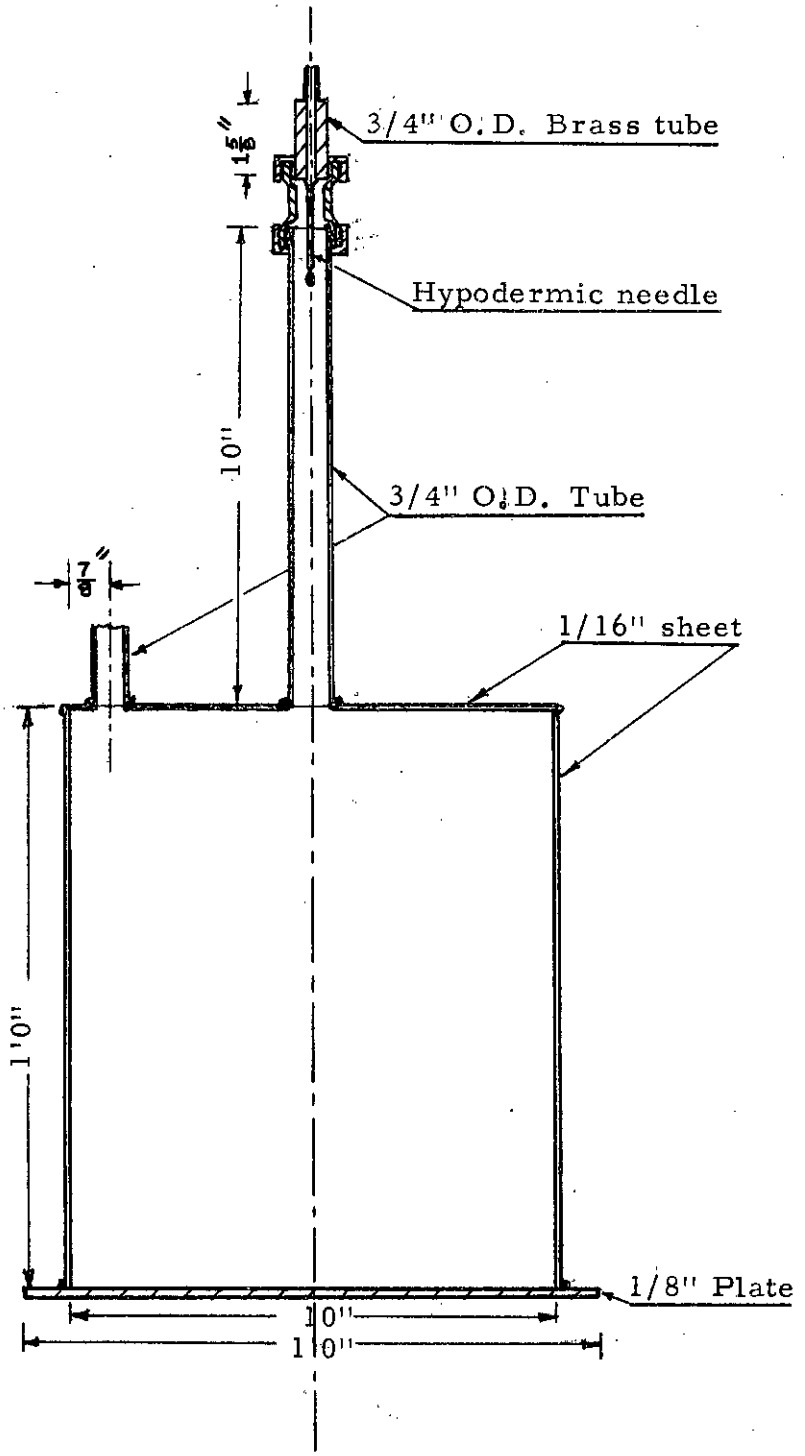

Material: Stainless Steel

Fig. 5.4 Boiler

Scale: $\frac{1}{4}$ Full Size

(e) Steam Superheater: A 1 ft. x 1 inch I.D. S.S. pipe, packed with fine S.S. gauge, carried the steam. This pipe was enclosed in a concentric ceramic pipe (1 ft. x $1\frac{1}{4}$ inch dia.) around which ni-chrome high resistance electric heating wire was wound. The two concentric pipes were held in position by two 'Sindanyo' (Asbestos) rings in the anular space on either side. The pipes were housed in a rectangular 'Sindanyo' box (1 ft. x 10 inch x 10 inch). The box was packed with chips of fire-bricks. The capacity of the heater was 2 KW.

(f) Differential Reactor: The reactor tube consisted of two pieces of 2 inch I.D. seamless Stainless Steel pipe (Fig. 5.5) joined together by a pair of S.S. flanges ($4\frac{1}{4}$ inch dia. x $\frac{1}{4}$ inch thick). Between these two flanges a S.S. ring (same size as that of flanges) was placed which held a 2.5/8 inch dia. S.S. Rigimesh Disc (100 microns) on which catalyst particles (500-600 microns) rested. The top piece was 9.1/4 inch long and a side arm (3/4 inch O.D. S.S. tube) was located 2 inch down the top at an angle of 30^{o} with the horizontal line. Two thermocouple wells (about 2.5 mm. dia.), located axially and along the wall, were suspended from a $\frac{1}{4}$ inch S.S. disc which closed the top of the reactor. The wells came down very close to the catalyst retainer. The bottom piece of the reactor contained a thermocouple well inserted from the side wall. The bottom of the reactor led to a 3/4 O.D. S.S. tube connection through a pair of S.S. flanges ($4\frac{1}{4}$ inch dia. x $\frac{1}{4}$ inch thick). Each pair of flanges was fastened by 8 2BA bolts and nuts. High temperature resistant gasket material was used between the flanges. Provision was kept to introduce the feed from the top or from the bottom of the reactor with the help of a number of two-way cocks.

(g) Condenser: It consisted of two concentric helical $\frac{1}{2}$ inch N.B. copper tubes connected in parallel, each having a length of 15 ft. These were housed in a big cylindrical brass tank (2 ft. dia. x 3 ft. high).

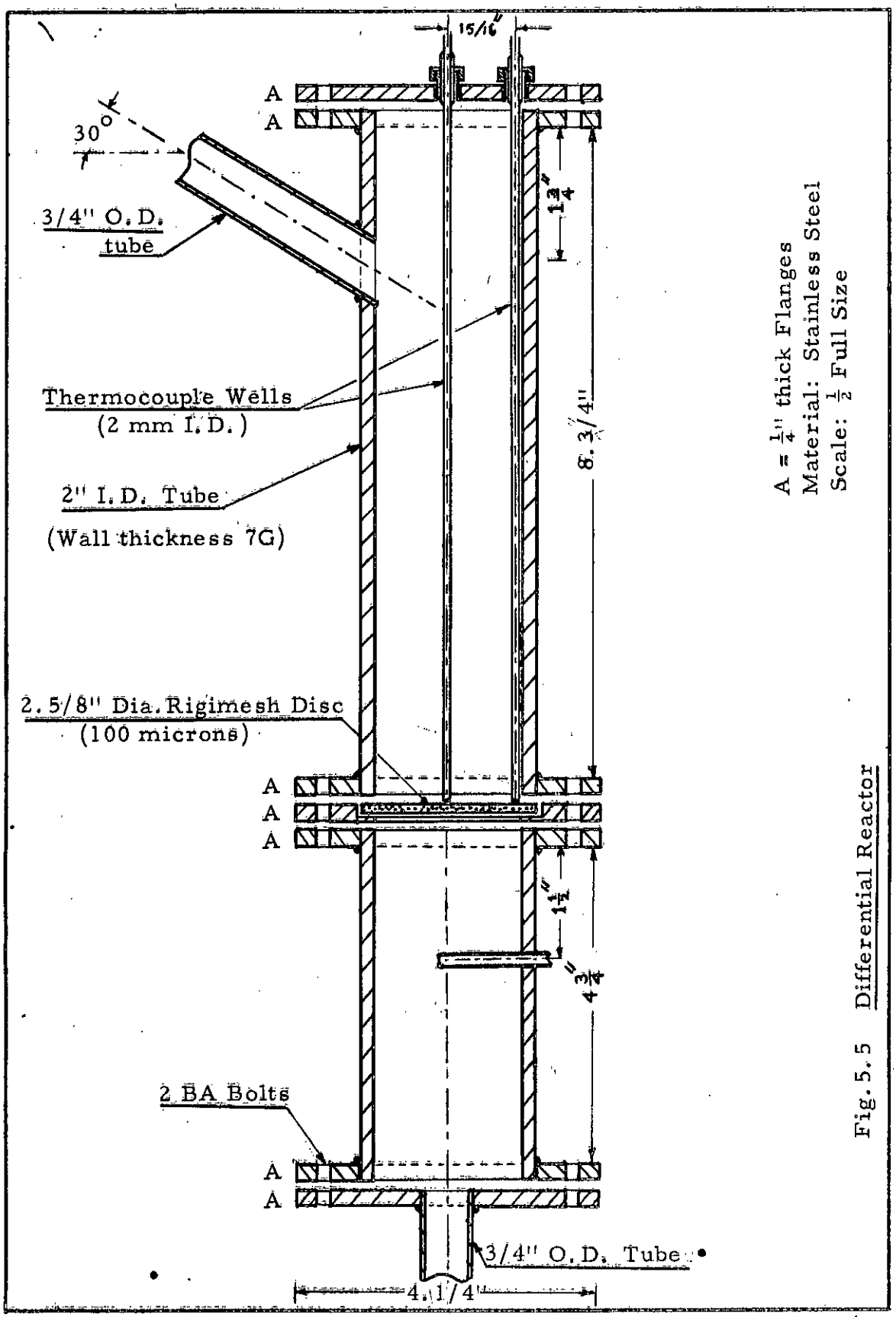

Fig. 5.5 Differential Reactor

Cooling water line was provided from the top and went deep down. An over-flow line was provided from the side wall near the top. A drain cum cooling water recirculating line was kept from the centre of the bottom. A centrifugal pump was used to recirculate the cooling water.

(h) Condensate Knock-Out Drum: This is a 9 inch dia. x 1 ft. high drum made with 1/16 inch brass sheet (Fig. 5.6) the bottom of which was a cone facing up with vertical height of $\frac{1}{2}$ inch. The condensate outlet was provided from the centre of the bottom through a $\frac{1}{4}$ inch N.B. copper tube. The gaseous mixture went out through a 3/4 inch N.B. copper tube from the centre of the top. A side arm of $\frac{1}{2}$ inch N.B. copper tube near the bottom was provided for the entrance of steam-gas mixture. Inside the drum 4 cones (8 inch in diameter at the base with $\frac{1}{4}$ inch vertical height) facing down and 3 transacted cones (9 inch in base diameter and 1 inch dia. at the other with vertical height of $\frac{1}{4}$ inch) facing up were used as baffles. These two types of cones were placed alternately as shown in the figure. The baffles were spaced $1\frac{1}{2}$ inch from each other and were held in position by two $\frac{1}{4}$ inch brass rods. All the seams were brazed.

(i) Condensate Tank: This is a 2 ft. long x 4 inch N.B. copper pipe with both ends closed. The condensate entered through a $\frac{1}{4}$ inch N.B. copper tube from the centre of the top. A drainage line with a stop cock was provided from the bottom. To read the water level in the tank a graduated gauge glass (1.3/4 ft. long) was provided. A purge line from this tank was kept.

The inter-connecting lines up to the condenser were of 3/4 inch O.D. S.S. tubes and which after the condenser were made of copper. The inter-connecting lines up to condenser and the boiler, the gas-steam mixer and reactor were electrically heated and heavily insulated by asbestos ropes.

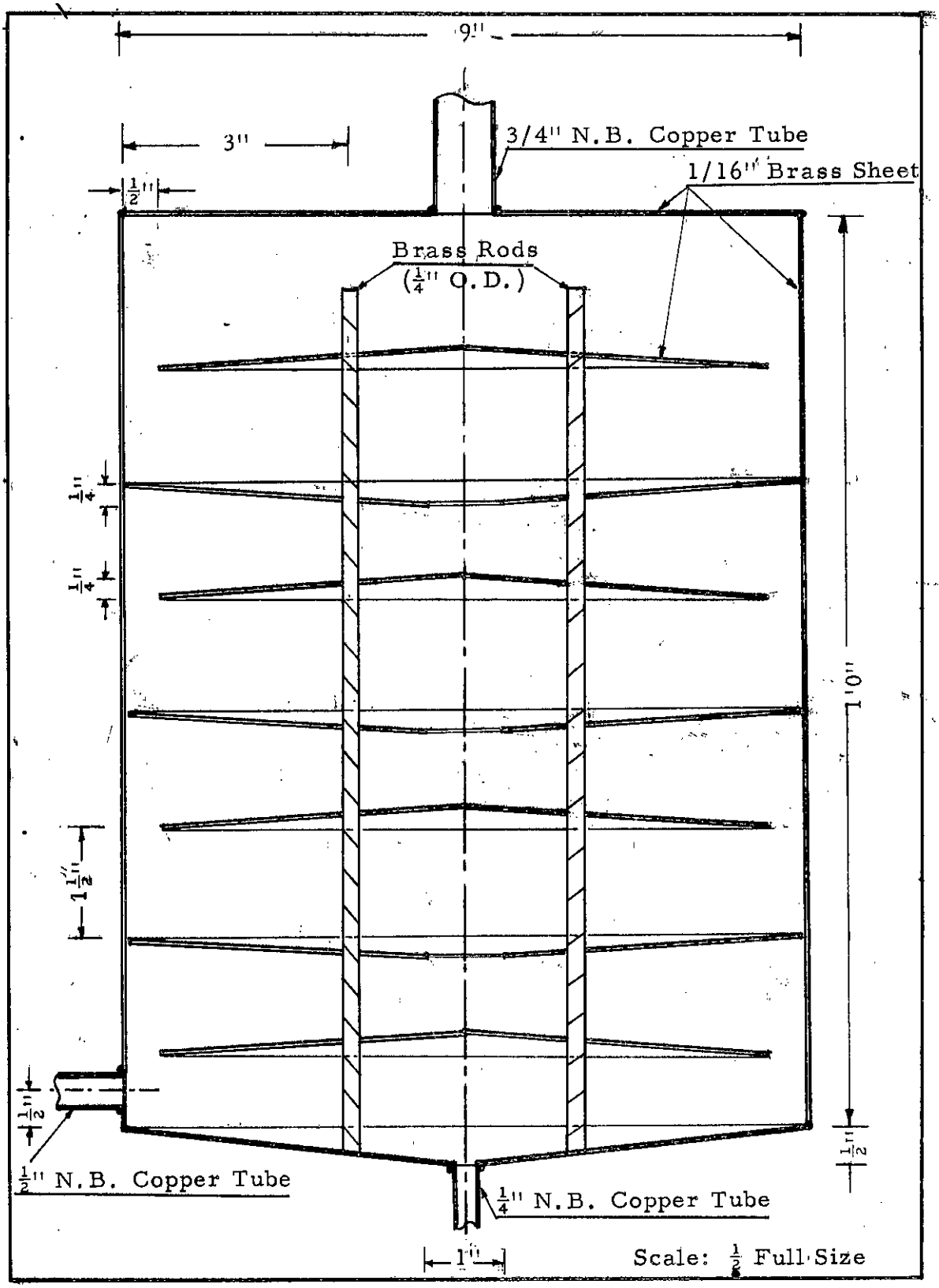

Fig. 5.6 Condensate Knock-Out Drum

The heating methods will be dealt with in the next section.

5.2 INSTRUMENTATION

(a) Temperature measurement: Temperatures at eight points were read. The positions of these are shown in Fig. 5.2. All the thermocouples used in temperature measurement were chromel-alumel in stainless steel sheathing (1 mm. dia.). $1\frac{1}{2}$ mm. in internal diameter stainless steel tube was used around the thermocouple wire for protection against mechanical damage and also acted as a smooth guide inside the thermocouple wells (2 mm. I.D. S.S. tube). The wells were held in position by 1/8 inch S.S. couplings, one end of each of which was silver-soldered on the flow lines and in the reactor top disc. Stainless steel sleeves were used between the couplings and well tubes. The seams of the sleeves were silver-soldered in the walls of the well tubes. The hot junctions (except the two in the reactor) were placed in the centre of the flow lines. The thermocouples along with the protection tubes and wells were calibrated at melting points of tin (231.75°C), lead (327.35°C) and zinc (419.50°C). The calibration table is given in Appendix 1. Very little difference was observed from the standard charts (40, 83). The cold junctions were protected from getting wet by glass tubes closed at one end. Chromel and alumel extension leads were used.

The potential differences were measured by a Cambridge mini potentiometer through a Cambridge 10-point double pole selector switch. This potentiometer was capable of reading to 1/100 millivolts. For the continuous recording of temperature in the reactor, parallel connections were made for two thermocouples in the reactor from the selector switch to a Kent Mark-3 Electronic 16 point Recorder.

(b) Pressure measurement: The pressure in the reactor was measured with the help of a Foxboro D/P cell pressure transmitter and a pressure indicator. The pressure connection was made just before the reactor entrance (in the present work the feed was introduced from the top). The connecting line (3/4 inch O.D. S.S. tube) between the reactor and the D/P cell was so aligned that any condensate formed in this line run back to the main flow system. The D/P cell was supplied with dust and oil free compressed air at 20 p.s.i.g. Compressed air was obtained from the departmental supply line at about 50 p.s.i.g. and was first passed through a filter and then reduced to 20 p.s.i.g. by a pressure regulator. The reduced pressure was read in a pressure gauge, the output pressure from the D/P cell being fed to the indicator which gave the corresponding reactor pressure. The indicator had a scale with a span from 10 to 20 p.s.i.g. and 1/10 of 1 p.s.i.a could easily be read. This calibrated scale was checked by means of a Fortin's barometer.

(c) Flow measurement: The flow rates of CO, CO_2, N_2 and H_2 were measured at 5 p.s.i.g. by 4 Fischer & Porter tri-flat type glass rotameters. The float material for N_2 was made of stainless steel, for CO and CO_2 of glass and for H_2 of sapphire. The rotameters were calibrated individually for the respective gases at 5 p.s.i.g. with the help of two wet-gas meters. The small one had a maximum capacity of 0.5 cu.ft./min. and for the other one it was 2 cu.ft./min. These two meters were checked against each other for calibration accuracy and later by chromatographic analysis of gas mixtures. The metering pressure (5 p.s.i.g.) was set by the respective cylinder head pressure regulators. The pressure setting was checked by a pressure gauge attached to a common manifold close to the rotameter entrance. The flow of each gas was regulated by a fine control valve placed just after the rotameter. The flow of steam was measured by

metering the distilled water with a metering pump (D. C. L.) having a capacity of 0-8 c.c./min. and then injecting through a fine bore hypodermic needle into the boiler. The boiler instantaneously transformed water to steam. The metering pump along with the injecting device was calibrated by collecting water for a certain period of time. The calibration was checked every time before the start of the experiment. The performance of the boiler was checked by measuring the condensate for corresponding calibrated flow of water.

(d) Heating of the system: As mentioned before the steam produced was superheated in the superheater by a 2 K.W. electric heater. To prevent the heat loss from the process line and process equipment between superheater and condenser were provided with electrically heating devices. Process line between superheater and gas-steam mixer was provided with 400 W. Electrothermal heating flexible cable. A 2 K.W. Pyrotenax heating cable was wound round the gas-steam mixer. Process line between gas-steam mixer and reactor, and between reactor and condenser had 1 K.W. Pyrotenax and 400 W. Electrothermal heating cables respectively. The power supply for these 4 heating units were controlled by four Sunvic Energy Regulators. The gas-steam mixture was brought to the reaction temperature by a 1 K.W. heater around the side arm of the reactor. The reactor had two 400 W. Electrothermal cable heaters controlled separately. The energy input for these 3 heaters and for the 2 K.W. superheater was controlled by two 13 amp. (230 V.) and two 3 amp. (230 V.) Claude Lyons Variacs. Each circuit was provided with a fuse, a switch and an indicating light.

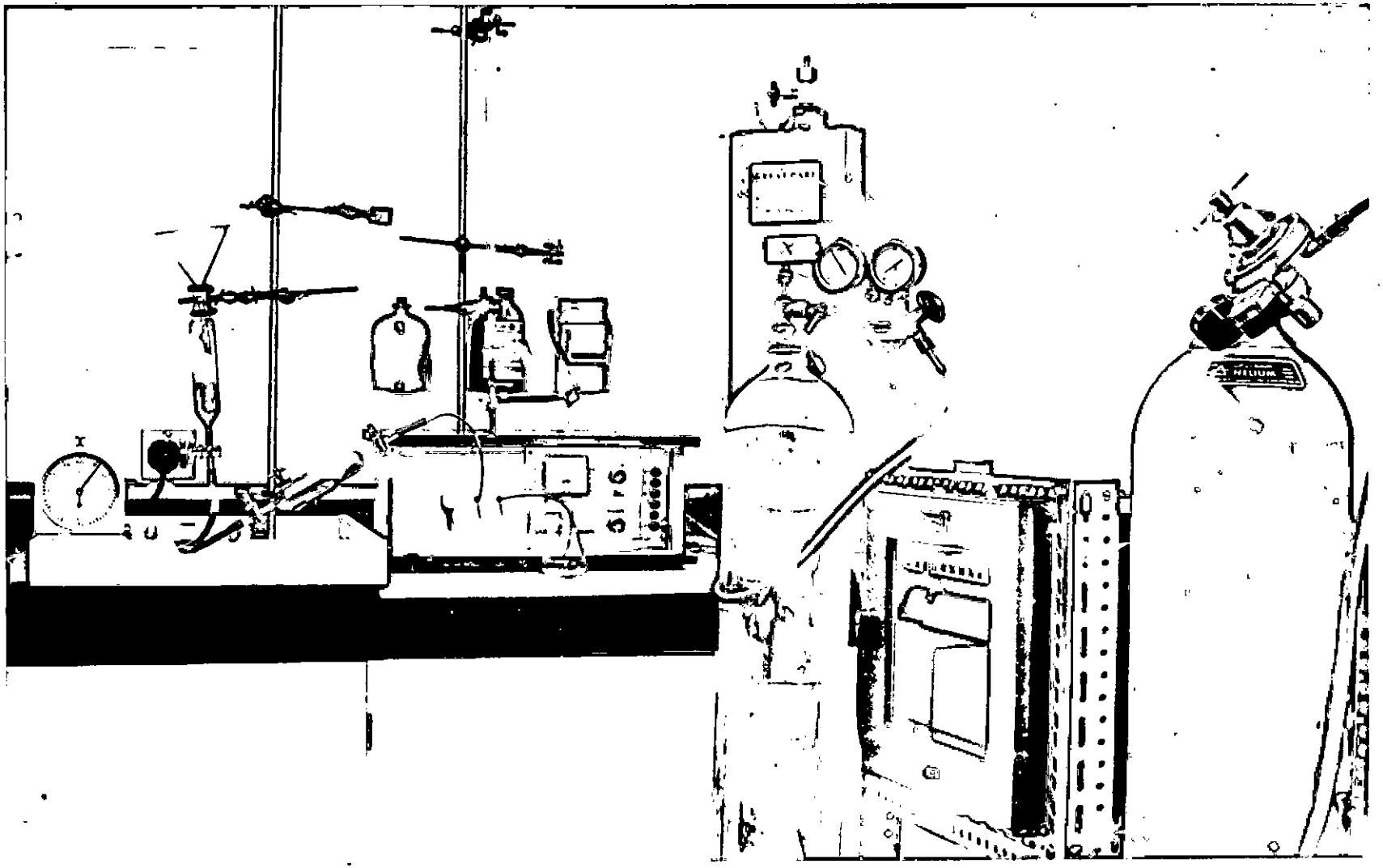

Fig. 5.7 General View of Gas Chromatography Equipment.

(e) Analysis of gaseous mixtures: This was accomplished by using a gas chromatography technic. A Fisher Gas-Partitioner-Model 25 V was used with a Honeywell Electronic Recorder (0-1 m.v.). A general view of the gas chromatography equipment is given in Fig. 5.7 and the line diagram is given below in Fig. 5.8.

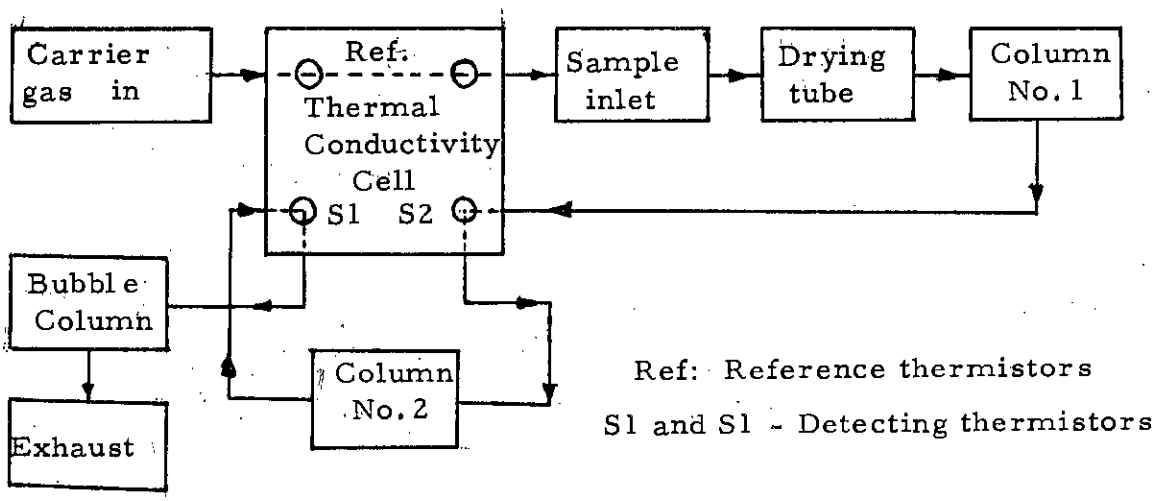

Fig. 5.8 Line Diagram of Gas Chromatography Equipment

During the experiment samples were collected in a number of 100 cc high vacuum gas sampling tubes. A "Speedivac" two stage vacuum pump was used to remove air from the sampling tubes before use. From the tube part of the sample was transferred into the sampling loop (0.5 cc) of the chromatograph by a mercury displacement method. A push on the plunger connected the loop with the carrier gas. The reproducibility of this method of sample introduction is within about $\pm$ 0.3%.

The Fisher Gas Partition - Model 25 V contains dual-column/dual-detector chromatographic system for separating and measuring CO_2, O_2, N_2, CH_4 and CO with helium as carrier gas. H_2 may be determined by using argon as carrier gas. These gases can be analysed in less than 5 minutes. When a mixture of gases is introduced into the instrument, it is swept through the two chromatographic columns by a continuous flow of carrier gas. All components of the gas sample, except CO_2, are swept quickly through column 1 and as they emerge, are detected by thermistor S1 and produce an electrical signal which is recorded on a chart of a millivolt recorder as a composite peak. This composite peak is of no analytical significance. CO_2, travelling slowly through the first column, is thus separated from the other gases, and as it emerges from column 1, is recorded immediately after the composite. The components of the composite mixture are separated in the second column. As the gases emerge individually from the column and pass over detector S2, a chromatogram of each peak is produced. CO_2 is permanently absorbed in the second column. Each gas in identified by its position on the chromatogram, and its concentration determined from the peak height. A typical chromatogram of an experimental sample is given in Fig. 5.9.

The first column is a 30 inch long by $\frac{1}{4}$ inch diameter packed with 30% HMPA on Columpak (60 to 80 mesh). The second one is a 6.5 ft. by 3/16 inch column packed with 42-60 mesh Molecular Sieve 13X. The function of the detectors S1 and S2 is to detect the presence of the sample in the carrier gas stream by monitoring a change in the thermal conductivity of the carrier gas and sample mixture. The column system is designed to operate at a carrier gas flow rate of 80 cc/minute. Before switching on the power in the detector system, the carrier gas flow rate

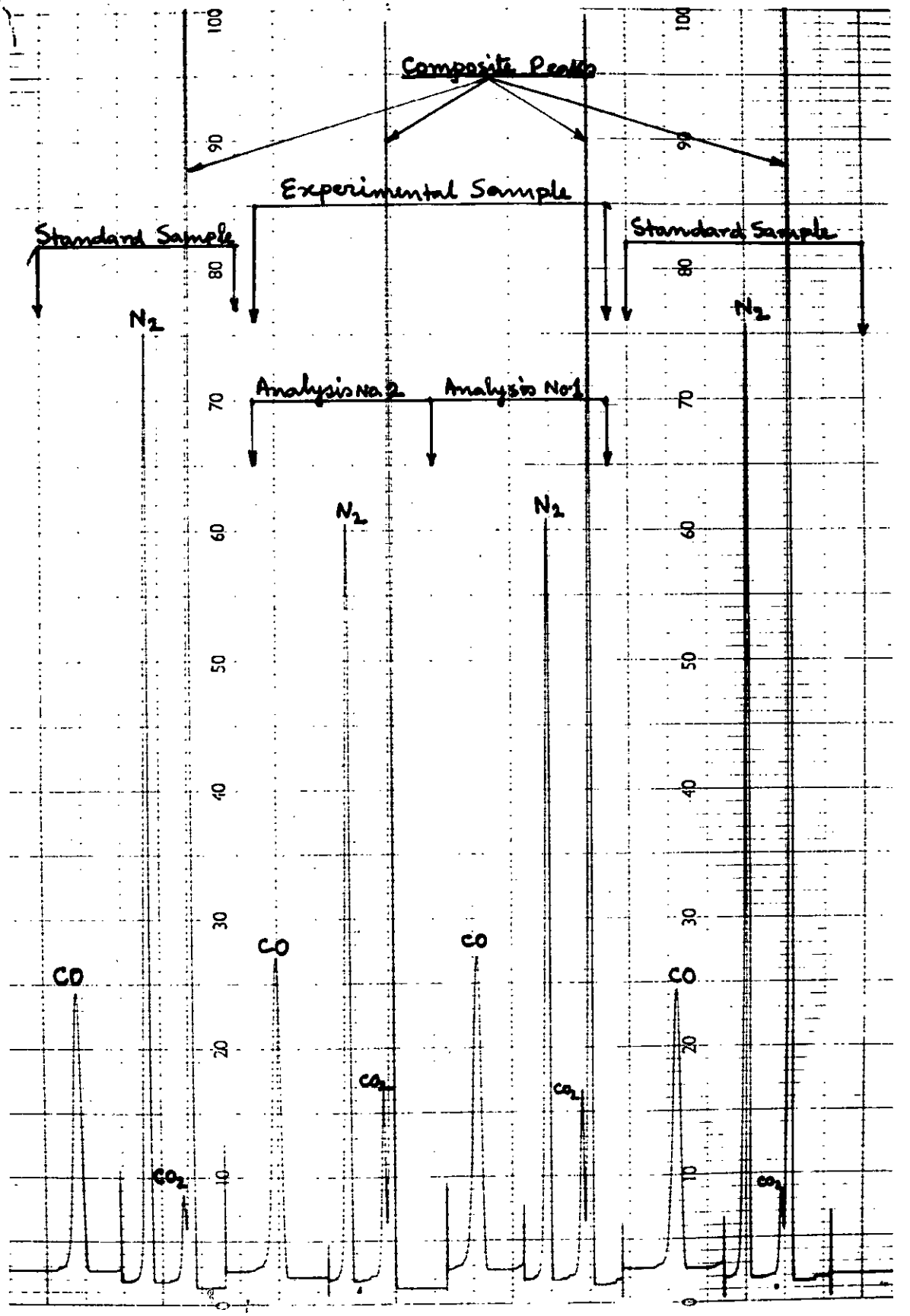

Fig. 5.9 Typical Chromatograms.

was adjusted with the help of a soap bubble column. The soap bubble column was made with a 100 cc. glass burette kept vertical from the bottom of which carrier gas was passed upward. Soap solution in little quantity was put in the gas stream through a side arm which produced soap bubbles climbing up the column. Timing the bubble rise from 0 cc. mark to 100 cc. mark gave the rate of flow.

5.3 EXPERIMENTAL PROCEDURE

At first the calibration of the metering pump was checked. Then the equivalent flow of nitrogen was maintained and heater switches were put on. The system was gradually brought to an average temperature of 250°C in about 4 hours. The ring gas burner underneath the boiler was lit and in about 20 minutes time the metering pump was switched on and CO, CO_2, H_2 gases were put into the system. According to the desired composition the rotameters and the metering pump were adjusted, N_2 being used as a balance. The variac settings for various flow rates and temperatures were obtained previously. As the temperature in the reactor was approaching the desired value, a sample of the gas mixture was taken in a sampling tube from the sampling line, provided just after the Jet mixer and was analysed in the gas chromatograph to check the calibration accuracy of the rotameters. The operating procedure of the chromatography equipment will be described later. The gradual rise in reactor temperature was recorded on the chart of the Kent recorder. By adjusting the power input in the two reactor heaters the axial and radial temperature gradient in the catalyst bed (2 inch in diameter and 2-4 mm. high) could be brought to less than 1°C. After the reaction temperature had reached a steady state (shown on the recorder), the equipment was ready to give the readings which were then taken as quickly as possible. The room temperature and the temperature of the water in the wet gas

meter were noted from the Hg-glass thermometers. The atmospheric pressure from a Fortin's barometer and the reactor pressure from the pressure indicator were taken. Temperatures shown by the two reactor thermocouples were read by the Cambridge potentiometer. The flow rate of the gaseous mixture was measured by timing, the wet gas meter pointer for 1 rev. (1 cu.ft.) and the average of three readings was noted. Two evacuated sampling tubes were used for taking samples from the sampling line provided from just before the wet test meter. First tube (100 cc.), by suction, emptied the sampling loop (30 cc.) and filled it with a representative sample. The second one then collected the sample. The rate of condensate collection was read from the sight glass of the condensate tank.

Now according to the experimental programme the mass flow rate, composition or/and reaction temperature were changed and readings were taken as described above and thus a number of samples were collected. These samples were brought to the constant temperature room (controlled at 22 $\pm$ 1°C) where the chromatographic equipment was kept (fig. 5.7). A carrier flow rate equivalent to 80 cc./min. of Helium (Argon for obtaining H_2) was established first with the help of a soap bubble column (fig. 5.8). The equipment was switched on for about 2-3 hours before use. The method of analysis was described in the previous section. Each experimental sample was analysed twice, any drift in the chromatograph being checked by running a standard gas sample at the beginning and end of each experimental sample analysis. From the ratio of sample and standard peak heights, the composition of the sample was calculated. The composition of the standard gas mixture was determined by a Mass-spectrometer.

Commercially available gases were used in the experiment. Impurity in CO was 0.2% CO_2, 0.15% O_2 and 0.6% N_2. Commercially pure grade CO_2 (liquid, bone dry, 99.8%), H_2 (99.7%) and Nitrogen (99.7%) were used. Two standard mixtures were used. One with the composition of 14.8% H_2, 35.2% N_2, 19.4% CO and 30.6% CO_2, and the other had 4.84% H_2, 81.07% N_2, 8.27% CO and 5.72% CO_2.

(a) Studies of Catalytic Activity of the Reactor Material: Experiments were carried out at mass velocities of 0.2808, 0.4571 and 0.5726 gm.mol./min and at the temperature of 400° to 450°C at all heating sections. No activity of the reactor material was observed except at 450°C and at 0.2808 gm.mol./min. (less than 5%). Though the mass velocity was changed, the composition was kept constant ($p_{CO} = p_{H_2O} = p_{H_2} = p_{CO_2} = 0.10$ atm.).

(b) Studies of Catalysts: Commercial catalysts used in the present work were of different sizes, their physical properties being given in Appendix II. All the catalysts were crushed down to small particles. Particles between 25 and 30 mesh sizes (500-599 microns) were used in all the experiments. By openings the top disc catalyst was introduced into the reactor and care was taken that the catalyst bed top was leveled. All the catalysts were reduced with a gas mixture having the composition of $p_{CO} = p_{H_2O} = p_{CO_2} = p_{H_2} = 0.10$ atm., and at the mass flow rate to be used in the actual experiment. The reduction temperature was raised very slowly up to 450°C (for the Girdler G-66 up to 320°C) and kept at that temperature for a considerable time. Activity fell very quickly at the beginning but eventually became quite steady.

5.4 EXPERIMENTAL ACCURACY

The flow rate of each gas was steady to within $\pm$ 1%. For a mixed gas flow rate the accuracy was within $\pm$ 1.5% of the total flow. The accuracy of metering distilled water by the metering pump was better than 1%.

Based on chromatographic analysis, the control of feed gas composition was within $\pm$ 0.2% of CO (i.e. $\pm$ 2% at the level of 10% CO) and the reaction rate calculation was based on the composition of CO. For N_2 and H_2 it was also within $\pm$ 2% but for CO_2 it was $\pm$ 2.5%. During chromatographic analysis, the variation of peak heights in consecutive analysis of the same sample was within $\pm$ 1% for CO, H_2 and N_2 and $\pm$ 2% for CO_2.

The control of reaction temperature in the reactor was within $\pm$ 1°C of the desired value and as mentioned earlier that in the catalyst bed (2 inch in dia. and 2-4 mm. high) the temperature gradient for both longitudinal and radial was within 1°C.

Chapter 6. RESULTS

Experiments were carried out at a mass flow rate (0.46 gm. mol./min.) at which the activity of the reactor material had no measurable effect and at a contact time of 0.181 hr.$^{-1}$cm.$^{-2}$ at which the resistance due to mass transfer (diffusional) was negligible. The results of the mass transfer studies are given in Fig. 6.1.

Kinetics studies on five commercial shift catalysts were carried out by using factorial experiments as described in chapter 4. The experimental data are given in chapter 10 and the results are given below. In the analysis of variance, the significance of the effects of factors are judged by the F-test based on replication error mean square value of respective factorial experiment. Although for the sake of uniformity experimental data are expressed to five decimal places, it is appreciated that in some cases the last two figures may not be significant.

SSV Catalyst (Fe_2O_3 - Cr_2O_3)

(a) 350°-380°C (Tables 10.1 and 10.10)

The significance test showed that at the 99% confidence limit the effects of p_{CO}, p_{H_2O}, T were strong, with a weaker effect (95% confidence limit) from p_{CO_2}. No interaction was significant.

(b) 400°-430°C (Tables 10.2 and 10.11)

On a 99% confidence limit the effects of p_{CO}, p_{H_2O} and T were significant and the effects of p_{CO_2} was significant at 95%. No interaction was significant.

Power-Gas Catalyst (Fe_2O_3 - Cr_2O_3)

(a) 350°-380°C (Tables 10.3 and 10.12)

The effects of p_{CO}, p_{H_2O}, p_{CO_2}, T, $p_{CO} \times p_{CO_2}$ and $p_{CO} \times p_{H_2}$ were significant on a 99% confidence limit and on a 95% confidence limit the effects of p_{H_2}, $p_{H_2O} \times p_{CO_2}$ and $p_{H_2} \times T$ were significant.

(b) 400°-430°C (Tables 10.4 and 10.13)

On a 99% confidence limit the effects of p_{CO}, p_{H_2O} and T, and on a 95% confidence limit p_{CO_2} and p_{H_2} were significant. No interactions was found to be important.

I.C.I. Catalyst (Fe_2O_3-Cr_2O_3)

(a) 350°-380°C (Tables 10.5 and 10.14)

The effects of p_{CO}, p_{H_2O}, p_{CO_2}, p_{H_2}, T and $p_{CO_2} \times T$ were significant at the 99% confidence limit with weaker effects (95% confidence limit) from $p_{CO} \times p_{CO_2}$ and $p_{H_2O} \times T$.

(b) 400°-430°C (Tables 10.6 and 10.15)

In this experiment the replication error mean square was very small (0.00005) compared with values of the order 0.0006 which were obtained in the experiments for the other three iron oxide based catalysts for the same temperature range. The significance test for this experiment was done on the basis of the latter value. On a 99% confidence limit p_{CO}, p_{H_2O}, p_{CO_2} and T were significant but at the 95% confidence limit only $p_{CO} \times T$

was significant.

Girdler G-3A Catalyst (Fe_2O_3-Cr_2O_3)

(a) 350°-380°C (Tables 10.7 and 10.16)

The significance test showed that on a 99% confidence limit the effects of p_{CO}, p_{H_2O}, T and $p_{H_2O} \times p_{CO_2}$ were significant but on a 95% confidence limit the effects of p_{CO_2}, $p_{CO} \times p_{H_2O}$, $p_{H_2O} \times T$, $p_{CO_2} \times T$ and $p_{H_2} \times T$ were significant.

(b) 400°-430°C (Tables 10.8 and 10.17)

The effects of p_{CO}, p_{H_2O}, p_{CO_2} and T were important on a 99% confidence limit, and on a 95% confidence limit the effects of p_{H_2} and $p_{CO_2} \times T$ were significant.

Girdler G-66 Catalyst (Oxides of Zn, Cu and Cr)

250°-285°C (Tables 10.9 and 10.18)

Based on the 99% confidence limit the effects of p_{CO}, p_{H_2O}, p_{H_2}, T, $p_{CO} \times p_{H_2O}$, $p_{CO_2} \times p_{H_2}$, $p_{CO_2} \times T$ and $p_{H_2} \times T$ were significant and the effects of $p_{CO} \times p_{CO_2}$, $p_{CO} \times T$, $p_{H_2O} \times p_{CO_2}$ and $p_{H_2O} \times p_{H_2}$ were significant at the 95% confidence limit.

In the significance tests it was observed that, except for SSV catalyst, some interactions were significant event at the 99% confidence limit. But the exponential form of rate equation (eqn. 4.5) will consider only the main effects. The experimental data were correlated with a linear regression equation of the form of Eqn. 4.7 by means of least squares.. The results

are given in Table 6.1

The apparent activation energy of each catalyst for the temperature range 350° to 450°C (for G-66 the range is 210°-310°C) was obtained by considering a rate equation with the average of the low (350°-380°C) and high (400°-430°C) temperature range values of a, b, c and d, and plotting log k vs 1/T from the experimental data (Tables 10.19 to 10.23). The results are shown in figures 6.2 to 6.6.

Table 6.1 Results of Data Fitting in Eqn. 4.7

Catalysts	Temperature range (°C)	A	$\frac{E}{2.303R}$	a	b	c	d	Residual Standard Deviation (log r)
SSV	350-380	7.50×10^5	4069.5 ± 385.2	0.630 ± 0.161	0.590 ± 0.159	-0.460 ± 0.176	0	0.063
	400-430	1.01×10^4	2571.3 ± 222.7	0.970 ± 0.083	0.640 ± 0.078	-0.470 ± 0.100	0	0.031
Power-Gas	350-380	1.08×10^5	3596.7 ± 464.1	0.918 ± 0.192	0.567 ± 0.190	-0.342 ± 0.214	-0.402 ± 0.208	0.075
	400-430	1.49×10^5	3494.4 ± 206.3	1.218 ± 0.075	0.560 ± 0.068	-0.517 ± 0.087	-0.332 ± 0.084	0.027
I.C.I.	350-380	2.46×10^8	6058.9 ± 483.1	1.133 ± 0.205	0.527 ± 0.198	-0.898 ± 0.227	-0.524 ± 0.219	0.078
	400-430	1.67×10^4	2740.6 ± 446.2	1.064 ± 0.156	0.803 ± 0.154	-0.521 ± 0.186	-0.210 ± 0.173	0.059
Girdler G-3A	350-380	3.80×10^4	3257.0 ± 718.9	1.415 ± 0.298	0.634 ± 0.290	-0.770 ± 0.309	-0.124 ± 0.307	0.115
	400-430	5.67×10^7	5398.3 ± 424.0	1.059 ± 0.158	0.772 ± 0.143	-0.539 ± 0.170	-0.309 ± 0.167	0.057
Girdler G-66	250-385	24.72	1130.8 ± 315.2	0.684 ± 0.208	0.573 ± 0.210	0	-0.704 ± 0.234	0.084

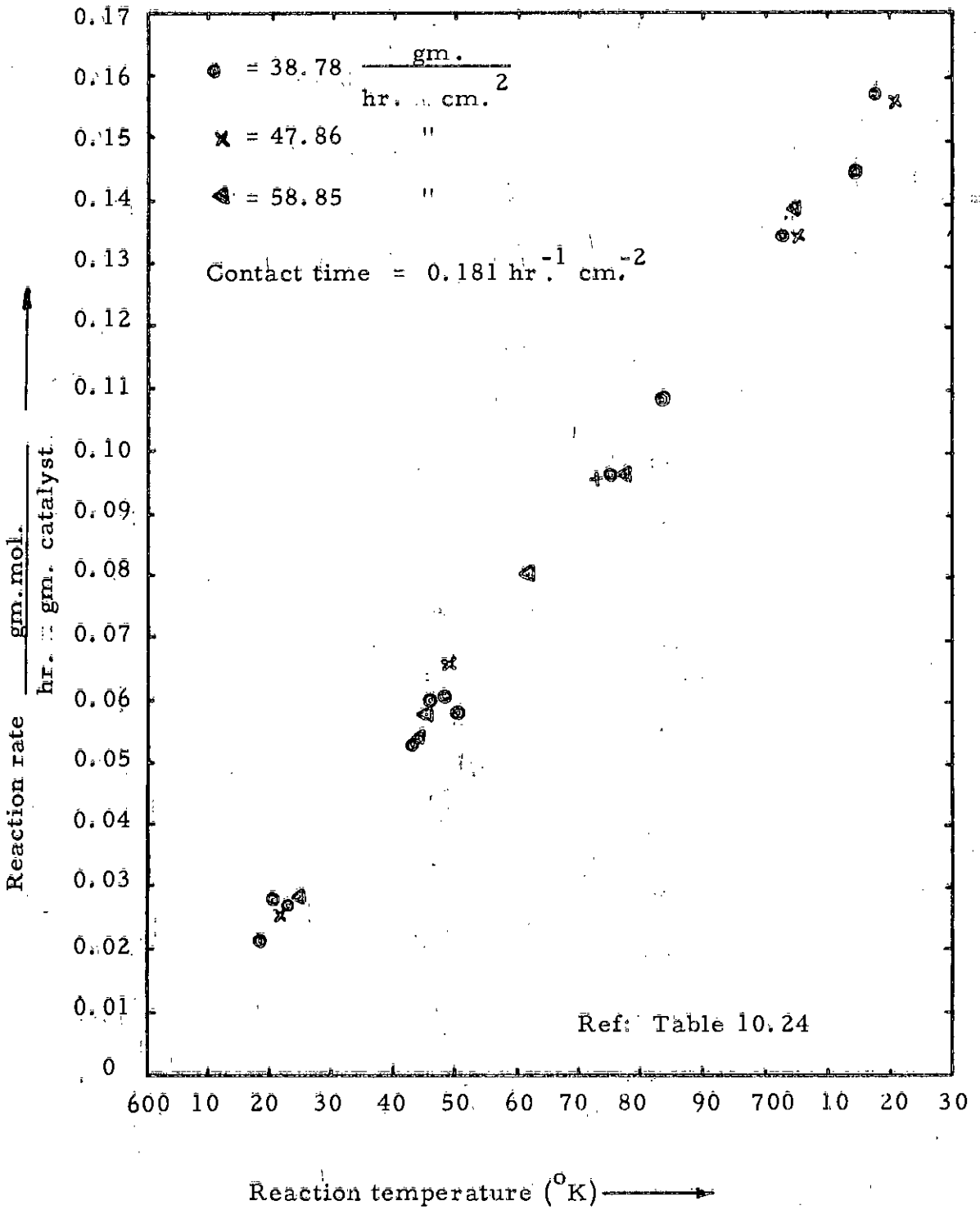

Fig. 6.1 Effect of Mass Velocity on Reaction Rate-SSV Catalyst

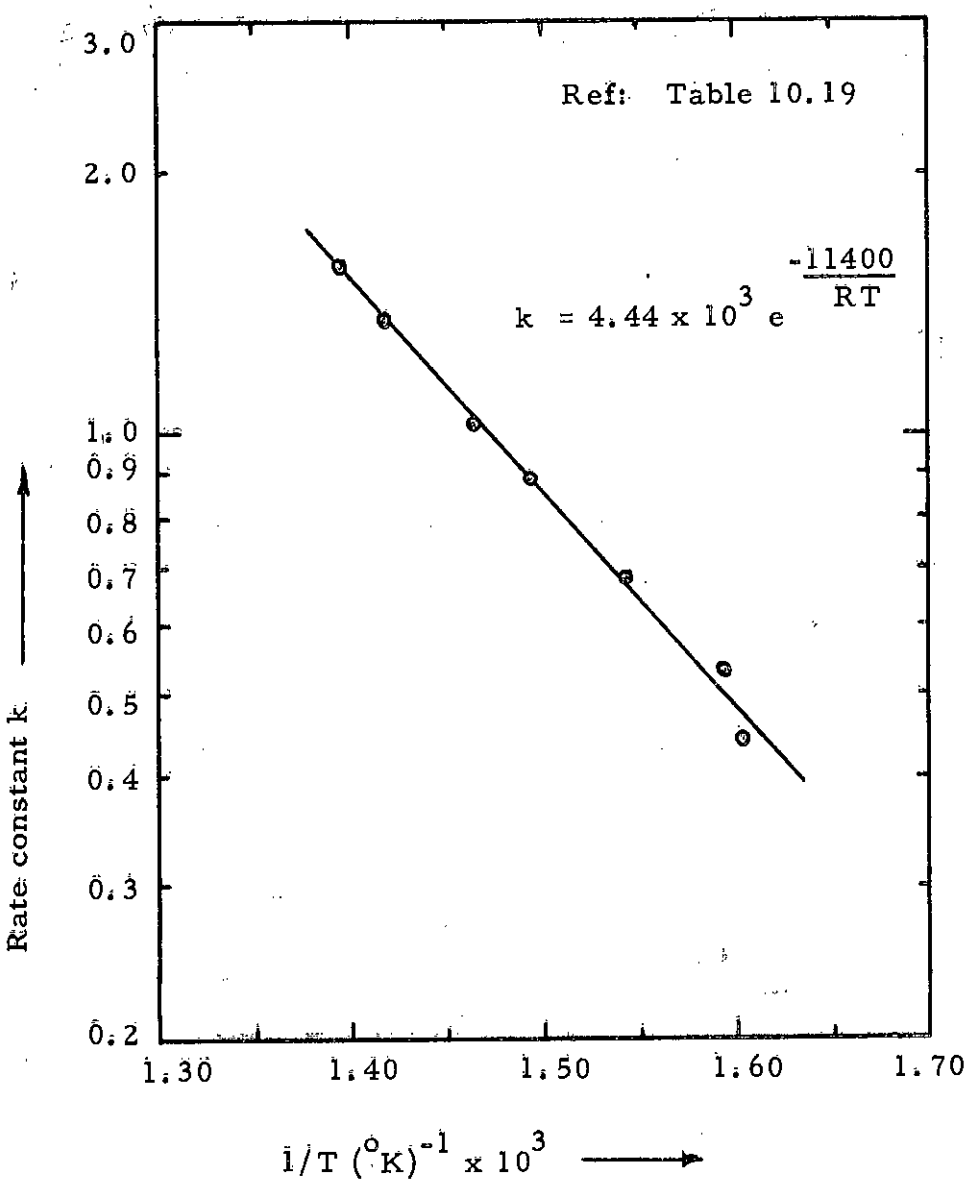

Fig. 6.2 Apparent Activation Energy of SSV Catalyst

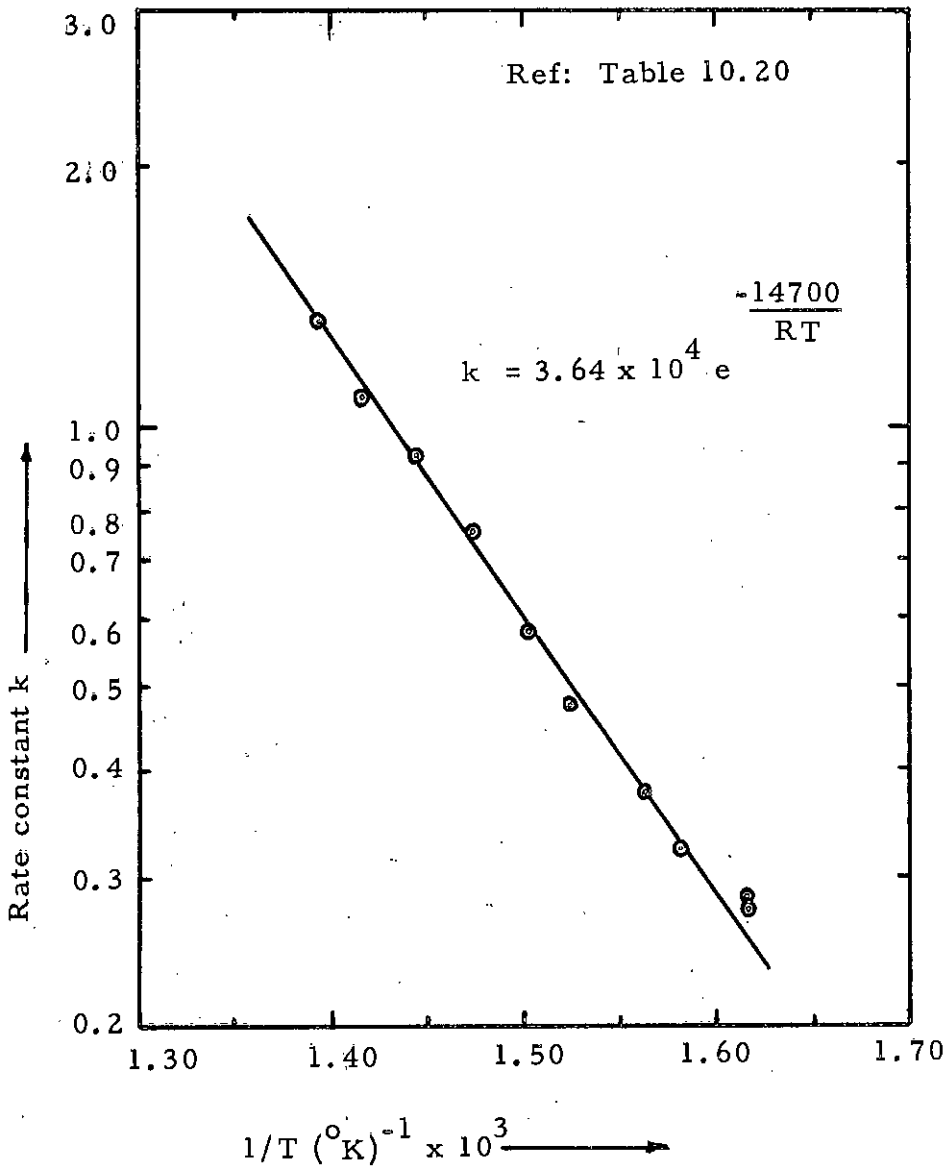

Fig. 6.3 Apparent Activation Energy of Power-Gas Catalyst

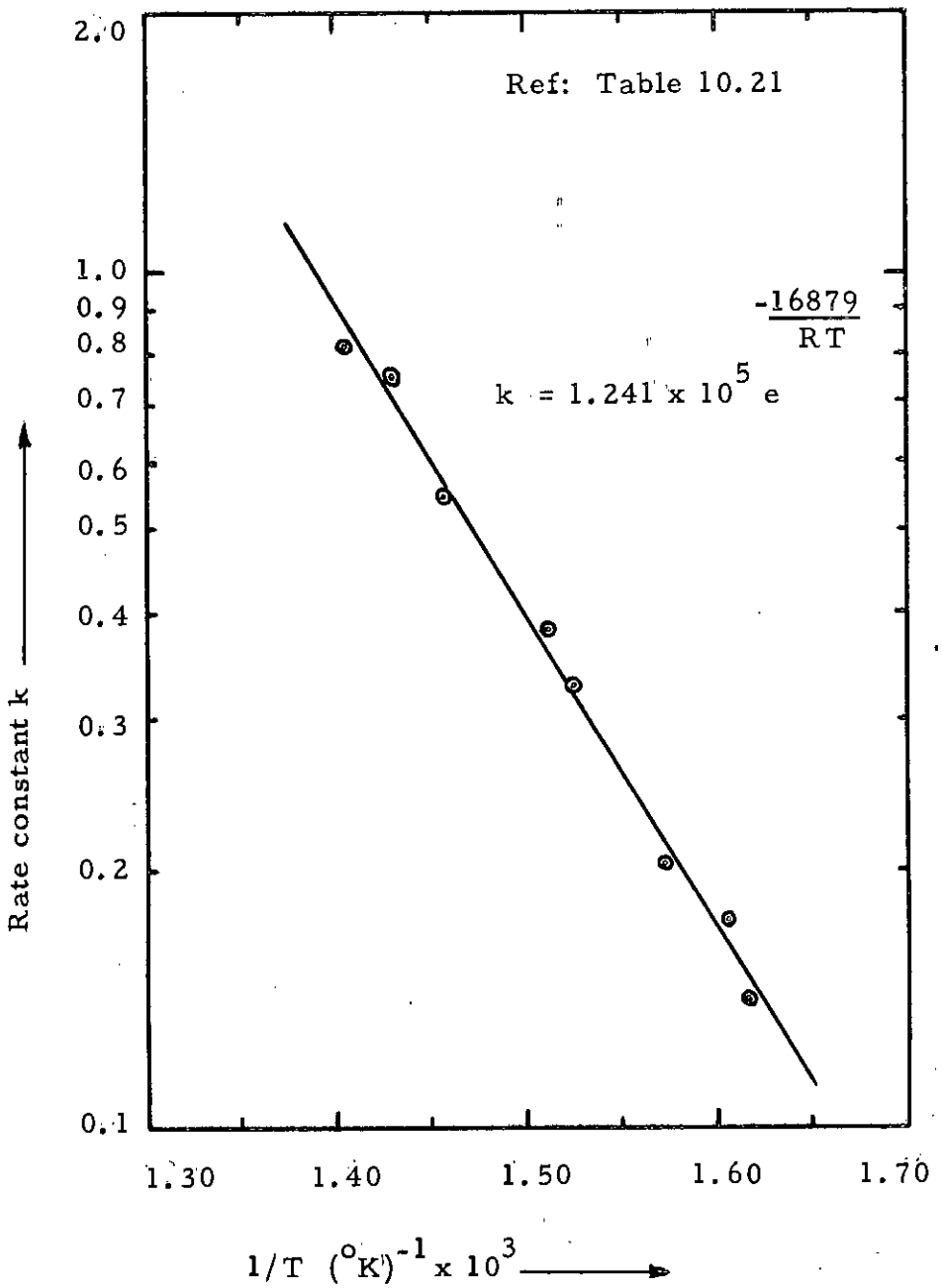

Fig. 6.4 Apparent Activation Energy of I.C.I. Catalyst

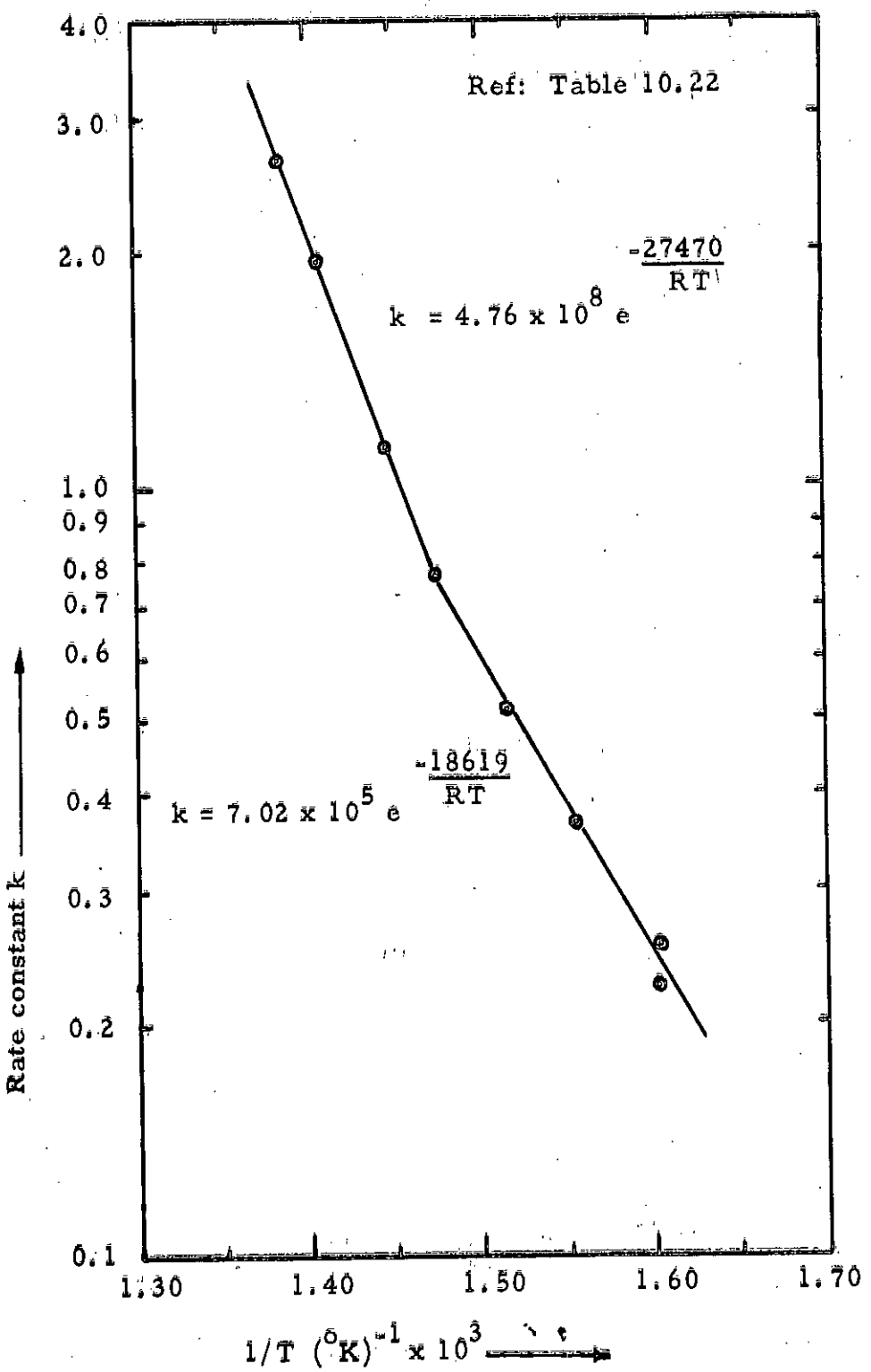

Fig.6.5 Apparent Activation Energy of Girdler G-3A Catalyst

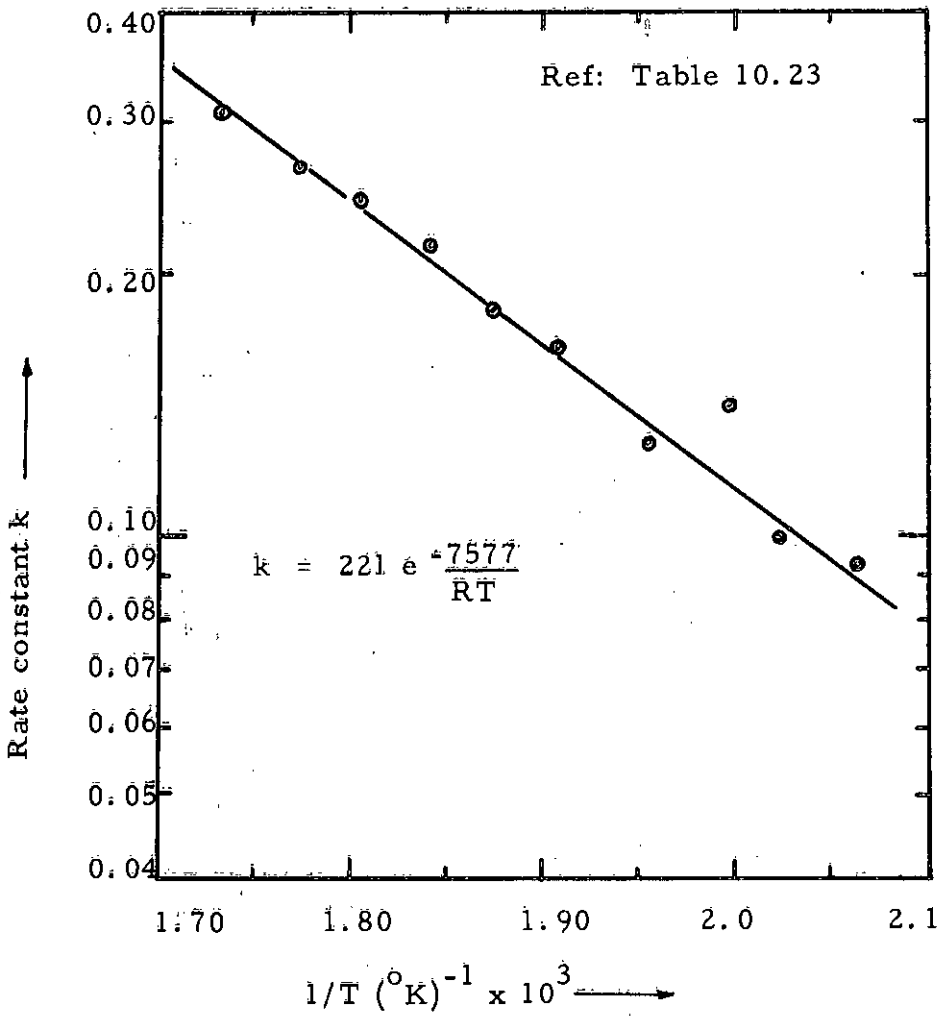

Fig. 6.6 Apparent Activation Energy of Girdler G-66 Catalyst

Chapter 7. DISCUSSION

In this chapter results obtained will be compared with the previous work and ways of expressing rate equations will be considered. The discussion falls naturally into two main sections - mass transfer effects and the kinetics of the reaction.

7.1 MASS TRANSFER EFFECTS

(a) External diffusion: The influence of mass transfer on the reaction rate of the shift reaction due to external diffusion has been studied by relatively few workers (section 3.2.4). In one case at reaction temperatures between 450° and 570°C and at volumetric flow rates between 3000 and 5000 cubic meters/hour the diffusional resistance was found to be negligible in comparison with the chemical resistance (64). On the other hand inhibition up to 10% has been observed at a temperature as low as 400°C (9). In the majority of work however mass transfer effects are assumed to be negligible without direct experimental tests.

In the present work mass transfer studies were carried out at a fixed contact time of 14.1 gms. of catalyst per gm.mol. of feed per minute (0.181 hr.$^{-1}$cm.$^{-2}$) and at three mass velocities (38.74, 47.86 and 58.85 gm.hr.$^{-1}$ cm.$^{-2}$) over a temperature range of 350° to 450°C. The results are shown in figure 6.1, where reaction rates for these three mass flow rates are plotted against reaction temperatures. It is evident that even at high temperatures reaction rate is independent of mass flow rate. If diffusion effects were important the plot would have produced three separate curves or straight lines. This result also showed that channelling in the bed was negligible and that catalyst distribution was uniform.

(b) Pore diffusion: Previous studies on shift catalysts (6, 9, 15, 64, 72, 84, 85) indicated that at relatively high temperatures (generally above 400°C) and down to a particle size of 2 mm. pore diffusion could be of importance. In order to avoid this complication catalyst particles with sizes between 0.6 and 0.5 mm. were used in the present work.

7.2 KINETICS OF THE REACTION

(a) Comparison of results with those obtained by previous workers: The summary of the results of previous kinetic studies on iron-oxide based shift catalysts given in Table 7.1 shows results that at first sight are quite conflicting. The forward reaction is first order with respect to CO (6, 9, 14 28, 42, 45, 58, 62, 64, 65, 68, 70, 72, 81, 84, 85, 86, 100), but fractional (11, 14, 57, 94) or zero (50) orders have been observed. The order with respect to H_2O may be zero (6, 9, 42, 45, 60, 70, 80, 84, 85), fractional (11, 14, 50, 58, 68, 85, 100), first order (28, 57, 72, 81, 86, 94) or even retarding (14). The forward reaction probably unaffected by H_2 (6, 9, 11, 14, 28, 42, 45, 57, 58, 64, 65, 68, 70, 72, 80, 81, 84, 85, 86, 89, 94, 100) although retardation (14, 62, 85) and acceleration (50) have been noted. Similarly authors find retardation by CO_2 (11, 14, 57, 58, 65, 68, 69, 89, 94, 100) but others find the rate unaffected (6, 9, 28, 42, 45, 50, 62, 64, 70, 72, 80, 81, 84, 85, 86).

Entries summarised in rows Y and Z in table 7.1 differed from the rest of the investigators by simply assuming either a straight forward first or second order rate equation.

Before attempting any comparison between these apparently widely divergent results and those obtained in the present work a number of difficulties inherent in any comparison must be considered.

Table 7.1 Summary of the results of previous kinetic studies on Iron-oxide based shift catalysts

Workers	Ref. No.	Order of reaction with respect to			
		CO	H_2O	CO_2	H_2
BELONOGOV and POPOV	9	1	0	-	-
BOHLBRO	11	0.8 to 1.0	0.2 to 0.35	-0.65 to -0.50	0
"	14	0.75	0.30	-0.35	-0.05
"	14	1.35	-0.15	-0.40	0
HEINZE and RIENACKER	42	1	0	-	-
HULBURT and SRINI VASAN	50	negligible	fractional	negligible	fractional (positive)
KIRILOV	57	0.5	1	-0.5	0
KODAMA et al	58	1	fractional	retarding	0
KULKOVA and TEMKIN	62	1	0.5	0	-0.5
POPOV	85	1	0, but fractional above 400°C	0	0, but retarding above 400°C
LAUPICHLER	64	1	-	-	-
LEBEDOR and POPOV	65	1	0, when used in large quantity	retarding	0
SAKSIN	94	0.5	1	-0.5	0
STELLING and KRUSENSTIERNA	100	1	fractional	retarding	0

Table 7.1 (cont'd)

Workers	Ref. No.	Order of reaction with respect to			
		CO	H_2O	CO_2	H_2
MARS	68	1	fractional	retard-ing	0
Y	28, 72, 81, 86.	1	1	-	-
Z	6, 45, 70, 80, 84.	1	0	-	-

Firstly in the vast majority of publications the actual composition of catalysts used is not given even when these have been produced by the workers concerned. Again when commercially made catalysts have been used their origin is not stated.

Secondly any comparison of the effect of concentration of molecular species on the reaction rate must be based on two distinct criteria. Stated in the simplest of terms these amount to whether a given species does affect the reaction rate and if so to what extent. The first criterion is not too difficult to determine and direct experimental evidence will usually provide an answer. It is possible however that the retarding effect of another species may mask the effect to a certain extent. The second criterion is usually expressed in terms of "molecularity" or "order of reaction" and here the difficulties often start. Determining this order of reaction usually means the correlation of experimental results by means of an equation derived on the basis of a given kinetic model. Since as pointed out in chapter 2 (page 15) two apparently dissimilar rate equations may correlate experimental results to an equal degree of accuracy divergence in order of reactions may be of doubtful significance. If results are expressed in terms of an exponential relationship then since this is a purely empirical procedure any indices determined in this way must be regarded with caution when considering reaction mechanism. In this case a comparison of indices is meaningful provided the statistical accuracy of the calculations is of the same order.

Thirdly in this and most of the other investigations conditions are chosen in such a manner as to minimise the effects of the backward reaction. In order to test for any possible contribution of the backward reaction this was expressed as a first approximation in the form:

$$r_b = \left[P_{CO_2}^{1+c} P_{H_2}^{1+d} P_{CO}^{1-a} P_{H_2O}^{1-b} \right] / K \qquad (7.1)$$

K, the equilibrium constant being obtained from the literature (section 3.1). The three relationships (eqn. 3.1, 3.2 and 3.3) gave at 430°C values of 8.83, 8.73 and 9.31 respectively, which are reasonably close. Equation 3.1 was actually used in the present calculation. For all iron-oxide based catalysts backward reaction rates were less than 10% of the forward reaction rate in the lower temperature range and less than 20% for the higher temperature range. For the Girdler G-66 catalyst backward rates were less than 5% of the forward rate. Since these values as shown in a later section fall well within the accuracy of the exponential relationship used, the effect of any backward reaction will not be considered significant for the purposes of further agreement.

Turning now to the results obtained in the present work the effect of individual molecular species will be discussed first before making any general comparisons.

Effect of Carbon monoxide

A strong effect of carbon monoxide on the reaction rate was found for all catalysts studied. Values of "a" the exponent of p_{CO} varied widely from 0.63 to 1.42 (SSV 0.63 and 0.97, Power-gas 0.92 and 1.22, I.C.I. 1.13 and 1.06, Girdler G-3A 1.42 and 1.06 and Girdler G-66 0.68). Direct comparison of these results with those obtained by previous workers is only possible in two cases, where known catalysts were used in conjunction with an exponential type of rate equation. The first (11) using the SSV catalyst obtained values of "a" between 0.8 to 1.0 (330°-500°C) which is in reasonable agreement with the present work. The other (14) used a laboratory made catalyst containing 1.9% NaOH at 380°C and gave a value of 1.35 for "a" which agrees with 1.42 for the Girdler catalyst

(350°-380°C).

Possible reasons for "a" being greater than 1.0 have been discussed by BOHLBRO (14) who considered the possibility of a compound consisting of more than one CO group taking part in the rate determining step. A mechanism given by BASOLO and PEARSON (8) comprising iron carbonyl and iron hydrocarbonyl in the presence of alkali might seem to be a possibility.

Most of the other workers either obtained or assumed "a" as unity.

Effect of Steam

The effect of steam on the forward reaction rate was also found to be quite marked. Values of "b" for all the catalysts were fractional and nearly uniform (SSV 0.59 and 0.64, Power-Gas 0.57 and 0.56, I.C.I. 0.53 and 0.80, Girdler G-3A 0.63 and 0.77 and Girdler G-66 0.57). This agrees reasonably well with the results from BOHLBRO'S study (11) on SSV catalyst and those of a large number of other workers (11, 14, 50, 58, 68, 85, 100).

Effect of Carbon dioxide

Quite a strong retardation of the rate of reaction was observed in keeping with the findings of other workers (11, 14, 57, 58, 65, 68, 69, 89, 94, 100) and individual values of "c" varied but little (SSV - 0.46 and -0.47, Power-Gas -0.34 and -0.52, I.C.I. -0.90 and -0.52 and Girdler G-3A -0.77 and -0.54). The exception to this proved to be the Girdler G-66 catalyst where the retardation was not large enough to be significant. Values for the SSV catalyst compared quite well with those of BOHLBRO (-0.65 to -0.5) (11).

Effect of Hydrogen

Looking at table 7.1 apparently contradictory results indicate no effect in some cases and a considerable retardation in others. In the present work hydrogen exhibited a retarding effect in some cases (Power-Gas

I.C.I. 350°-380°C, Girdler G-3A 400°-430°C and Girdler G-66) whilst for the rest of the catalysts no significant effect was observed. Although not significant values of "d" are given for the purpose of comparison for catalysts where a significant effect was observed in a higher or lower temperature range. Again results in the case of the SSV catalyst agrees with previous work in showing no significant retarding effect.

Overall comparison

It appears from the previous discussion that these seemingly contradictory results obtained by various workers can be valid, any divergence being due to the different detailed composition of the catalyst. Again it must be noted that not only catalyst composition but also temperature could be responsible for different effects of molecular species on the reaction rate. A similar effect has been observed in the catalytic oxidation of carbon monoxide to carbon dioxide on a ferric oxide catalyst where the reaction is first order below about 300°C but tends to zero order at higher temperatures.

Unfortunately even if the detailed compositions of the commercial catalysts used in the present investigation were known it would be extremely difficult to account either qualitatively or quantitatively for the effects observed. This does not mean that mechanisms could not be postulated but that the difficulty would be to substantiate the postulated mechanism. For a considerable time to come the design engineer will have to be satisfied with expressing results in terms of an exponential expression obtained by experiment. The value of such expressions will be discussed in the next section.

(b) The suitability of the exponential expression for the correlation of the data: As mentioned previously in chapter 6 though some interactions were large anough to be significant, these were not considered during correlations of the present data. The exponential form of equation considered for this reaction (eqn. 4.6) is not able to deal directly with any form of interaction. When considering the statistical significance of main effects and interactions care must be taken that an apparent non significance is not caused by too close an interval between two levels of a particular variable. For the present work this was avoided by choosing uniform values at both levels for all partial pressures of the constituents.

How well the rates can be expressed by equation 4.6, which only considered the main effects is shown in figures 7.1 to 7.5. It is observed that at the high temperature range for all the iron oxide based catalysts (except I.C.I.) the rates were very well predicted. At the low temperature range and for Girdler G-66 catalyst the predicted rates were not as good as that obtained at high temperatures. This is partly due to small reaction rate values at low temperatures at which experimental errors are magnified and partly due to presence of interactions in some of the experimental data. Generally at low temperatures more interactions were obtained than at high temperatures. Before attaching much importance to the interactions further factorial experiments should be performed with the factors involved in the interactions at 3 or more levels. It should also be stressed that values obtained in the present work are applicable only in the range of variables covered.

Table 7.2 shows results depicted in fig. 7.1 to 7.5 in numerical form where error is defined as

$$\left[\frac{r_{calculated} - r_{experimental}}{r_{experimental}} \right] 100$$

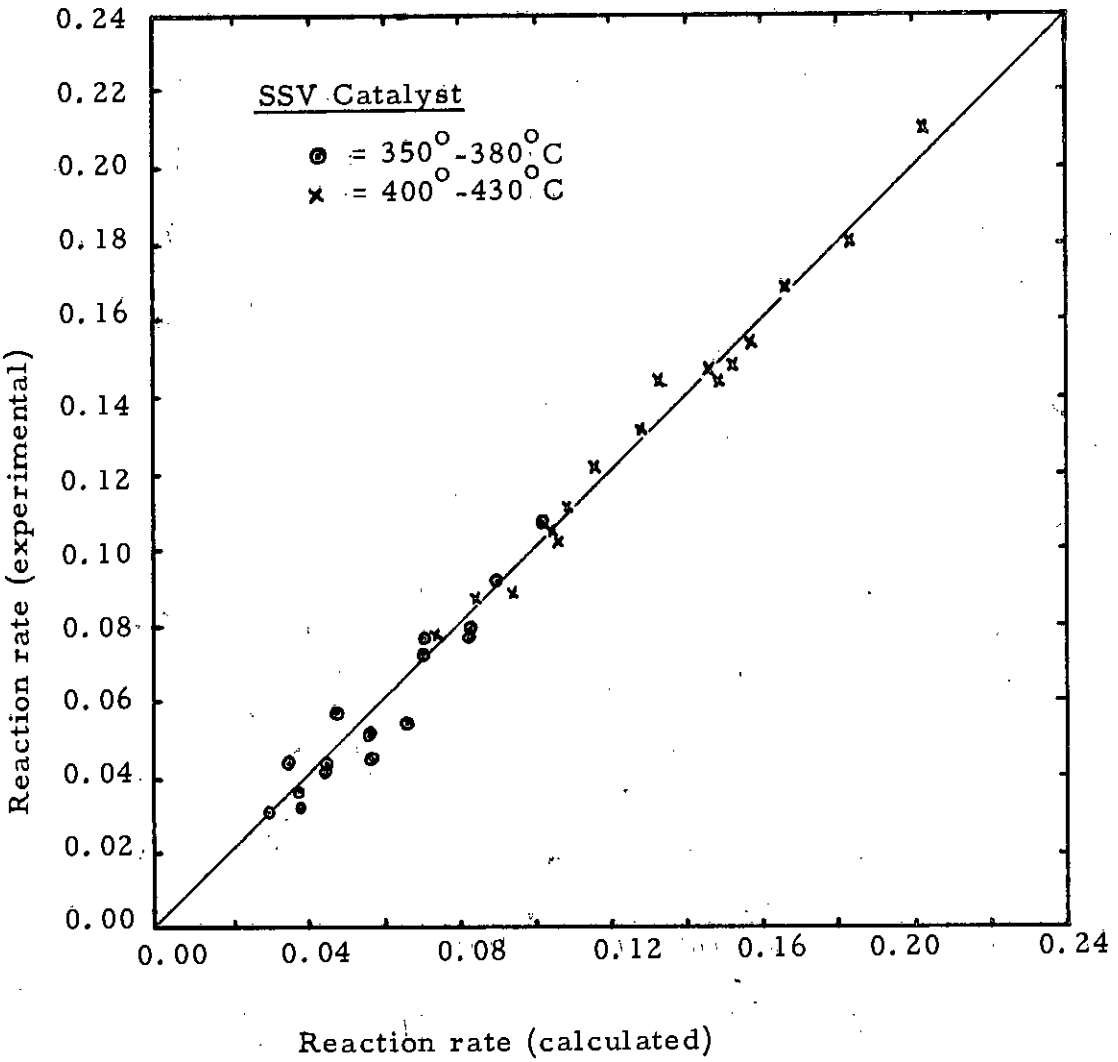

Fig. 7.1 Comparison of experimental and calculated rates

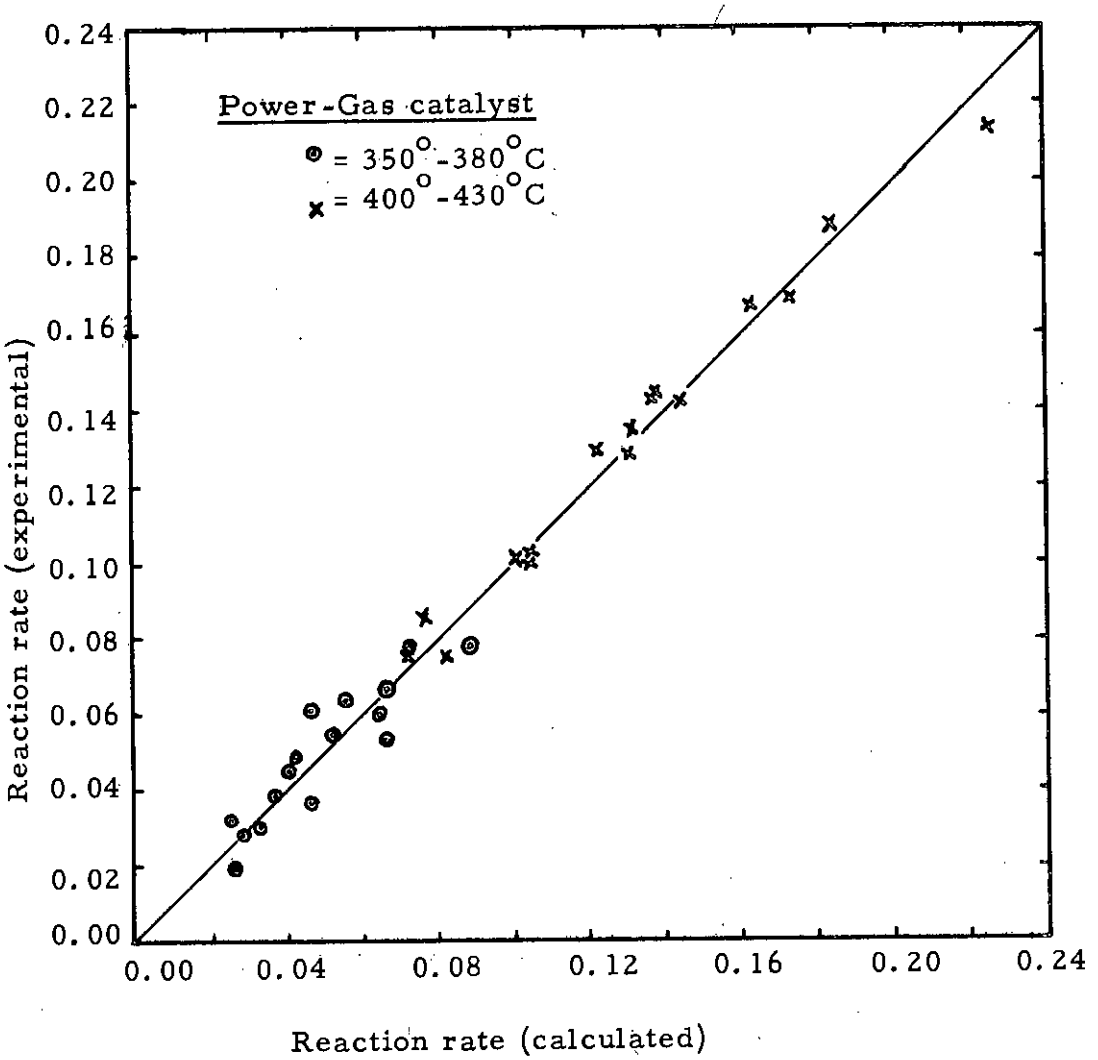

Fig. 7.2 Comparison of experimental and calculated rates

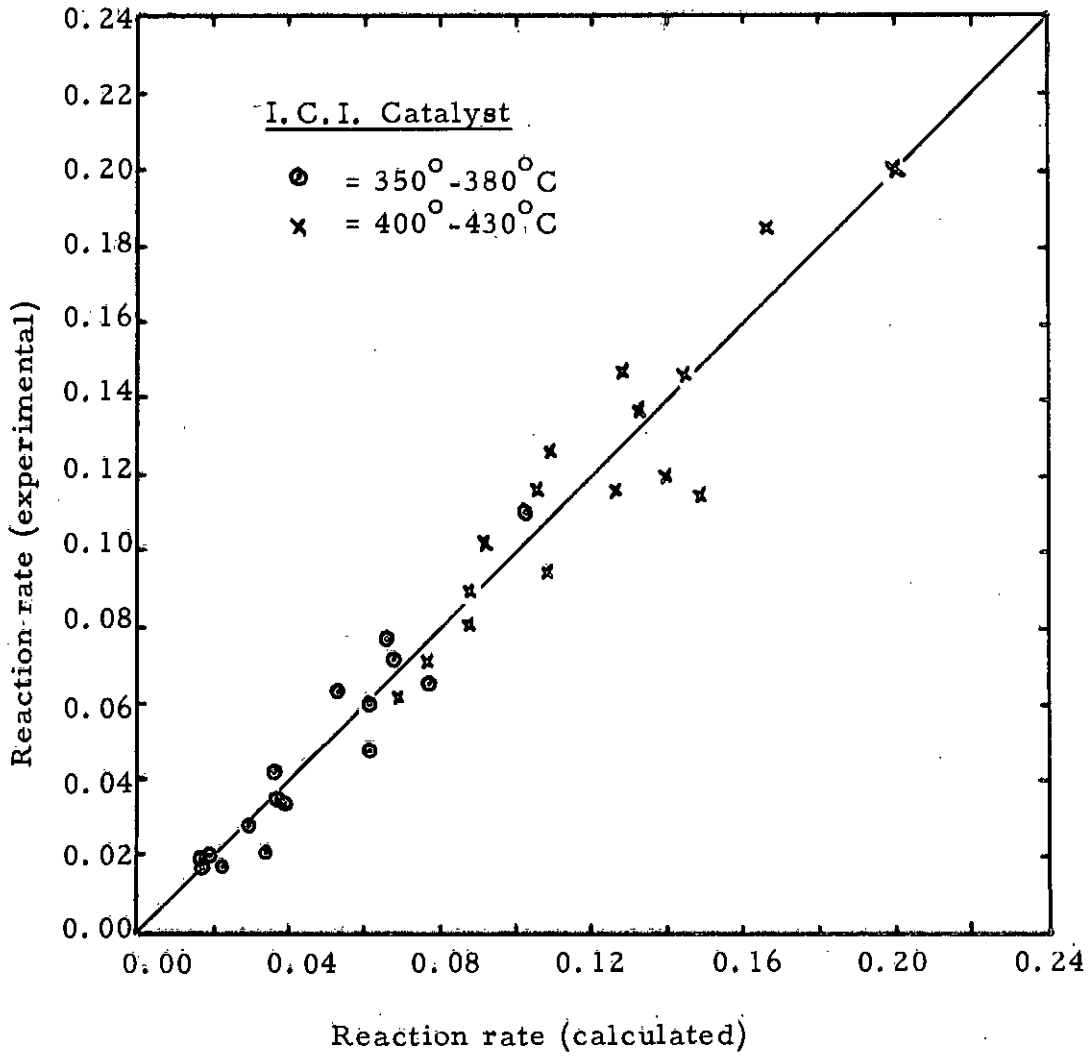

Fig. 7.3 Comparison of experimental and calculated rates

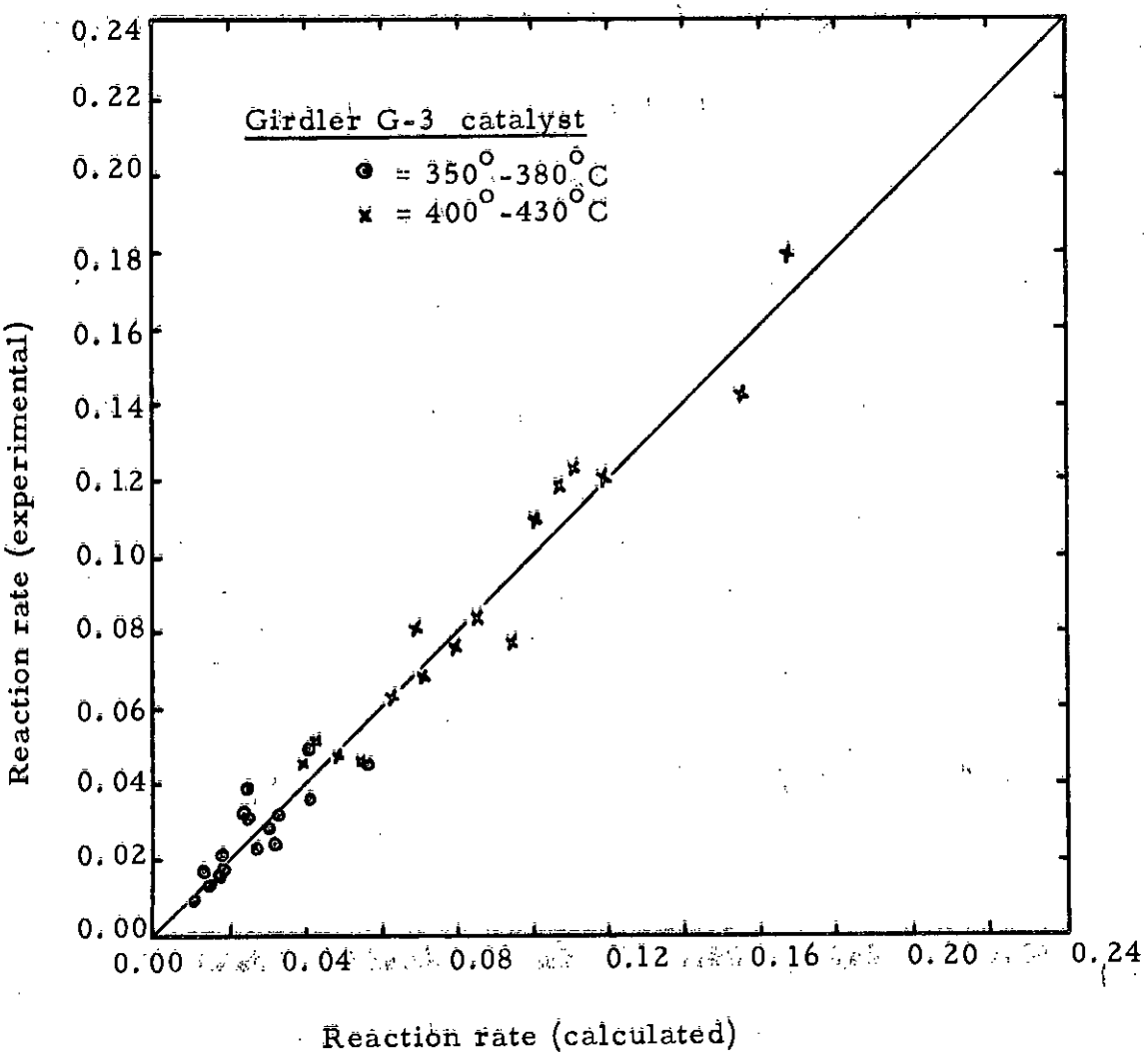

Fig. 7.4 Comparison of experimental and calculated rates

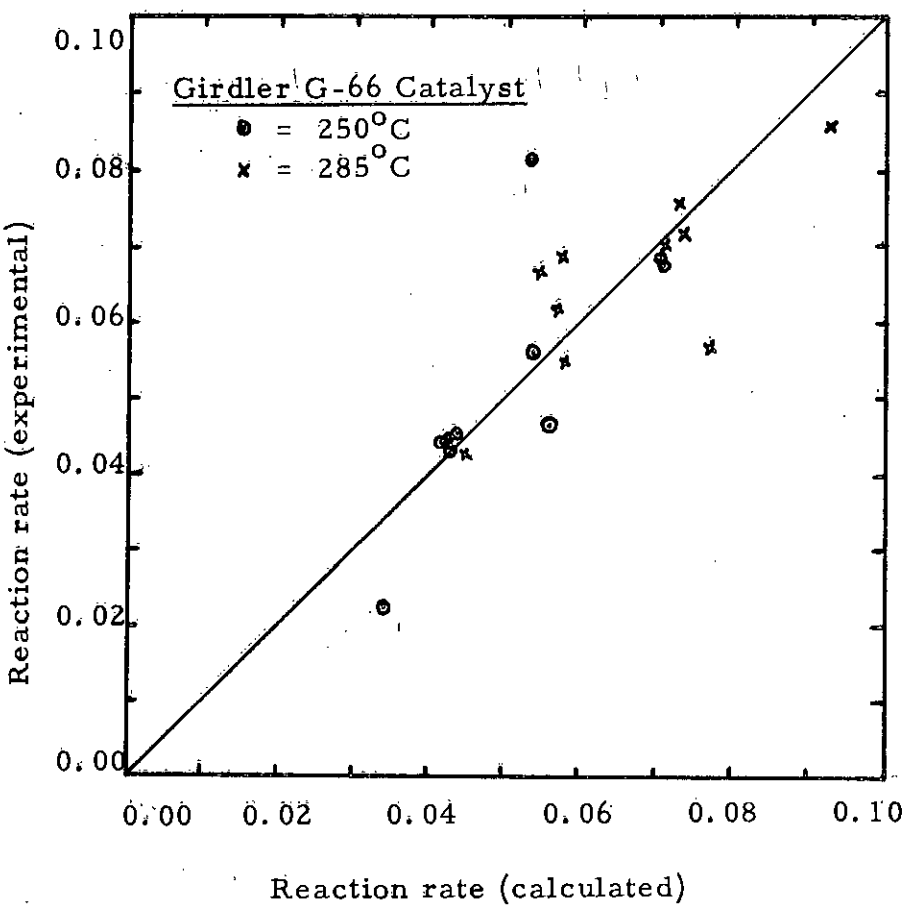

Fig. 7.5 Comparison of experimental and calculated rates

Table 7.2 Error in correlation of experimental data by the exponential type rate expression

Catalysts	Temperature range (°C)	Percentage error		
		- Maximum	+	Mean
SSV	350-380	19.0	28.0	10.2
	400-430	13.6	8.0	4.6
Power-Gas	350-380	23.1	38.8	13.4
	400-430	9.8	10.2	4.0
I.C.I.	350-380	16.8	53.2	12.6
	400-430	13.6	28.5	9.7
Girdler G-3A	350-380	35.6	45.0	18.3
	400-430	17.5	24.6	9.8
Girdler G-66	250-285	34.9	52.7	13.8

Agreement between experimental values and those obtained by using the exponential expression is as good as can be obtained using a more complex expression based on a Hougen-Watson or Langmuir - Hinshelwood model and should therefore be used for design purposes.

(c) The relative activity of the catalysts used: It was realised from the outset that the 2^5 factorial design was unsuitable for the accurate determination of apparent activation energies since the two temperature levels were too close together. Nevertheless plots of log k against 1/T were done in order to see whether the slope gave apparent activation energies of reasonable order of magnitude. An average rate equation was used for each catalyst although values for a, b, c and d sometimes differed significantly at the two temperature ranges.

A straight line was obtained for each catalyst (Fig. 6.2, 6.3, 6.4 and 6.6) with the exception of Girdler G-3A (Fig. 6.5) where a distinct discontinuity in slope was observed at 405°C. This type of temperature dependence of rate constants has not been reported before for the shift catalysts but has been observed in the case of some other reactions. This type of behaviour may be explained by the assumption that the rate constant is really composed of two each with its own energy of activation (23).

Considering figures 6.2 to 6.6 and 10.1 to 10.5 it is evident that catalysts can be arranged in order of decreasing activity: Girdler G-66, SSV, Power-Gas, I.C.I., Girdler G-3A (at low temperatures). A previous study (70) also gave the same order for the Power-Gas, I.C.I. and Girdler G-3A catalysts. A.B. Svenska Saltpeterverken in their commercial literature claim a very high activity for their catalyst. This agrees with the present findings.

(d) Consideration of possible mechanisms: As often stated in the literature (17, 100, 109) it is necessary to apply the utmost caution when trying to deduce a mechanism from the rate expression since different mechanisms may very well yield rate expressions which are approximation to each other.

A number of mechanisms have been presented for the water-gas shift reaction on iron-oxide based catalysts. A rate determining step (11, 58, 100) could be the reaction between gaseous CO and oxidised surface sites, or perhaps chemisorption of CO. CO_2 and H_2O are assumed to be strongly adsorbed on the surface, where as H_2 is considered as not adsorbed. The rate controlling step (14) could also be a surface reaction between adsorbed CO and oxidised surface. Other mechanisms in which reaction occurs between the gaseous components and reduced and unreduced surface sites have been suggested by many investigators. In one case the reduction of surface by CO was found to be rate controlling (62) and the oxidation reaction was considered to be in equilibrium. It has also been suggested (85) that the oxidation of CO could involve the ferric-ferrous iron equilibrium on the catalyst surface. Even the oxidation of surface by H_2O has been considered as the rate controlling step (50) with the ferric-ferrous iron in equilibrium.

As mentioned previously determination of a possible reaction mechanism was not the primary object of this work. It would be interesting however to fit the experimental data by a Hougen-Watson type of rate expression based on a probable reaction mechanism. The reaction mechanism considered consists of the following steps:

$$CO + Ol \rightleftharpoons CO.Ol \qquad k_1, k_1' \qquad (7.2)$$

$$CO.Ol \rightleftharpoons CO_2.1 \qquad k_2, k_2' \qquad (7.3)$$

$$CO_2.1 \rightleftharpoons CO_2 + 1 \qquad k_3, k_3' \qquad (7.4)$$

$$H_2O + 1 \rightleftharpoons H_2O.1 \qquad k_4, k_4' \qquad (7.5)$$

$$H_2O.1 \rightleftharpoons H_2.Ol \qquad k_5, k_5' \qquad (7.6)$$

$$H_2.Ol \rightleftharpoons H_2 + Ol \qquad k_6, k_6' \qquad (7.7)$$

where Ol = oxidised surface site

1 = reduced surface site

k_1, k_2, etc. = forward rate constants

k_1', k_2' etc. = backward rate constants.

and $K_1 = k_1/k_1'$

Amongst the above mentioned six steps the adsorption of CO is considered to be rate controlling. The total number of surface sites of all types is given by

$$L = [Ol]\ (p_{H_2O} + A\, p_{H_2}\, p_{H_2O} + B\, p_{H_2} + C\, p_{CO_2}\, p_{H_2})/p_{H_2O} \qquad (7.8)$$

where $A = (1 + K_5)/K_5K_6$

$B = 1/K_4K_5K_6$

$C = (1 + K_2)/K_2K_3K_4K_5K_6$

The rate of reaction $r = k_1\, p_{CO}\ [Ol]$ (7.9)

or $r = k_1 L\, p_{CO}\, p_{H_2O}/(p_{H_2O} + A\, p_{H_2}\, p_{H_2O} + B\, p_{H_2} + C\, p_{CO_2}\, p_{H_2})$ (7.10)

$$\text{or } \frac{1}{r} = \frac{1}{k_1 L} \cdot \frac{1}{p_{CO}} + \frac{A}{k_1 L} \cdot \frac{p_{H_2}}{p_{CO}} + \frac{B}{k_1 L} \cdot \frac{p_{H_2}}{p_{CO} p_{H_2O}} +$$

$$\frac{C}{k_1 L} \cdot \frac{P_{CO_2} P_{H_2}}{P_{CO} P_{H_2O}} \qquad (7.11)$$

Experimental data showing strong interactions with temperature suggest a kinetic expression with more than one temperature dependent rate constant. For this reason experimental data for Girdler G-3A (350°-380°C) were chosen to try out equation 7.11, although it was realised that this expression showed a strong dependence on H_2.

A multiple regression fitting gave the values of

$$\frac{1}{k_1 L} = 5.45 \pm 3.36$$

$$\frac{A}{k_1 L} = -32.56 \pm 34.87$$

$$\frac{B}{k_1 L} = 1.04 \pm 3.95$$

$$\frac{C}{k_1 L} = 22.18 \pm 22.50$$

and shows that it was not a good correlation. Moreover the -ve value of the coefficient, according to Hougen-Watson, automatically rejects the mechanism. The mean percentage error in predicting rates by using equation 7.11 was $\pm$ 32.4 (maximum +74% and -50.8%).

Due to lack of time it was not possible to test equations 3.5a (58) and 3.14 (100) which agree qualitatively with the findings for the SSV catalyst. It is hoped to do this for a paper arising out of this work. It is also evident, that for the low temperature catalyst (Girdler G-66) a mechanism radically different from those applying to an iron oxide based catalyst must

be postulated. One possibility might be the reduction of surface by gaseous CO as the rate controlling step in a mechanism where the reaction occurs between the gaseous components and reduced and unreduced surface sites (62).

Chapter 8. CONCLUSIONS

(a) Using a contact time of 0.181 hr.$^{-1}$ cm.$^{-2}$ no appreciable mass transfer effects were noticed even at the lowest mass flow rate (38.74 gm. hr.$^{-1}$ cm.$^{-2}$) and highest temperature (450°C).

(b) The rate of reaction increases with the partial pressure of carbon monoxide for all the catalysts.

(c) The rate of reaction also increases with the partial pressure of water for all the catalysts but the effect is relatively smaller than that of carbon monoxide.

(d) The partial pressure of carbon dioxide strongly reduces the reaction rate for all the catalysts except for Girdler G-66, where the effect was negligible.

(e) The rate was not affected by the partial pressure of hydrogen for SSV, I.C.I. (400°-430°C) and Girdler G-3A (350°-380°C) catalysts but reduced the rates for the rest.

(f) Any divergence in the results obtained by other workers (table 7.1) may be due to the different composition of the catalysts. Temperature may also modify the reaction path.

(g) The exponential form of rate expression is sufficiently accurate for representing the experimental data and thus can be used with confidence for design purposes.

(h) On an experimental basis the commercial catalysts used can be arranged in order of decreasing activity: Girdler G-66, SSV, Power-Gas, I.C.I., Girdler G-3A (at low temperatures).

Chapter 9. RECOMMENDATIONS FOR FURTHER WORK

The findings of the present work require confirmation by repeating the factorial experiments at higher partial pressures of the components involved.

Experiments similar to the present work should be carried out with a number of laboratory prepared catalysts with different and known compositions.

To confirm the presence of interactions observed in the present work further factorial experiments should be performed varying only factors involved in interactions at three or more levels.

Chapter 10 EXPERIMENTAL DATA

Table 10.1 Factorial Experiment: SSV Catalyst (350°-380°C)

Treatment Combination Number	Average of inlet and outlet partial pressures (atm.)				Total flow rate (gm.mol/min)	r = reaction rate gm.mol./hr.(gm. of catalyst)
	p_{CO}	p_{H_2O}	p_{CO_2}	p_{H_2}		
TCN-1	0.14401	0.09427	0.10539	0.10469	0.4598	0.04289
TCN-2	0.09509	0.14520	0.10529	0.10548	0.4531	0.04155
TCN-3	0.09653	0.09654	0.15538	0.10378	0.4518	0.03089
TCN-4	0.14309	0.14309	0.15562	0.10689	0.4551	0.05624
TCN-5	0.09507	0.09507	0.10342	0.15605	0.4510	0.04343
TCN-6	0.14392	0.14392	0.10644	0.15488	0.4587	0.04504
TCN-7	0.14529	0.09556	0.15611	0.15312	0.4599	0.03224
TCN-8	0.09523	0.14580	0.15542	0.15464	0.4537	0.03591
TCN-9	0.09301	0.09301	0.10634	0.10628	0.4583	0.05445
TCN-10	0.13576	0.13576	0.11588	0.11199	0.4604	0.10692
TCN-11	0.14006	0.09030	0.16113	0.10875	0.4594	0.07594
TCN-12	0.09130	0.14128	0.15849	0.10888	0.4545	0.07173
TCN-13	0.13917	0.08969	0.11042	0.15775	0.4646	0.07728
TCN-14	0.09020	0.14010	0.10820	0.15955	0.4561	0.07943
TCN-15	0.09363	0.09363	0.15713	0.15576	0.4573	0.05015
TCN-16	0.13815	0.13815	0.16038	0.16057	0.4589	0.09215
TCN-1R	0.14409	0.09436	0.10619	0.10455	0.4600	0.04200
TCN-5R	0.09497	0.09497	0.10316	0.15538	0.4537	0.04200
TCN-10R	0.13452	0.13452	0.11366	0.11328	0.4591	0.12180
TCN-13R	0.13786	0.08819	0.10937	0.16016	0.4611	0.09206

Table 10.2 Factorial Experiment: SSV Catalyst (400°-430°C)

Treatment Combination Number	Average of inlet and outlet partial pressures (atm.)				Total flow rate (gm.mol/min)	r = reaction rate gm.mol./hr.(gm. of catalyst)
	p_{CO}	p_{H_2O}	p_{CO_2}	p_{H_2}		
TCN-1	0.13291	0.08339	0.11720	0.11481	0.4648	0.13137
TCN-2	0.08648	0.13642	0.11281	0.11329	0.4606	0.11059
TCN-3	0.09054	0.09054	0.15961	0.10907	0.4613	0.07657
TCN-4	0.13213	0.13213	0.16751	0.11710	0.4624	0.14418
TCN-5	0.08931	0.08931	0.11070	0.16019	0.4614	0.08668
TCN-6	0.13091	0.13091	0.12170	0.16611	0.4689	0.14776
TCN-7	0.13703	0.08723	0.16530	0.16180	0.4631	0.10271
TCN-8	0.08917	0.13912	0.16055	0.16058	0.4605	0.08848
TCN-9	0.08478	0.08478	0.11543	0.11408	0.4648	0.12197
TCN-10	0.12367	0.12367	0.12874	0.12427	0.4673	0.21000
TCN-11	0.13077	0.08095	0.16819	0.11830	0.4630	0.15483
TCN-12	0.08230	0.13237	0.16490	0.11797	0.4583	0.14641
TCN-13	0.12880	0.07922	0.11723	0.16865	0.4675	0.16683
TCN-14	0.08214	0.13198	0.11650	0.16701	0.4627	0.14516
TCN-15	0.08730	0.08730	0.15800	0.16313	0.4580	0.10558
TCN-16	0.12520	0.12520	0.16580	0.17101	0.4643	0.18170
TCN-1R	0.13427	0.08470	0.11737	0.11357	0.4676	0.12089
TCN-4R	0.13198	0.13198	0.16790	0.11772	0.4607	0.14722
TCN-11R	0.13215	0.08228	0.16270	0.11719	0.4620	0.14444
TCN-15R	0.08863	0.08863	0.15800	0.16129	0.4595	0.09358

Table 10.3 Factorial Experiment: Power Gas Catalyst (350°-380°C)

Treatment Combination Number	Average of inlet and outlet partial pressures (atm.)				Total flow rate (gm.mol/min)	r = reaction rate $\frac{\text{gm.mol.}}{\text{hr.}\ (\text{gm. of catalyst})}$
	P_{CO}	P_{H_2O}	P_{CO_2}	P_{H_2}		
TCN-1	0.14416	0.09415	0.10535	0.10586	0.4630	0.04854
TCN-2	0.09550	0.14557	0.10691	0.10481	0.4616	0.03851
TCN-3	0.09816	0.09816	0.15402	0.10299	0.4578	0.01979
TCN-4	0.14417	0.14417	0.15815	0.10868	0.4527	0.06116
TCN-5	0.09627	0.09627	0.10421	0.15393	0.4623	0.03152
TCN-6	0.14555	0.14555	0.10688	0.15450	0.4629	0.03707
TCN-7	0.14695	0.09675	0.15155	0.15424	0.4594	0.03000
TCN-8	0.09765	0.14821	0.15223	0.15519	0.4528	0.02830
TCN-9	0.09367	0.09367	0.10584	0.10717	0.4592	0.05552
TCN-10	0.14031	0.14031	0.11055	0.10953	0.4629	0.07889
TCN-11	0.14281	0.09249	0.15788	0.10876	0.4573	0.06663
TCN-12	0.09459	0.14512	0.15828	0.10754	0.4534	0.05257
TCN-13	0.14264	0.09270	0.11356	0.15702	0.4641	0.05973
TCN-14	0.09264	0.14286	0.11091	0.15850	0.4589	0.06420
TCN-15	0.09522	0.09522	0.15785	0.15660	0.4563	0.04504
TCN-16	0.14201	0.14201	0.15949	0.16140	0.4527	0.07862
TCN-4R	0.14465	0.14465	0.15679	0.10830	0.4524	0.05767
TCN-8R	0.09762	0.14810	0.15301	0.15474	0.4544	0.02704
TCN-9R	0.09373	0.09373	0.10870	0.10690	0.4602	0.05427
TCN-10R	0.13950	0.13950	0.11264	0.11140	0.4597	0.09089

Table 10.4 Factorial Experiment: Power Gas Catalyst (400^{o}-430^{o}C)

Treatment Combination Number	Average of inlet and outlet partial pressures (atm.)				Total flow rate (gm.mol/min)	r = reaction rate $\frac{\text{gm.mol.}}{\text{hr. (gm.of catalyst)}}$
	p_{CO}	p_{H_2O}	p_{CO_2}	p_{H_2}		
TCN-1	0.13450	0.08437	0.11383	0.11603	0.4570	0.12960
TCN-2	0.08828	0.13878	0.11147	0.11371	0.4499	0.10240
TCN-3	0.09173	0.09173	0.15843	0.11104	0.4464	0.07719
TCN-4	0.13437	0.13437	0.16585	0.11999	0.4434	0.14490
TCN-5	0.09038	0.09038	0.10730	0.16218	0.4496	0.08570
TCN-6	0.13333	0.13333	0.11801	0.16875	0.4525	0.14350
TCN-7	0.13892	0.08848	0.16000	0.16375	0.4507	0.10030
TCN-8	0.09181	0.14239	0.15731	0.16608	0.4484	0.07504
TCN-9	0.08482	0.08482	0.11853	0.11664	0.4522	0.12890
TCN-10	0.12444	0.12444	0.12844	0.12603	0.4553	0.21310
TCN-11	0.13077	0.08019	0.17106	0.12209	0.4486	0.16830
TCN-12	0.08451	0.13523	0.16463	0.11849	0.4459	0.13530
TCN-13	0.12955	0.07952	0.11964	0.17062	0.4583	0.16840
TCN-14	0.08277	0.13299	0.11512	0.16836	0.4548	0.14400
TCN-15	0.08828	0.08828	0.15983	0.16334	0.4528	0.10050
TCN-16	0.12803	0.12803	0.16899	0.17485	0.4502	0.18880
TCN-3R	0.09250	0.09250	0.15856	0.10969	0.4490	0.06913
TCN-4R	0.13421	0.13421	0.16892	0.12000	0.4438	0.14560
TCN-9R	0.08567	0.08567	0.11517	0.11469	0.4572	0.11830

Table 10.5 Factorial Experiment: I.C.I. Catalyst (350°-380°C)

Treatment Combination Number	Average of inlet and outlet partial pressures (atm.)				Total flow rate (gm.mol/min)	r = reaction rate $\frac{\text{gm.mol.}}{\text{hr.}(\text{gm. of catalyst})}$
	P_{CO}	P_{H_2O}	P_{CO_2}	P_{H_2}		
TCN-1	0.14431	0.09445	0.10726	0.10497	0.4588	0.04325
TCN-2	0.09626	0.14620	0.10618	0.10350	0.4572	0.02964
TCN-3	0.09805	0.09805	0.15354	0.10250	0.4536	0.01809
TCN-4	0.14729	0.14729	0.15523	0.10270	0.4562	0.02212
TCN-5	0.09720	0.09720	0.10607	0.15218	0.4584	0.02095
TCN-6	0.14518	0.14518	0.10753	0.15389	0.4590	0.03582
TCN-7	0.14776	0.09776	0.15595	0.15226	0.4561	0.01836
TCN-8	0.09787	0.14791	0.15330	0.15253	0.4547	0.01863
TCN-9	0.09396	0.09396	0.10942	0.10579	0.4572	0.04845
TCN-10	0.13574	0.13574	0.11592	0.11281	0.4615	0.11070
TCN-11	0.14068	0.09069	0.16023	0.10815	0.4564	0.07585
TCN-12	0.09261	0.14288	0.15680	0.10845	0.4513	0.06412
TCN-13	0.14102	0.09135	0.10949	0.15699	0.4623	0.06609
TCN-14	0.09227	0.14211	0.10923	0.15689	0.4592	0.06080
TCN-15	0.09530	0.09530	0.15680	0.15400	0.4587	0.03627
TCN-16	0.14096	0.14096	0.16041	0.15908	0.4560	0.07397
TCN-1R	0.14432	0.09446	0.10712	0.10496	0.4588	0.04316
TCN-7R	0.14713	0.09708	0.15460	0.15408	0.4552	0.02165
TCN-9R	0.09348	0.09348	0.10670	0.10613	0.4579	0.05185
TCN-10R	0.13580	0.13580	0.11548	0.11325	0.4601	0.11270

Table 10.6 Factorial Experiment: I.C.I. Catalyst (400°-430°C)

Treatment Combination Number	Average of inlet and outlet partial pressures (atm.)				Total flow rate (gm.mol/min.)	r = reaction rate $\frac{\text{gm.mol.}}{\text{hr.(gm. of catalyst)}}$
	P_{CO}	P_{H_2O}	P_{CO_2}	P_{H_2}		
TCN-1	0.13462	0.08464	0.12065	0.11530	0.4589	0.12600
TCN-2	0.08858	0.13871	0.11245	0.11194	0.4562	0.09546
TCN-3	0.09286	0.09286	0.16177	0.10807	0.4544	0.06188
TCN-4	0.13409	0.13409	0.16813	0.11768	0.4522	0.13750
TCN-5	0.09114	0.09114	0.11254	0.15863	0.4595	0.07218
TCN-6	0.13247	0.13247	0.11800	0.16818	0.4566	0.14610
TCN-7	0.13825	0.08795	0.16444	0.16356	0.4532	0.10270
TCN-8	0.09089	0.14136	0.16057	0.16146	0.4502	0.08104
TCN-9	0.08614	0.08614	0.11757	0.11501	0.4538	0.11720
TCN-10	0.12542	0.12542	0.12641	0.12416	0.4601	0.20050
TCN-11	0.13543	0.08534	0.16606	0.11504	0.4569	0.12150
TCN-12	0.08629	0.13657	0.16797	0.11487	0.4534	0.11610
TCN-13	0.13556	0.08576	0.11506	0.16346	0.4617	0.11530
TCN-14	0.08263	0.13306	0.12224	0.16953	0.4508	0.14720
TCN-15	0.08963	0.08963	0.16402	0.16206	0.4525	0.08955
TCN-16	0.12842	0.12842	0.17682	0.17446	0.4500	0.18550
TCN-4R	0.13393	0.13393	0.16908	0.11878	0.4507	0.14040
TCN-8R	0.09091	0.14137	0.16112	0.16143	0.4502	0.08086
TCN-9R	0.08569	0.08569	0.11791	0.11522	0.4545	0.12020
TCN-15R	0.09003	0.09003	0.16230	0.16179	0.4520	0.08659

Table 10.7 Factorial Experiment: Girdler G-3A Catalyst (350°-380°C)

Treatment Combination Number	Average of inlet and outlet partial pressures (atm.)				Total flow rate (gm.mol/min)	r = reaction rate $\frac{\text{gm.mol.}}{\text{hr.}(\text{gm. of catalyst})}$
	P_{CO}	P_{H_2O}	P_{CO_2}	P_{H_2}		
TCN-1	0.14746	0.09738	0.10489	0.10292	0.4635	0.02302
TCN-2	0.09824	0.14839	0.10419	0.10231	0.4624	0.01684
TCN-3	0.09921	0.09921	0.15433	0.10126	0.4627	0.00851
TCN-4	0.14650	0.14650	0.15246	0.10547	0.4579	0.03860
TCN-5	0.09849	0.09849	0.10153	0.15153	0.4649	0.01263
TCN-6	0.14704	0.14704	0.10486	0.15230	0.4670	0.02203
TCN-7	0.14835	0.09807	0.15412	0.15330	0.4599	0.02033
TCN-8	0.09838	0.14861	0.15106	0.15278	0.4607	0.01719
TCN-9	0.09635	0.09635	0.10487	0.10382	0.4641	0.03107
TCN-10	0.14457	0.14457	0.10625	0.10537	0.4651	0.04495
TCN-11	0.14652	0.09688	0.15495	0.10412	0.4626	0.03206
TCN-12	0.09696	0.14738	0.15372	0.10470	0.4573	0.03170
TCN-13	0.14380	0.09390	0.10403	0.15554	0.4670	0.04916
TCN-14	0.09673	0.14680	0.10518	0.15360	0.4638	0.02821
TCN-15	0.09837	0.09837	0.15433	0.15232	0.4624	0.01575
TCN-16	0.14634	0.14634	0.15441	0.15495	0.4610	0.03555
TCN-1R	0.14847	0.09638	0.10305	0.10398	0.4633	0.02152
TCN-2R	0.09776	0.14787	0.10230	0.10264	0.4631	0.02024
TCN-9R	0.09641	0.09641	0.10443	0.10392	0.4628	0.03161
TCN-15R	0.09887	0.09887	0.15528	0.15215	0.4609	0.01390

Table 10.8 Factorial Experiment: Girdler G-3A Catalyst (400°-430°C)

Treatment Combination Number	Average of inlet and outlet partial pressures (atm.)				Total flow rate (gm.mol.)/min	r - reaction rate gm.mol./hr. (gm. of catalyst)
	P_{CO}	P_{H_2O}	P_{CO_2}	P_{H_2}		
TCN-1	0.14068	0.09049	0.11035	0.11027	0.4615	0.08176
TCN-2	0.09285	0.14315	0.10971	0.10834	0.4596	0.06376
TCN-3	0.09523	0.09523	0.15653	0.10649	0.4563	0.04522
TCN-4	0.14196	0.14196	0.15990	0.11002	0.4577	0.07567
TCN-5	0.09432	0.09432	0.10657	0.15702	0.4601	0.05122
TCN-6	0.14086	0.14086	0.10910	0.16095	0.4595	0.08265
TCN-7	0.14552	0.09520	0.15627	0.15641	0.4591	0.04478
TCN-8	0.09538	0.14593	0.15428	0.15738	0.4550	0.04666
TCN-9	0.09103	0.09103	0.11168	0.10957	0.4622	0.07674
TCN-10	0.12860	0.12860	0.12152	0.12159	0.4643	0.17890
TCN-11	0.13618	0.08576	0.16668	0.11591	0.4574	0.12350
TCN-12	0.08756	0.13818	0.16600	0.11449	0.4557	0.10990
TCN-13	0.13535	0.08545	0.11797	0.16405	0.4669	0.12000
TCN-14	0.08620	0.13648	0.11554	0.16521	0.4598	0.11830
TCN-15	0.09225	0.09225	0.16089	0.15887	0.4609	0.06770
TCN-16	0.13385	0.13385	0.16941	0.16864	0.4574	0.14250
TCN-2R	0.09350	0.14383	0.10713	0.10781	0.4590	0.05883
TCN-7R	0.14480	0.09446	0.15771	0.15724	0.4588	0.05113
TCN-9R	0.09044	0.09044	0.11167	0.11025	0.4618	0.08194
TCN-16R	0.13440	0.13440	0.16972	0.16970	0.4593	0.13630

Table 10.9 Factorial Experiment: Girdler G-66 Catalyst (250°-285°C)

Treatment Combination Number	Average of inlet and outlet partial pressures (atm.)				Total flow rate gm.mol./min.	r = reaction rate gm.mol./hr.(gm. of catalyst)
	P_{CO}	P_{H_2O}	P_{CO_2}	P_{H_2}		
TCN-1	0.14067	0.09046	0.10895	0.11036	0.4574	0.08149
TCN-2	0.09339	0.14350	0.10850	0.10702	0.4592	0.05606
TCN-3	0.09530	0.09530	0.15598	0.10587	0.4558	0.04316
TCN-4	0.14268	0.14268	0.15785	0.10914	0.4545	0.06851
TCN-5	0.09734	0.09734	0.10607	0.15280	0.4606	0.02239
TCN-6	0.14420	0.14420	0.10796	0.15540	0.4624	0.04639
TCN-7	0.14645	0.09574	0.15392	0.15780	0.4584	0.04558
TCN-8	0.09557	0.14611	0.15602	0.15714	0.4514	0.04460
TCN-9	0.09293	0.09293	0.10832	0.10791	0.4573	0.06134
TCN-10	0.13936	0.13936	0.11266	0.11011	0.4631	0.08561
TCN-11	0.14357	0.09340	0.16098	0.10726	0.4581	0.05686
TCN-12	0.09203	0.14233	0.15790	0.10912	0.4559	0.06976
TCN-13	0.14231	0.09144	0.10799	0.15784	0.4638	0.06868
TCN-14	0.09225	0.14250	0.10703	0.15880	0.4573	0.06689
TCN-15	0.09532	0.09532	0.15684	0.15606	0.4561	0.04272
TCN-16	0.14210	0.14210	0.15936	0.16070	0.4527	0.07540
TCN-4R	0.14297	0.14297	0.15900	0.10925	0.4531	0.06788
TCN-8R	0.09562	0.14622	0.15534	0.15734	0.4505	0.04486
TCN-9R	0.09378	0.09378	0.10740	0.10708	0.4572	0.05445
TCN-16R	0.14250	0.14250	0.15999	0.16006	0.4535	0.07119

Table 10.10 Analysis of Variance, log r. SSV Catalyst (350°-380°C)

Source of Variation	Effect	Degree of Freedom	Mean Square
Main effects:			
$\log p_{CO}$	-0.10165	1	0.041327 **
$\log p_{H_2O}$	-0.10669	1	0.045529 **
$\log p_{CO_2}$	+0.04888	1	0.009555 *
$\log p_{H_2}$	+0.02302	1	0.002120
$1/T$	-0.26353	1	0.277794 **
Interactions			
$(\log p_{CO})(\log p_{H_2O})$	-0.01529	1	0.000935
$(\log p_{CO})(\log p_{CO_2})$	-0.02395	1	0.002296
$(\log p_{CO})(\log p_{H_2})$	+0.04632	1	0.008581
$(\log p_{CO})(1/T)$	-0.04089	1	0.006689
$(\log p_{H_2O})(\log p_{CO_2})$	-0.02994	1	0.003586
$(\log p_{H_2O})(\log p_{H_2})$	+0.02199	1	0.001935
$(\log p_{H_2O})(1/T)$	-0.02942	1	0.003462
$(\log p_{CO_2})(\log p_{H_2})$	+0.03889	1	0.006049
$(\log p_{CO_2})(1/T)$	-0.01083	1	0.000469
$(\log p_{H_2})(1/T)$	-0.01092	1	0.000477

Error mean square based on 4 replicates = 0.001159

** - significant at 99% confidence limit

* - " " 95% " "

Table 10.11 Analysis of Variance, log r. SSV Catalyst (400°-430°C)

Source of Variation	Effect	Degree of Freedom	Mean Square
Main Effects:			
$\log p_{CO}$	-0.15030	1	0.090340 **
$\log p_{H_2O}$	-0.09430	1	0.035550 **
$\log p_{CO_2}$	+0.05287	1	0.011770 *
$\log p_{H_2}$	+0.02950	1	0.003480
1/T	-0.14497	1	0.084060 **
Interactions:			
$(\log p_{CO})(\log p_{H_2O})$	+0.00225	1	0.000020
$(\log p_{CO})(\log p_{CO_2})$	+0.00040	1	0.000000
$(\log p_{CO})(\log p_{H_2})$	+0.00218	1	0.000020
$(\log p_{CO})(1/T)$	+0.01128	1	0.000509
$(\log p_{H_2O})(\log p_{CO_2})$	-0.01113	1	0.000496
$(\log p_{H_2O})(\log p_{H_2})$	+0.00865	1	0.000300
$(\log p_{H_2O})(1/T)$	-0.00250	1	0.000025
$(\log p_{CO_2})(\log p_{H_2})$	+0.00972	1	0.000380
$(\log p_{CO_2})(1/T)$	-0.01426	1	0.000813
$(\log p_{H_2})(1/T)$	-0.00533	1	0.000110

Error mean square based on 4 replicates = 0.000632
** - significant at 99% confidence limit
* - " " 95% " "

Table 10.12 Analysis of Variance, log r. Power Gas Catalyst (350^{o}-380^{o}C)

Source of Variation	Effect	Degree of Freedom	Mean Square
Main Effects:			
$\log p_{CO}$	-0.14405	1	0.083000 **
$\log p_{H_2O}$	-0.09469	1	0.035860 **
$\log p_{CO_2}$	+0.05739	1	0.013174 **
$\log p_{H_2}$	+0.05138	1	0.010563 *
1/T	-0.24595	1	0.241980 **
Interactions:			
$(\log p_{CO})(\log p_{H_2O})$	-0.00155	1	0.000096
$(\log p_{CO})(\log p_{CO_2})$	-0.07100	1	0.020163 **
$(\log p_{CO})(\log p_{H_2})$	+0.06745	1	0.018204 **
$(\log p_{CO})(1/T)$	+0.02753	1	0.003031
$(\log p_{H_2O})(\log p_{CO_2})$	-0.05623	1	0.012649 *
$(\log p_{H_2O})(\log p_{H_2})$	+0.01509	1	0.000911
$(\log p_{H_2O})(1/T)$	+0.01604	1	0.001029
$(\log p_{CO_2})(\log p_{H_2})$	-0.01406	1	0.000791
$(\log p_{CO_2})(1/T)$	-0.02447	1	0.002396
$(\log p_{H_2})(1/T)$	-0.03813	1	0.005806 *

Error mean square based on 4 replicates = 0.000615

** - significant at 99% confidence limit

* - " " 95%

Table 10.13 Analysis of Variance, log r. Power Gas Catalyst (400°-430°C)

Source of Variation	Effect	Degree of Freedom	Mean Square
Main Effects:			
$\log p_{CO}$	-0.17257	1	0.119130 **
$\log p_{H_2O}$	-0.07481	1	0.022380 **
$\log p_{CO_2}$	+0.05944	1	0.014130 *
$\log p_{H_2}$	+0.04231	1	0.007160 *
1/T	-0.16514	1	0.109090 **
Interactions:			
$(\log p_{CO})(\log p_{H_2O})$	-0.01423	1	0.000811
$(\log p_{CO})(\log p_{CO_2})$	-0.01945	1	0.001514
$(\log p_{CO})(\log p_{H_2})$	-0.00034	1	0.000000
$(\log p_{CO})(1/T)$	+0.00885	1	0.000313
$(\log p_{H_2O})(\log p_{CO_2})$	-0.00683	1	0.000187
$(\log p_{H_2O})(\log p_{H_2})$	-0.00112	1	0.000005
$(\log p_{H_2O})(1/T)$	-0.00755	1	0.000228
$(\log p_{CO_2})(\log p_{H_2})$	+0.02050	1	0.001682
$(\log p_{CO_2})(1/T)$	-0.01232	1	0.000607
$(\log p_{H_2})(1/T)$	-0.00897	1	0.000322

Error mean square based on 3 replicates = 0.00061

** - significant at 99% confidence limit

* - " " 95% " "

Table 10.14 Analysis of Variance, log r. I.C.I. Catalyst (350°-380°C)

Source of Variation	Effect	Degree of Freedom	Mean Square
Main Effects:			
$\log p_{CO}$	-0.15696	1	0.098544 **
$\log p_{H_2O}$	-0.09020	1	0.032544 **
$\log p_{CO_2}$	+0.13310	1	0.070861 **
$\log p_{H_2}$	+0.08556	1	0.029273 **
1/T	-0.41619	1	0.692870 **
Interactions:			
$(\log p_{CO})(\log p_{H_2O})$	+0.03717	1	0.005525
$(\log p_{CO})(\log p_{CO_2})$	-0.04234	1	0.007169 *
$(\log p_{CO})(\log p_{H_2})$	+0.01387	1	0.000769
$(\log p_{CO})(1/T)$	-0.03744	1	0.005606
$(\log p_{H_2O})(\log p_{CO_2})$	+0.01076	1	0.000484
$(\log p_{H_2O})(\log p_{H_2})$	-0.03793	1	0.005754
$(\log p_{H_2O})(1/T)$	-0.04958	1	0.009833 *
$(\log p_{CO_2})(\log p_{H_2})$	-0.00393	1	0.000062
$(\log p_{CO_2})(1/T)$	-0.07861	1	0.024724 **
$(\log p_{H_2})(1/T)$	+0.01040	1	0.000431

Error mean square based on 4 replicates = 0.00076
** - significant at 99% confidence limit
* - " " 95% " "

Table 10.15 Analysis of Variance, log r_o - I.C.I. Catalyst (400°-430°C)

Source of Variation	Effect	Degree of Freedom	Mean Square
Main Effects:			
$\log p_{CO}$	-0.16740	1	0.112144**
$\log p_{H_2O}$	-0.13317	1	0.070934**
$\log p_{CO_2}$	+0.06051	1	0.014647**
$\log p_{H_2}$	+0.01713	1	0.001183
1/T	-0.12715	1	0.064669**
Interactions:			
$(\log p_{CO})(\log p_{H_2O})$	-0.02060	1	0.001718
$(\log p_{CO})(\log p_{CO_2})$	-0.02873	1	0.003299
$(\log p_{CO})(\log p_{H_2})$	+0.01262	1	0.000637
$(\log p_{CO})(1/T)$	+0.05166	1	0.010675*
$(\log p_{H_2O})(\log p_{CO_2})$	-0.00193	1	0.000149
$(\log p_{H_2O})(\log p_{H_2})$	-0.02326	1	0.002164
$(\log p_{H_2O})(1/T)$	-0.02578	1	0.002662
$(\log p_{CO_2})(\log p_{H_2})$	-0.03248	1	0.004220
$(\log p_{CO_2})(1/T)$	-0.00152	1	0.000093
$(\log p_{H_2})(1/T)$	+0.00045	1	0.000001

Error mean square based on 4 replicates = 0.000052
** - significant at 99% confidence limit
* - " " 95% " "

Table 10.16 Analysis of Variance, log r. Girdler G-3A Catalyst (350°-380°C)

Source of Variation	Effect	Degree of Freedom	Mean Square
Main Effects:			
$\log p_{CO}$	-0.23337	1	0.217846 **
$\log p_{H_2O}$	-0.11969	1	0.057298 **
$\log p_{CO_2}$	+0.06311	1	0.015930 *
$\log p_{H_2}$	+0.04739	1	0.008982
1/T	-0.24368	1	0.237517 **
Interaction:			
$(\log p_{CO})(\log p_{H_2O})$	+0.05334	1	0.011384 *
$(\log p_{CO})(\log p_{CO_2})$	-0.03862	1	0.005968
$(\log p_{CO})(\log p_{H_2})$	+0.00606	1	0.000147
$(\log p_{CO})(1/T)$	+0.04335	1	0.007519
$(\log p_{H_2O})(\log p_{CO_2})$	-0.11343	1	0.051465 **
$(\log p_{H_2O})(\log p_{H_2})$	+0.04941	1	0.009766
$(\log p_{H_2O})(1/T)$	+0.05272	1	0.011120 *
$(\log p_{CO_2})(\log p_{H_2})$	+0.01610	1	0.000451
$(\log p_{CO_2})(1/T)$	+0.06988	1	0.019531 *
$(\log p_{H_2})(1/T)$	+0.01810	1	0.013108 *

Error mean square based on 4 replicates = 0.00128

** - significant at 99% confidence limit

* - " " 95% " "

Table 10.17 Analysis of Variance, log r. Girdler G-3A Catalyst (400°-430°C)

Source of Variation	Effect	Degree of Freedom	Mean Square
Main Effects:			
$\log p_{CO}$	-0.15865	1	0.100680**
$\log p_{H_2O}$	-0.12190	1	0.059438**
$\log p_{CO_2}$	+0.082780	1	0.027409**
$\log p_{H_2}$	+0.054798	1	0.012011*
1/T	-0.27610	1	0.304931**
Interactions:			
$(\log p_{CO})(\log p_{H_2O})$	+0.00487	1	0.000095
$(\log p_{CO})(\log p_{CO_2})$	+0.01375	1	0.000756
$(\log p_{CO})(\log p_{H_2})$	+0.02881	1	0.003320
$(\log p_{CO})(1/T)$	-0.02827	1	0.003197
$(\log p_{H_2O})(\log p_{CO_2})$	-0.00660	1	0.000174
$(\log p_{H_2O})(\log p_{H_2})$	-0.01377	1	0.000758
$(\log p_{H_2O})(1/T)$	-0.03659	1	0.005354
$(\log p_{CO_2})(\log p_{H_2})$	-0.03583	1	0.005134
$(\log p_{CO_2})(1/T)$	-0.03960	1	0.006272*
$(\log p_{H_2})(1/T)$	-0.02136	1	0.001826

Error mean square based on 4 replicates = 0.000716
** - significant at 99% confidence limit
* - " " 95% " "

Table 10.18 Analysis of Variance, log r. Girdler G-66 Catalyst (250°-285°C)

Source of Variation	Effect	Degree of Freedom	Mean Square
Main effects:			
$\log p_{CO}$	-0.12539	1	0.062891**
$\log p_{H_2O}$	-0.10177	1	0.041412**
$\log p_{CO_2}$	+0.02167	1	0.001878
$\log p_{H_2}$	+0.11931	1	0.056942**
1/T	-0.12922	1	0.066786**
Interactions:			
$(\log p_{CO})(\log p_{H_2O})$	+0.06411	1	0.016442**
$(\log p_{CO})(\log p_{CO_2})$	+0.03338	1	0.004456*
$(\log p_{CO})(\log p_{H_2})$	-0.02062	1	0.001700
$(\log p_{CO})(1/T)$	+0.04684	1	0.008777*
$(\log p_{H_2O})(\log p_{CO_2})$	-0.02994	1	0.003586*
$(\log p_{H_2O})(\log p_{H_2})$	-0.03380	1	0.004568*
$(\log p_{H_2O})(1/T)$	-0.01546	1	0.000956
$(\log p_{CO_2})(\log p_{H_2})$	-0.05603	1	0.013050**
$(\log p_{CO_2})(1/T)$	+0.04734	1	0.008965**
$(\log p_{H_2})(1/T)$	+0.08219	1	0.027021**

Error mean square based on 4 replicates = 0.000415
** - significant at 99% confidence limit
* - " " 95% " "

Table 10.19 Determination of Apparent Activation Energy SSV Catalyst (350^{o}-450^{o}C)

$$r = k\, p_{CO}^{0.80}\, p_{H_2O}^{0.615}\, p_{CO_2}^{-0.465}$$

Run Number	Reaction Temp. (^{o}C)	Average of inlet and outlet partial pressures (atm.)				r = reaction rate $\frac{\text{gm.mol.}}{\text{hr.} \cdot \text{gm. catalyst}}$	$\frac{1}{T}$ ($^{o}K^{-1}$)	Rate Const. k	Total flow rate $\frac{\text{gm.mol}}{\text{min}}$
		P_{CO}	P_{H_2O}	P_{CO_2}	P_{H_2}				
SSV-1.1	354	0.09401	0.09401	0.10385	0.10421	0.05390	0.001595	0.5338	0.4680
SSV-1.2	396	0.09002	0.09002	0.10865	0.10872	0.08300	0.001495	0.8923	0.4740
SSV-1.3	431	0.08609	0.08609	0.11124	0.11296	0.11860	0.001420	1.3730	0.4706
SSV-1.4	350	0.09483	0.09483	0.10235	0.10329	0.04580	0.001605	0.4449	0.4696
SSV-2.1	375	0.09220	0.09220	0.10563	0.10521	0.06680	0.001543	0.6850	0.4614
SSV-2.2	407	0.08896	0.08896	0.10948	0.10948	0.09242	0.001467	1.0140	0.4631
SSV-2.3	442	0.08417	0.08417	0.11344	0.11421	0.13119	0.001398	1.5820	0.4646

Table 10.20 Determination of Apparent Activation Energy Power-Gas Catalyst (350°-450°C)

$$r = k\, P_{CO}^{1.068}\, P_{H_2O}^{0.5637}\, P_{CO_2}^{-0.4293}\, P_{H_2}^{-0.3669}$$

Run Number	Reaction Temp (°C)	Average of inlet and outlet partial pressures (atm.)				r = reaction rate $\frac{\text{gm.mol}}{\text{hr.} \cdot \text{gm. catalyst}}$	$\frac{1}{T}$ ($^{\circ}K^{-1}$)	Rate Const. k	Total flow rate $\frac{\text{gm.mol}}{\text{min.}}$
		P_{CO}	P_{H_2O}	P_{CO_2}	P_{H_2}				
PG.1.1	367	0.09407	0.09407	0.10339	0.10574	0.04809	0.001563	0.3767	0.4602
PG.1.2	392	0.09120	0.09120	0.10803	0.10769	0.06860	0.001504	0.5798	0.4645
PG.1.3	420	0.08746	0.08746	0.11180	0.11137	0.09949	0.001444	0.9252	0.4647
PG.1.4	444	0.08401	0.08401	0.11472	0.11542	0.12994	0.001395	1.3210	0.4620
PG.1.5	346	0.09584	0.09584	0.10160	0.10485	0.03707	0.001617	0.2788	0.4585
PG.2.1	346	0.09582	0.09582	0.10321	0.10805	0.03770	0.001616	0.2857	0.4547
PG.2.2	359	0.09495	0.09495	0.10364	0.10534	0.04210	0.001581	0.3246	0.4518
PG.2.3	384	0.09305	0.09305	0.10835	0.10744	0.05812	0.001523	0.4756	0.4510
PG.2.4	406	0.08985	0.08985	0.11105	0.11200	0.08450	0.001473	0.7514	0.4498
PG.2.5	432	0.08659	0.08659	0.11316	0.11483	0.11310	0.001418	1.0870	0.4488

Table 10.21 Determination of Apparent Activation Energy I.C.I. Catalyst (350°-450°C)

$$r = k\, P_{CO}^{1.098}\, P_{H_2O}^{0.6654}\, P_{CO_2}^{-0.7096}\, P_{H_2}^{-0.3669}$$

Run Number	Reaction Temp. (°C)	Average of inlet and outlet partial pressures (atm.)				r = reaction rate gm. mol. / hr. gm. catalyst	$\frac{1}{T}$ ($^{\circ}K^{-1}$)	Rate Const. k	Total flow rate gm. mol / min.
		P_{CO}	P_{H_2O}	P_{CO_2}	P_{H_2}				
ICI 1.1	350	0.09649	0.09649	0.10629	0.10424	0.03188	0.001605	0.1751	0.4593
ICI 1.2	383	0.09351	0.09351	0.10926	0.10690	0.05525	0.001524	0.3301	0.4607
ICI 1.3	440	0.08651	0.08651	0.11519	0.11369	0.11240	0.001403	0.8180	0.4617
ICI 2.1	346	0.09710	0.09710	0.10607	0.10341	0.02610	0.001614	0.1411	0.4611
ICI 2.2	363	0.09587	0.09587	0.10614	0.10473	0.03654	0.001572	0.2030	0.4607
ICI 2.3	388	0.09272	0.09272	0.11117	0.10797	0.06286	0.001512	0.3874	0.4603
ICI 2.4	413	0.08994	0.08994	0.11214	0.11005	0.08346	0.001458	0.5497	0.4635
ICI 2.5	427	0.08715	0.08715	0.11444	0.11174	0.10660	0.001429	0.7569	0.4636

Table 10.22 Determination of Apparent Activation Energy Girdler G-3A Catalyst (350°-450°C)

$$r = k\, P_{CO}^{1.237}\, P_{H_2O}^{0.7033}\, P_{CO_2}^{-0.6543}\, P_{H_2}^{-0.2166}$$

Run Number	Reaction Temp. (°C)	Average of inlet and outlet partial pressures (atm.)				r = reaction rate $\frac{\text{gm.mol.}}{\text{hr.} :: \text{gm. catalyst}}$	$\frac{1}{T}$ ($^{\circ}K^{-1}$)	Rate Const. k	Total flow rate $\frac{\text{gm.mol.}}{\text{min.}}$
		P_{CO}	P_{H_2O}	P_{CO_2}	P_{H_2}				
G-3A 1.1	352	0.09818	0.09818	0.10521	0.10251	0.01791	0.001601	0.2263	0.4613
G-3A 1.2	387	0.09563	0.09563	0.10628	0.10506	0.03895	0.001516	0.5143	0.4613
G-3A 1.3	418	0.09144	0.09144	0.11121	0.10981	0.07379	0.001448	1.1270	0.4611
G-3A 1.4	449	0.08398	0.08398	0.11957	0.11729	0.13680	0.001386	2.621	0.4587
G-3A 2.1	351	0.09750	0.09750	0.10321	0.10241	0.02033	0.001604	0.2571	0.4632
G-3A 2.2	371	0.09668	0.09668	0.10449	0.10344	0.02830	0.001554	0.3675	0.4622
G-3A 2.3	405	0.09349	0.09349	0.10833	0.10642	0.05364	0.001476	0.7658	0.4633
G-3A 2.4	437	0.08662	0.08662	0.11588	0.11408	0.11300	0.001409	1.9860	0.4596

Table 10.23 Determination of Apparent Activation Energy. Girdler G-66 Catalyst (210°-310°C)

$$r = k\, p_{CO}^{0.6841}\, p_{H_2O}^{0.5729}\, p_{H_2}^{-0.7043}$$

Run Number	Reaction Temp. (°C)	Average of inlet and outlet partial pressures (atm.)				r = reaction rate $\frac{\text{gm.mol.}}{\text{hr.} \cdot \text{gm. catalyst}}$	$\frac{1}{T}$ ($^{\circ}K^{-1}$)	Rate Const. k	Total flow rate $\frac{\text{gm.mol.}}{\text{min.}}$
		p_{CO}	p_{H_2O}	p_{CO_2}	p_{H_2}				
G-66 1.1	212	0.09726	0.09726	0.10316	0.10316	0.02445	0.002064	0.09241	0.4626
G-66 1.2	228	0.09596	0.09596	0.10469	0.10469	0.03609	0.001998	0.14020	0.4615
G-66 1.3	251	0.09514	0.09514	0.10415	0.10525	0.04191	0.001908	0.16520	0.4627
G-66 1.4	270	0.09369	0.09369	0.10621	0.10648	0.05319	0.001842	0.21550	0.4637
G-66 1.5	291	0.09238	0.09238	0.10713	0.10765	0.06349	0.001775	0.26390	0.4644
G-66 2.1	222	0.09710	0.09710	0.10442	0.10346	0.02615	0.002022	0.09926	0.4593
G-66 2.2	239	0.09604	0.09604	0.10415	0.10405	0.03313	0.001955	0.12800	0.4615
G-66 2.3	260	0.09463	0.09463	0.10565	0.10565	0.04549	0.001876	0.18100	0.4606
G-66 2.4	281	0.09294	0.09294	0.10740	0.10739	0.05966	0.001805	0.24560	0.4604
G-66 2.5	304	0.09139	0.09139	0.10891	0.10891	0.07236	0.001733	0.30720	0.4606

Table 10.24 Effect of Mass Velocity on Reaction Rate

SSV Catalyst (350°-450°C)

p_{CO} inlet = p_{H_2O} inlet = p_{CO_2} inlet = p_{H_2} inlet = 0.10 atm.

Run Number	Mass flow rate $\frac{gm}{hr. \cdot cm^2}$	Bed Height (mm.)	Reaction Temp. (°K)	Reaction rate $\frac{gm.mol.}{hr. \cdot gm.catalyst}$
SSV 1.1/1	38.74	2.62	643	0.05349
SSV 1.1/2			646	0.06051
SSV 1.1/3			717	0.15883
SSV 1.1/4			620	0.02837
SSV 1.2/1			675	0.09634
SSV 1.2/2			703	0.13423
SSV 1.2/3			648	0.06103
SSV 1.2/4			623	0.02717
SSV 1.3/1			650	0.05837
SSV 1.3/2			683	0.10829
SSV 1.3/3			714	0.1444
SSV 1.3/4			618	0.2186

Table 10.24 Effect of Mass Velocity on Reaction Rate (Cont'd)

SSV Catalyst (350^{o}-450^{o}C)

p_{CO} inlet = p_{H_2O} inlet = p_{CO_2} inlet = p_{H_2} inlet = 0.10 atm.

Run Number	Mass flow rate $\frac{gm.}{hr. \cdot cm^2}$	Bed Height (mm.)	Reaction Temp. (°K)	Reaction rate $\frac{gm.mol.}{hr. \quad gm. \text{ catalyst}}$
SSV 2.1/1	47.86	3.30	648	0.06612
SSV 2.1/2			673	0.09577
SSV 2.1/3			705	0.13430
SSV 2.2/1			721	0.15680
SSV 2.2/2			621	0.02560
SSV 3.1/1	58.85	4.08	644	0.05438
SSV 3.1/2			677	0.09617
SSV 3.1/3			645	0.05823
SSV 3.2/1			624	0.02860
SSV 3.2/2			662	0.08027
SSV 3.2/3			705	0.13890

Reactor x - area = 20.25 cm^2.

$$\text{Contact time} = 14.06 \frac{\text{gm. Catalyst}}{\text{gm.mol. feed/min}} = 0.181 \text{ hr.}^{-1}\text{cm.}^{-2}$$

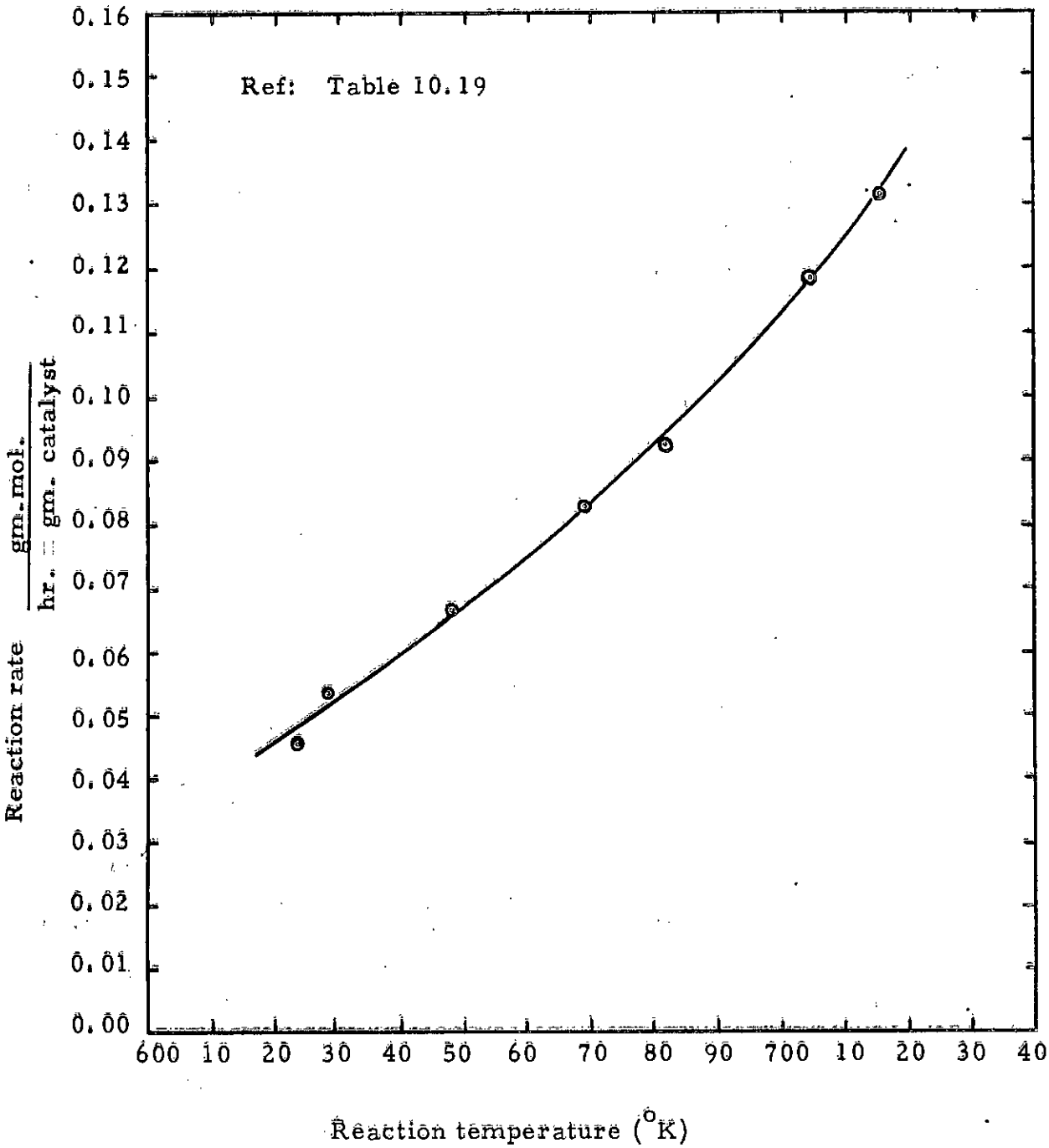

Fig. 10.1 Performance of SSV Catalyst

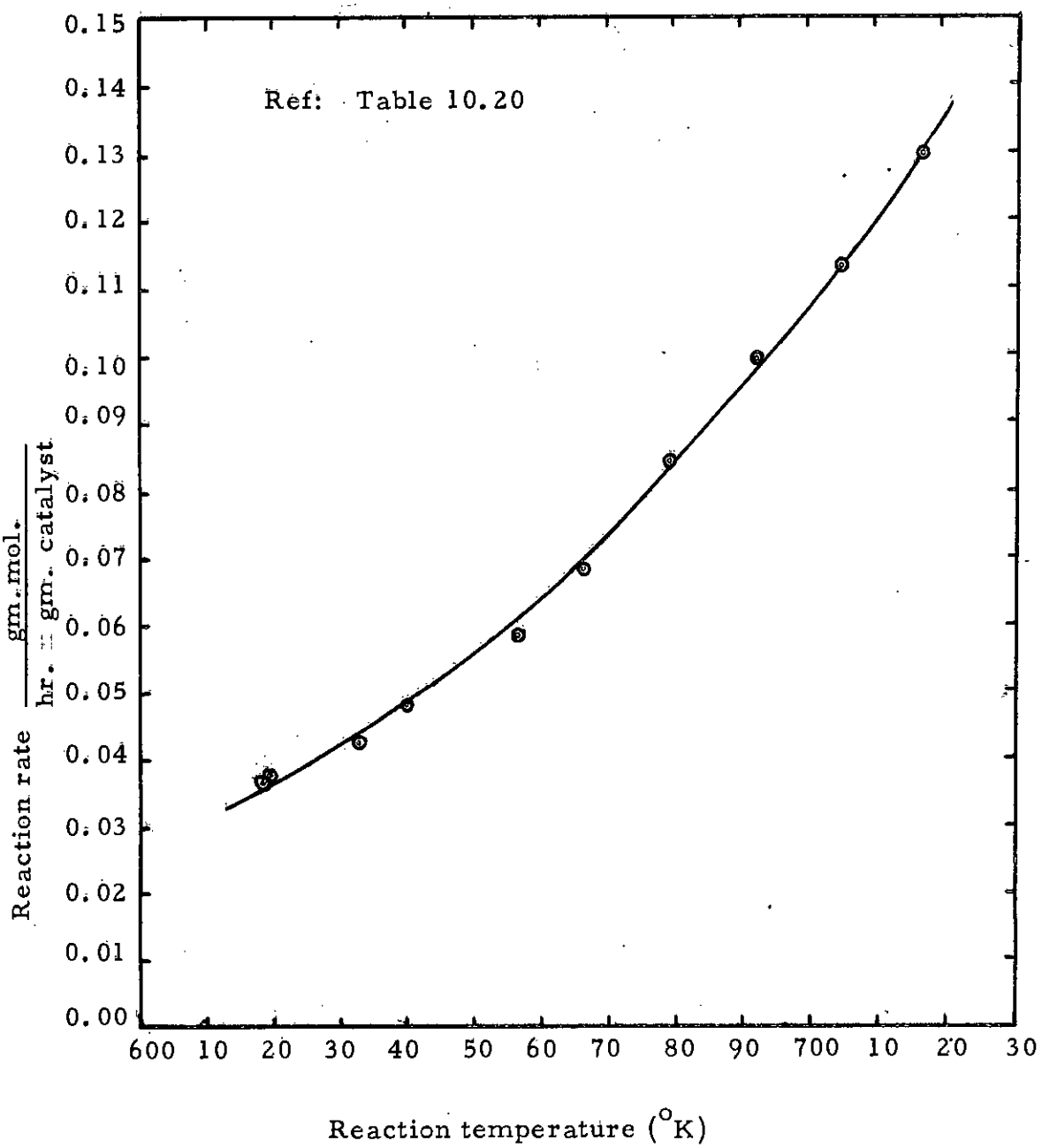

Fig. 10.2 Performance of Power-Gas Catalyst

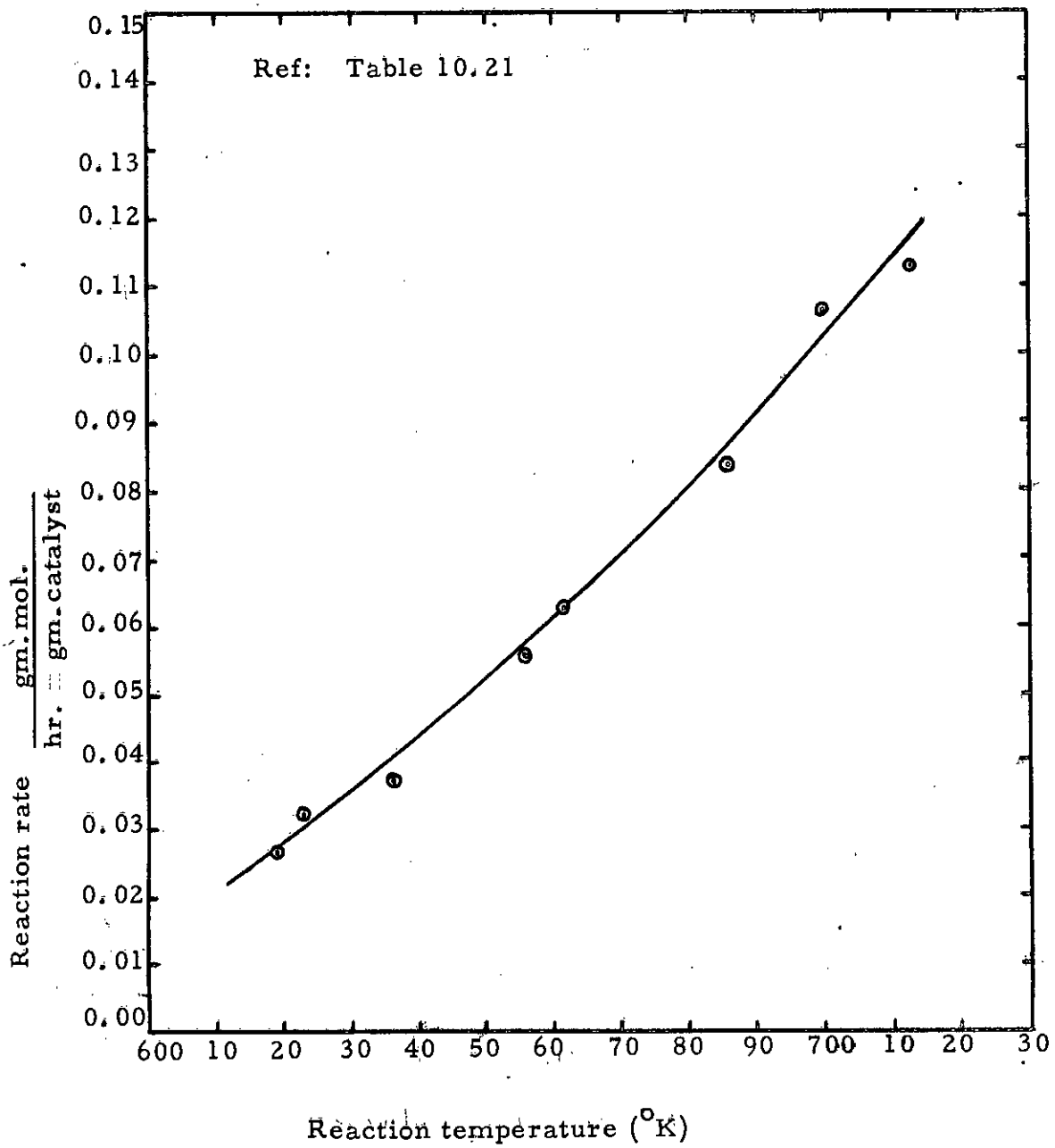

Fig. 10.3 Performance of I.C.I. Catalyst

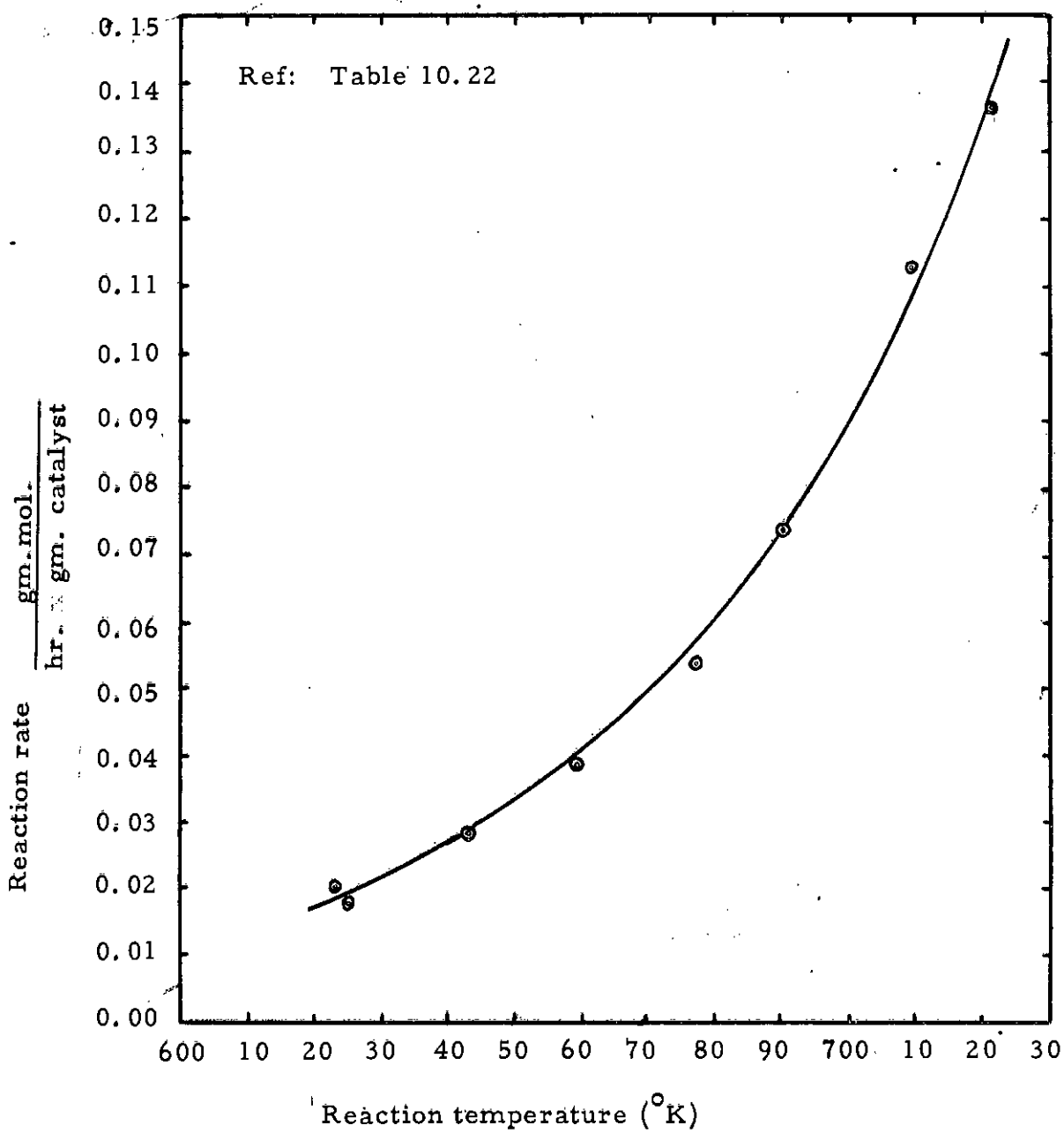

Fig. 10.4 Performance of Girdler G-3A Catalyst

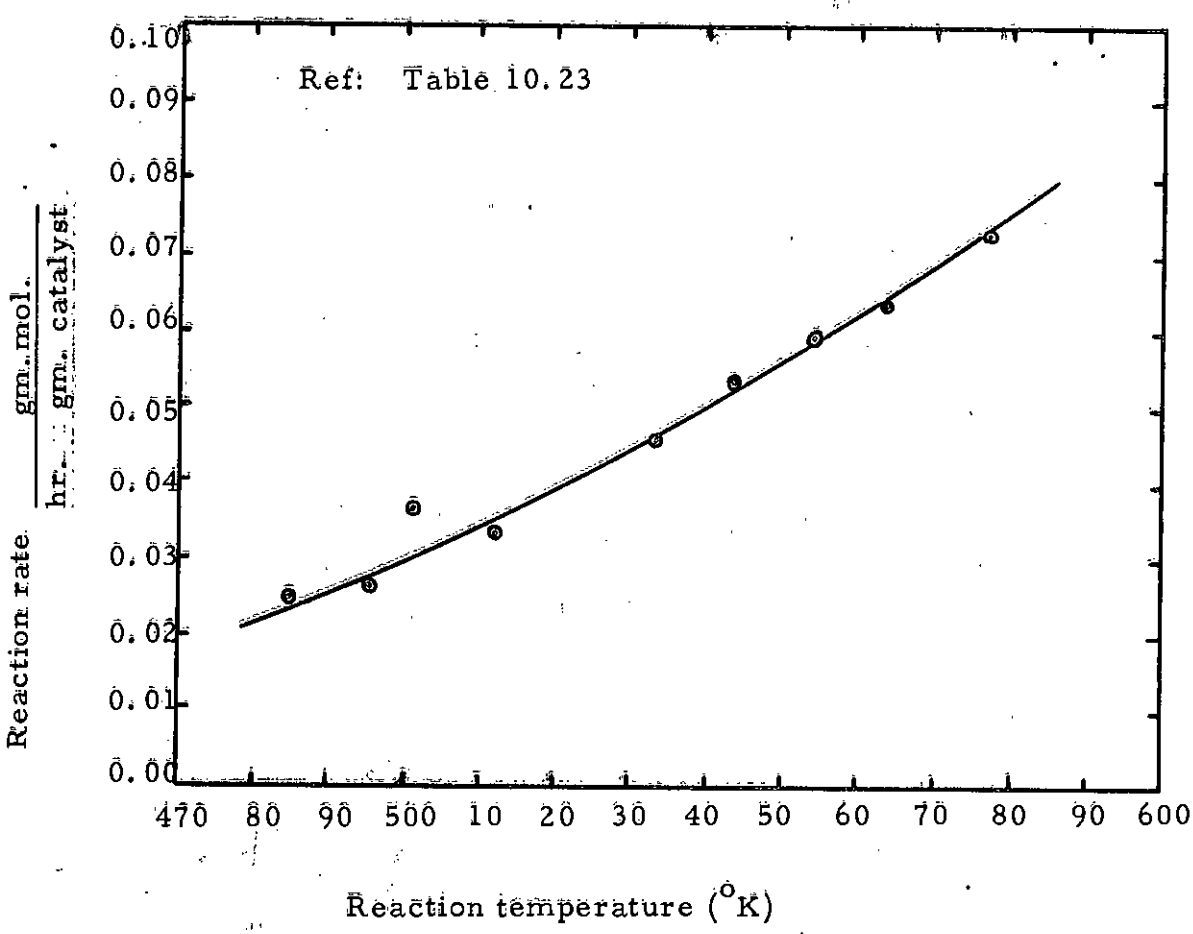

Fig. 10.5 Performance of Girdler G-66 Catalyst

Chapter 11. SAMPLE CALCULATIONS

Experimental data have been taken at random to illustrate the calculation of results.

11.1 CALCULATION OF REACTION RATE "r"

The method of obtaining basic experimental data is given in section 5.3. Run number TCN 9 from Table 10.7 (Girdler G-3A catalyst - 350° to 380°C) is chosen for the illustration.

Basic experimental data

Room temperature = 24°C

Wet test meter water temperature = 72.8°F ≡ 22.7°C

Reactor pressure = 14.84 psia. ≡ 767.2 mm. of Hg.

Atmospheric pressure = 762 mm. of Hg.

Average time taken for = 2 min. 42.2 seconds

1 rev. of Wet test meter ≡ 2.703 minutes

pointer (≡ 1 cu.ft.)

$$\text{Saturated gaseous flow rate} = \frac{1}{2.703} = 0.37 \text{ cu.ft./min.}$$

$$\text{Dry gaseous flow rate} = 0.37 \left(\frac{762-20.69}{762}\right) = 0.3599 \text{ cu.ft./min.}$$

(20.69 mm. of Hg is the vapour pressure of water at atmospheric pressure and at 22.7°C)

$$= 0.3599 \times \frac{1}{0.03532} = 10.19 \text{ litres/min.}$$

$$= \left(\frac{10.19}{22.4}\right)\left(\frac{273}{295.7}\right)\left(\frac{762}{760}\right) = 0.4211 \frac{\text{gm.mol.}}{\text{min.}}$$

The exit sample was analysed in the gas chromatograph and the results are given below.

Peak heights of standard sample (cm.)

	1st analysis	2nd analysis	average	composition
CO_2	1.88	1.84	1.86	5.72%
N_2	19.50	19.30	19.40	81.07%
CO	13.62	13.52	13.57	8.27%
H_2	7.10	7.20	7.15	4.84%

Peak heights of experimental sample (cm.)

	1st analysis	2nd analysis	average	composition	%
CO_2	3.90	3.96	3.93	$\frac{3.93 \times 5.72}{1.86}$	= 12.10
N_2	15.70	15.80	15.75	$\frac{15.75 \times 81.07}{19.40}$	= 65.72
CO	16.70	16.82	16.76	$\frac{16.76 \times 8.27}{13.57}$	= 10.22
H_2	17.42	17.66	17.54	$\frac{17.54 \times 4.84}{7.15}$	= 11.86

For the mass balances the calibrated values of inlet composition and mass flow rate were taken as given below and were checked just before the actual experiment. The effects due to small changes in room temperature and atmospheric pressure were neglected.

Average composition and mass flow rate for TCN 9

CO_2	= 10.00%	0.04649	gm.mol/min.
N_2	= 60.00%	0.27894	"
CO	= 10.00%	0.04649	"
H_2	= 10.00%	0.04649	"
H_2O	= 10.00%	0.04649	"
		0.46490	"

The reaction rate calculation was based on the mass balance on CO.

Moles of CO in = 0.04649 gm.mol./min.

Moles of CO out = $\frac{0.4211 \times 10.22}{100}$ = 0.04302 $\frac{\text{gm.mol.}}{\text{min.}}$

∴ Moles of CO reacted = 0.04649 - 0.04302

= 0.00347 gm.mol./min.

Reaction rate "r" = $\frac{0.00347 \times 60}{6.7}$

= 0.03107 $\frac{\text{gm.mol.}}{\text{hr. (gm. of catalyst)}}$

Now in the mass balance it was considered that moles of CO converted ≡ moles of H_2O converted. So the mass balance and outlet composition will be

N_2 = $\frac{0.4211 \times 65.72}{100}$ = 0.2768 $\frac{\text{gm.mol.}}{\text{min.}}$ (≡ N_2 in)

CO_2 = $\frac{0.4211 \times 12.10}{100}$ - (moles of CO converted = 0.00347)

= 0.05094 - 0.00347 = 0.04747 $\frac{\text{gm.mol.}}{\text{min.}}$ (should be equal to CO_2 in)

H_2 = $\frac{0.4211 \times 11.86}{100}$ - (moles of CO converted = 0.00347)

= 0.04996 - 0.00347 = 0.04649 $\frac{\text{gm.mol.}}{\text{min.}}$ (= H_2 in)

The total flow rate after the reaction would be the dry gaseous flow rate ($0.4211 \frac{gm.mol.}{min.}$) plus the unreacted H_2O flow rate ($0.04302 \frac{gm.mol.}{min.}$), which is equal to $0.46412 \frac{gm.mol.}{min.}$.

The outlet composition will therefore be:

CO_2	= 0.05094	$\frac{gm.mol.}{min.}$	10.98%
N_2	= 0.27680	"	60.03%
CO	= 0.04302	"	9.27%
H_2	= 0.04996	"	10.76%
H_2O	= 0.04302	"	9.27%
	0.46412	"	100.31

11.2 ANALYSIS OF VARIANCE

For an example table 10.1 is taken, whose analysis of variance is given in table 10.10. To illustrate the calculations a main effect and an interaction are considered.

Calculation of main effects

For the main effect of log p_{CO}, 8 values of log r at the higher (+) values of p_{CO}, and 8 values of log r at the lower (-) values of p_{CO}, were added separately. Dividing the difference between these two by 8 gave the effect of the factor, since this "difference" was virtually the sum of differences of 8 pairs.

Hence the effect of the factor log p_{CO}

$$= \left[(\Sigma \log r \text{ for all "+" } p_{CO}) - (\Sigma \log r \text{ for all "-" } p_{CO})\right] / 8 .$$

$$= (9.69349 - 10.50665)/8$$

= -0.81316/8 = -0.10165

sum of squares = $(-0.81316)^2$/(number of treatment combinations in the experiment)

= 0.66123/16 = 0.041327

Degree of freedom of p_{CO} = 2 - 1 = 1

∴ Mean square = 0.041327/1 = 0.041327

Calculation of interactions (two factors)

The method is the same as shown above except that the level of the interaction like log p_{CO} x log p_{H_2O} is decided in the following way.

In a treatment combination if p_{CO} is at the higher level (+) and p_{H_2O} at the lower level (-) or vice versa, then the interaction will be at lower level (-). In a treatment combination if both p_{CO} and p_{H_2O} are at the higher level (+) or both at lower level (-), then the interation will be at the higher level (+). These are true for other interactions. The degree of freedom of each interaction will still be 1.

The effect of (log p_{CO}) (log p_{H_2O}) = (10.03891 - 10.16123)/8

= -0.12232/8

= -0.01529

sum of squares = $(-0.12232)^2$/16

= 0.014962/16

= 0.000935

mean square = 0.000935/1

= 0.000935

Significance test

Table 10.1 is also taken here as an example. The significance test is based on error mean square calculations which are again based on

replicated runs. The calculations involved are shown below.

	variation	$(\text{variation})^2$
log r of TCN 1 - log r of TCN 1R =	0.00911	0.000083
log r of TCN 5 - log r of TCN 5R =	0.01454	0.000212
log r of TCN 10 - log r of TCN 10R =	0.05659	0.003202
log r of TCN 13 - log r of TCN 13R =	0.07600	0.005776
		0.009273

Error mean square = 0.009273/(number of runs involved = 8)

= 0.001159

According to the F-test (27, 103) any mean square value greater than 0.001159 x 7.71 = 0.008936 will be significant at the 95% confidence limit, and any mean square value greater than 0.001159 x 21.2 = 0.024571 will be significant at the 99% confidence limit. 7.71 and 21.2 are the F-values at 1 and 4 degrees of freedom for 95% and 99% confidence limits respectively.

11.3 CORRELATION OF EXPERIMENTAL DATA

The experimental data for each factorial experiment were correlated by fitting a linear regression equation of the form of equation 4.7, with the help of the least squares method. This was done by using the English Electric KDF9 digital computer of this University. The programme is stored in the library of the computing laboratory under the programme identifier KALMAY DHCL 085 - - KP4. Parameters A, E/R, a, b, c and d were thus evaluated and the results are given in table 6.1.

11.4 CALCULATION OF APPARENT ACTIVATION ENERGY

The rate equation over the range 350°-450°C for each catalyst(for G-66 - 210° to 310°C) takes the average value of each parameter a, b, c and d as evaluated (section 11.3) from the 350°-380°C and 400°-430°C factorial experiments. For example the rate equation of the Power-Gas catalyst for the range 350° to 450°C is:

$$r = k\, p_{CO}^{1.068}\, p_{H_2O}^{0.5637}\, p_{CO_2}^{-0.4293}\, p_{H_2}^{-0.3669}$$

From the experimental data given in table 10.20 a number of k values were calculated by means of the above equation and log k vs 1/T was plotted according to the Arrhenius relationship $k = A\, e^{-E/RT}$. The resulting plot was a straight line (fig. 6.3), the slope of which gave E/R (2.303) and the intercept A. Since R = 2 cal./gm.mol., the value of apparent activation energy E was thus obtained.

For the Girdler G-66 catalyst, since only one factorial experiment was performed, the values of a, b, c and d for 250°-285°C were used for the whole range (210°-310°C).

Chapter 12 APPENDICES

Appendix 1. Chromel-Alumel Thermocouple Calibration Chart

Cold Junction 0°C.

°C	mV		°C	mV	
100	4.10		400	16.34	
110	4.51		410	16.76	
120	4.92		419.50	17.16	Zinc M.P
130	5.33		420	17.18	
140	5.73		430	17.61	
150	6.13		440	18.03	
160	6.53		450	18.45	
170	6.93		460	18.88	
180	7.33		470	19.30	
190	7.73		480	19.73	
200	8.13		490	20.16	
210	8.54		500	20.59	
220	8.94				
230	9.34				
231.75	9.41	Tin M.P.			
240	9.75				
250	10.15				
260	10.56				
270	10.96				
280	11.37				
290	11.77				
300	12.18				
310	12.60				
320	13.00				
327.35	13.31	Lead M.P.			
330	13.42				
340	13.84				
350	14.25				
360	14.66				
370	15.08				
380	15.50				
390	15.93				

Appendix II. Physical Properties of Catalysts

Manufacturer	Basic Catalyst material	Shape and size	Specific Surface Area ($m^2/gm.$)	Specific weight
Svenska Salpeterverken (Sweden)	Iron oxide and chromium oxide	Pellets 9 mm. dia. x 9 mm. high	70-80	5.18 $\frac{gm}{cm^3}$
Power-Gas Corp. (U.K.)	Iron oxide and chromium oxide	Pellets (curved faces) 3/8 inch dia. x $\frac{1}{4}$ inch thick	80-85	2.2 $\frac{gm}{cm^3}$
Imperial Chemical Industries (U.K.)	Catalyst No. 15-2 - Iron oxide and chromium oxide	Pellets 8.5 mm. dia. x 11.3 mm. long	150-160	84 $\frac{lbs}{ft^3}$
Chemitron Chemicals - Girdler Catalyst Dept. (U.S.A.)	Catalyst No. G-3A Iron oxide and chromium oxide	Pellets 3/8 inch dia. x 3/8 inch high	-	72 $\frac{lbs}{ft^3}$
	Catalyst No. G-66 Oxides of Zinc, Copper and chromium	Pellets 3/16 inch dia. x 3/16 inch high	-	85 $\frac{lbs}{ft^3}$

Chapter 13. NOMENCLATURE

E = activation energy.

f_a = complete partition function of adsorbed molecules.

k = reaction rate constant.

k_f = rate constant for forward reaction.

k_b = rate constant for backward reaction.

K = thermodynamic equilibrium constant.

K_A, K_B = adsorption equilibrium constant.

p = partial pressure of reacting components.

P = total pressure.

q = heat of adsorption.

r = differential reaction rate.

r_f = forward reaction rate.

r_b = backward reaction rate.

R = gas constant.

Δt = rise in temperature in an adiabatic reactor.

T = absolute temperature.

V = volume of the reactor.

Θ = coverage of active sites.

Chapter 14 REFERENCES

1. ANOKHIN, TRAKER and MUKHLENOV, Zhur. Priklad, Khim., 33 (1960) p. 1740.

2. ARMSTRONG, E.F. and HILDITCH, T.P., Proc.Roy.Soc. (Lond.), 97A (1920) p. 265.

3. ATROSHCHENKO, V.J. and BIBR, B., Zhur. Priklad, Khim., 32 (1959) p. 997; Chem.Abstr. 53 (1959) 15735.

4. ATROSHCHENKO, V.I. and IVANOVA, L.N., Zhur. Prikl.Khimii, 37 (1964) p. 517; Brit.Chem.Eng.(Abstr.), Sept. 1964.

5. ATWOOD, K. and ARNOLD, M.R., Ind.Eng.Chem., 45 (1953) p. 424.

6. ATWOOD, K., ARNOLD, M.R. and APPEL, E.G., Ind.Eng.Chem., 42 (1950) p. 1600.

7. BARKLEY, L.W., CORRIGAN, T.E., WAINWRIGHT, H.W. and SANDS, A.E., Ind.Eng.Chem., 44 (1952) p. 1066.

8. BASOLO, F. and PEARSON, R.G., "Mechanism of Inorganic Reactions Wiley, N.Y., 1958 (p. 349).

9. BELONOGOV, K.N. and POPOV, B.I., Zhur.Fiz.Khim., 29 (1955) p. 1383; Chem.Abstr., 51 (1957) 818.

10. BELONOGOV, K.N. and POPOV, B.I., Zhur.Fiz.Khim., 29 (1955) p. 1187; Chem.Abstr., 50 (1956) 7557.

11. BOHLBRO, H., Acta Chem.Scand., 15 (1961) p. 502.

12. BOHLBRO, H., Acta Chem.Scand., 16 (1962) p. 431.

13. BOHLBRO, H., Acta Chem.Scand., 17 (1963) p. 1001.

14. BOHLBRO, H., Journal of Catalysis, 3 (1964) p. 207.

15. BOKHOVEN, C. and HOOGSCHAGEN, J., J. Chem. Phys., 21 (1953) p. 159.

16. BOSCH, C. and WILD, U.S. Patent No. 1,157,669 (Oct. 26, 1914).

17. BOUDART, M., A.I.Ch.E. Journal, 2 (1956) p. 62.

18. BRIDGER, G.L., GERNES, D.C. and THOMPSON, H.L., Chem. Eng. Progr., 44 (1948) p. 363.

19. British Patent No. 639,652; "Improvements in the Methods for Eliminating Carbon Monoxide from Gaseous Mixture".

20. British Patent No. 857,136; "Improvements in or relating to Catalysts for Carbon Monoxide Conversion".

21. British Patent No. 946,429; "Operating a Carbon Monoxide Conversion Plant".

22. CHRISTAIN, D.C. and BOYD, P.B. Jr., Chem. Eng., May, 1949, p. 148.

23. CHRISTIANSEN, J.A., Advan. in Catalysis, 5 (1953) p. 311.

24. CORRIGAN, T.E., Chem. Eng., 1954 Nov. p. 236 - 1955 July p. 227.

25. CRIBB, G.S., and MARSH, J.D.F., Trans. Inst. Gas Engrs. (London), 109 (1959-60) p. 714.

26. DANNHAUSER, W. and VAUGHN, P.A., J. Am. Chem. Soc., 77 (1955) p. 896.

27. DAVIES, O.L., (Editor) "The Design and Analysis of Industrial Experiments" Oliver & Boyd, 1963 (p. 247, 367 and 440).

28. DeBAUN, R.M. and ADLER, S.F., Chem. Eng. Progr., 56 (1960) No. 12, p. 24.

29. DE BRUIJN, H., Discussions Farady Soc., 8 (1950) p. 69.

30. DELORME, C., Acta Cryst., 9 (1956) p. 200.

31. DENBIGH, K.G. and PRINCE, A.J., J. Chem. Soc., 1947, p. 790.

32. DODGE, B.F., Ge'nie Chemique, 87 (1962) p.169.

32a. DOEHLEMAN, E., Z.Elektrochem., 44 (1938) p.178.

33. ELLIS, Sir C., J.Inst.Gas Engrs., 2 (1962) p.3.

34. EMMET, P.H., "Catalysis" Reinhold Publ.Co., N.Y., 1955, Vol.II, p.150

35. EMMET, P.H., "Catalysis" Reinhold Publ.Co., N.Y., 1955, Vol.III, p.318 and 338.

36. EVANS and NEWTON, Ind.Eng.Chem., 18 (1926) p.513.

37. FAUSER, G., Chemica Industria, 33 (1951) p.193.

38. FUKUDOME and KUSANO, Koggo Kagaku Zasshi, 63 (1960) p.1186.

39. HABER, Z.Physic.Chem., 68 (1909) p.731.

40. "Hand Book of Chemistry and Physics" - 44th Edition (1962-63), p.2702 (Chemical Rubber Publishing Co., Cleveland, U.S.A.).

41. HAYWARD, D.O. and TRAPNELL, M.W., "Chemisorption" 2nd Edition (Butterworth, London) 1964.

42. HEINZE, H. and RIENÄCKER, G., J.Prakt.Chem., 6 (1958) p.315; Chem.Abstr. 53 (1959) 5640.

43. HOLROYD, R., U.S. Bur.Mines, Inform.Circ.7375 (Aug,1946).

44. HOOGSCHAGEN, J., Ind.Eng.Chem., 47 (1955) p.906.

45. HOOGSCHAGEN, J., and ZWIETERING, P., J.Chem.Phys., 21 (1953) p.2224.

46. HORIUTI, J., J.Res.Inst.Catalysis, Hokkaido Univ., 5 (1957) p.1.

47. HORIUTI, J., and NAKAMURA, T., Z.Physik.Chem. (Neue Folge), 11 (1957) p.358.

48. HOUGEN, O.A., and WATSON, K.M., "Chemical Process Principles" - Part III, John Wiley & Sons Ltd., 1961 (Eighth Printing).

49. HOUGEN, O.A., and WATSON, K.M., Ind.Eng.Chem., 35 (1943) p.529.

50. HULBURT, H.M., and SRINI VASAN, C.D., A.I.Ch.E. Journal, 7 (1961) p.143.

51. IVANOVSKII, F.P., SHORINA, E.D. and DREITSER, I.G., Zhur.Khim. Prom., 14 (1937) p.567; Chem.Abstr. 31 (1937) 5956.

52. IVANOVSKII, et al, report in Proplemy Kinetika i Kataliza Nank S.S.S.R 10 (1960) p.90.

53. JOHNSON, J.Y., British Patent No.27,963, (1913).

54. JORDI, F., Monatsbull. Schweiz, Ver.Gas-u. Wasserfachm., 39 (1959) p.251.

55. KASSEL, L., Chemical Reviews, 18 (1936) p.299.

56. KIRCHER, O. and HOUGEN, O.A., A.I.Ch.E.Journal, 3 (1957) p.331.

57. KIRILLOV, I.P., Trans.Iranov Inst.of Chem.Tech., No.5, (1956) p.45; Chem.Abstr., 53 (1959) 11969.

58. KODAMA, S., FUKUI, K., TAME, T., and KINOSHITA, M., Catalyst (Japan), 8 (1952) p.50; Chem.Abstr.47 (1953), 11920.

59. KODAMA, S., MAZUME, A., FUKUBA, K. and FUKUI, K., Bull.Chem. Soc.Japan, 28 (1955) p.318; Chem.Abstr.52 (1958) 7661.

60. KRAMERS, H. and WESTERTERP, K.R., "Elements of Chemical Reactor Design and Operation"., Chapman & Hall 1963 (p.137).

61. KULKOVA, N.V., KUZNETS, Z.D. and TEMKIN, M.I., Dokl.Akad Nank, 90 (1953) p.1067; Chem.Abstr. 49 (1955) 8634.

62. KULKOVA, N.V. and TEMKIN, M.I., J.Phys.Chem. U.S.S.R., 23 (1949) p.695; Chem.Abstr.43 (1949) 7308.

63. LAIDLER, K.J., "Chemical Kinetics" McGraw Hill, N.Y., (1950).

64. LAUPICHLER, F.G., Ind.Eng.Chem., 30 (1938) p.578.

65. LEBEDER, A.T. and POPOV, B.I., Trudy Ivanovsk. Khim. - Teknol. Inst., No. 7 (1958) p. 53; Chem. Abstr, 54 (1960) p. 8251.

66. LEVENSPIEL, O., "Chemical Reaction Engineering - An Introduction to the Design of Chemical Reactors", John Wiley & Sons, 1962 (p. 426).

67. MANES, M., HOFER, L.J.E. and WELLER, S., J. Chem. Phys., 18 (1950) p. 1355.

68. MARS, P., Chem. Eng. Sci., 14 (1961) p. 375.

69. MARS, P., GORGELS, M.J. and ZWIETERING, P., in "Actes du Deuxième Congrés International de Catalyse", 1961, p. 2429 (Paris : Technipres).

70. MARSH, J.D.F. and ROBSON, R., "Catalysis in Practice," 1963 (London : Instn. Chem. Engrs.).

71. MILNER, M.J., C.P.E., 46 (1965) p. 208.

72. MOE, J.M., Chem. Eng. Progr., 58 (1962) p. 33.

73. MOE, J.M., Paper presented at the Am. Chem. Soc. Symp. "Production of Hydrogen" (N.Y., 1963).

74. MOND, L., and LANGER, C., Brit. Pat. No. 12,608 (1888).

75. MÜLLER, H., Gas-u. Wasserfach, 81 (1938) p. 590.

76. NAKANISHI, J. (Miss) and TAMARU, K., Trans. Faraday Soc., 59 (1963) p. 1470.

77. NATTA, G. and RIGAMONTI, R., Chimica e Industria (Italy), 18 (1936) p. 623; Chem. Abstr. 31 (1937), 2365[5].

78. NEUMANN, B. and KOHLER, G., Electrochem., 34 (1928) p. 218.

79. NEWLING, W.B.S. and MARSH, J.D.F., Gas Council Research Communication, GC86, 1962.

80. OLIVER, G., and BELA, B., Mag. Chem. Fóly., 66 (1960) p. 365.

81. PADOVANI, C., and LOTTERI, A., J. Soc. Chem. Ind., 56 (1937) p. 391T.

82. PARATELLA, A., Chimica Industria, 41 (1957) p. 1157.

83. PERRY, J.H. (Editor), "Chemical Engineers Hand Book", McGraw Hill.

84. POPOV, B.I., "Investigation of the Role of Mass Transfer Processes in the Carbon Monoxide Shift Reaction" - Dissertation, 1951, The D.I. Mendeleev Moscow Institute of Chemical Engineering.

85. POPOV, B.I., Zhur. Fiz. Khim., 31 (1957) p. 1033.

86. RI, KI CHIN, J. Soc. Chem. Ind. (Japan), 45 (1942) p. 35; Chem. Abstr. 43 (1949) 1945.

87. RIGAMONTI, R. and AGLIARDI, N., Chimica e Industria (Milan), 29 (1947) p. 145; Chem. Abstr. 44 (1950) 9784.

88. RIPPIN, D.W.T., and KISIEL, A.J., Private Communication.

89. ROITER, V.A., GAUKHMAN, S.S., PISARZHEVSKAYA, N.P. and GVALIYA, T.M., Zhur. Priklad. Khim., 18 (1945) p. 439; (Translation: C.F. Report 119, 385); Chem. Abstr. 40 (1946) 4593.

90. ROSSINI, F.D., et al, Nat. Bur. Stand., Circ. C461 (1947) p. 369.

91. ROSSINI, F.D., "Selected values of Physical and Thermodynamic Properties of Hydrocarbons and Related Compounds", Carnegie Press, Pittsburgh, Pa. (1953).

92. ROSSINI, F.D., J. Res. Nat. Bur. Stand., 34 (1945) p. 1634.

93. ROYEN, V.P. and EHRHARD, F., Erdöl und Kohle, 9 (1956) p. 19.

94. SAKSIN, V.F., "A study of the Kinetics of the Water-Gas Shift Reaction", The D.I. Mendeleev Moscow Institute of Chemical Engineering.

95. SARTORI, G. and NEWITT, D.M., Inst.Gas. Engrs., 222 (1939).

96. SCHUSTER, F., Gas-u. Wasserfach, 79 (1936) p.450.

97. SMITH, J.M., "Chemical Engineering Kinetics", McGraw Hill, 1956 (p.231, 280 and 318).

98. SORGATO, I. and ANGELIN, L., Chem.Eng.Sci., 20 (1965) p.431.

99. SPIERS, H.M. (Editor), "Technical Data on Fuel", 1962 (p.109 and 214).

100. STELLING, OTTO, and KRUSENSTIERNA, OTTO VON, Acta Chem.Scand. 12 (1958) p.1095.

101. STORCH, H.H. and PINKEL, I.I., Ind.Eng.Chem., 29 (1937) p.715.

101a. TATIEVSKAYA, E. and CHUFAROV, G., J.Phys.Chem. (U.S.S.R.), 8 (1936) p.933.

102. TEMKIN, M.I., "Problems in Kinetics and Catalysis", Moscow, 1949.

103. VOLK, "Applied Statistics for Engineers", McGraw Hill, N.Y..

104. WAGMAN, D.D., J.Res.Nat.Bur.Stand., 34 (1945) p.143.

105. WALAS, S.M., "Reaction Kinetics for Chemical Engineers", McGraw Hill, N.Y., 1959 (p.149 and 228).

106. WARD, R., in "Progress in Inorganic Chemistry", Vol.I, p.465-536, Interscience Publ., 1959.

107. WEISZ, P.B., Z.Physik.Chem. (Neue Folge), 11 (1957) p.1.

108. WEISZ, P.B. and PRATER, C.D., "Advances in Catalysis", 6 (1954) p.143; Chem.Eng.Progr.Symp.Ser.No.25 (1959) p.55.

109. WELLER, S., A.I.Ch.E.Journal, 2 (1956) p.59.

110. WHITE, E.C. and SCHULTZ, J.F., Ind.Eng.Chem., 26 (1934) p.95.

111. YANG, K.H. and HOUGEN, O.A., Chem. Eng. Progr., 46 (1950) p. 146.

112. "Chemitron Claim New Shift Catalyst will Revolutionise Hydrogen Plant Design" - Chemical Age, 89, No. 2273 (2nd Feb., 1963) p. 181.

113. U.S. Dept. Commerce, Office of Technical Services, Technical Oil Mission Reel 132, Item 26 (1947).